MONTHLY NOTICES

OF THE

ROYAL ASTRONOMICAL SOCIETY

Vol. 114 No. 6 1954

Published and Sold by the

ROYAL ASTRONOMICAL SOCIETY

BURLINGTON HOUSE

LONDON, W. 1

Price Thirteen Shillings and Sixpence

NOTICE TO AUTHORS

1. *Communications.*—Papers must be communicated to the Society by a Fellow. They should be accompanied by a summary at the *beginning* of the paper conveying briefly the content of the paper, and drawing attention to important new information and to the main conclusions. The summary should be intelligible in itself, without reference to the paper, to a reader with some knowledge of the subject; it should not normally exceed 200 words in length. **Authors are requested to submit MSS. in duplicate. These should be typed using double spacing and leaving a margin of not less than one inch on the left-hand side. Corrections to the MSS. should be made in the text and not in the margin.** Unless a paper reaches the Secretaries more than seven days before a Council meeting it will not normally be considered at that meeting. By Council decision, MSS. of accepted papers are retained by the Society for one year after publication; unless their return is then requested by the author, they are destroyed.

2. *Presentation.*—Authors are allowed considerable latitude, but they are requested to follow the general style and arrangement of *Monthly Notices*. References to literature should be given in the standard form, including a date, for printing either as footnotes or in a numbered list at the end of the paper. Each reference should give the **name and initials** of the author cited, irrespective of the occurrence of the name in the text (some latitude being permissible, however, in the case of an author referring to his own work). The following examples indicate the style of reference appropriate for a paper and a book, respectively :—

A. Corlin, *Zs. f. Astrophys.*, **15**, 239, 1938.

H. Jeffreys, *Theory of Probability*, 2nd edn., section 5.45, p. 258, Oxford, 1948.

3. *Notation.*—For technical astronomical terms, authors should conform closely to the recommendations of Commission 3 of the International Astronomical Union (*Trans. I.A.U.*, Vol. VI, p. 345, 1938). Council has decided to adopt the I.A.U. 3-letter abbreviations for constellations where contraction is desirable (Vol. IV, p. 221, 1932). In general matters, authors should follow the recommendations in *Symbols, Signs and Abbreviations* (London : Royal Society, 1951) except where these conflict with I.A.U. practice.

4. *Diagrams.*—**These should be designed to appear upright on the page, drawn about twice the size required in print and prepared for direct photographic reproduction except for the lettering, which should be inserted in pencil. Legends should be given in the manuscript indicating where in the text the figure should appear.** Blocks are retained by the Society for 10 years; unless the author requires them before the end of this period they are then destroyed.

5. *Tables.*—**These should be arranged so that they can be printed upright on the page.**

6. *Proofs.*—Costs of alterations exceeding 5 per cent of composition must be borne by the author. Fellows are warned that such costs have risen sharply in recent years, and it is in their own and the Society's interests to seek the maximum conciseness and simplification of symbols and equations consistent with clarity.

7. *Revised Manuscripts.*—When papers are submitted in revised form it is especially requested that they be accompanied by the original MSS.

Reading of Papers at Meetings

8. When submitting papers authors are requested to indicate whether they will be willing and able to read the paper at the next or some subsequent meeting, and approximately how long they would like to be allotted for speaking.

9. Postcards giving the programme of each meeting are issued some days before the meeting concerned. Fellows wishing to receive such cards whether for Ordinary Meetings or for the Geophysical Discussions or both should notify the Assistant Secretary.

MONTHLY NOTICES

OF THE

ROYAL ASTRONOMICAL SOCIETY

Vol. 114 No. 6

MEETING OF 1954 NOVEMBER 12

Dr J. Jackson, President, in the Chair

The election by the Council of the following Fellows was duly confirmed :—

Frederick Benario, 151–10 State Street, Flushing 54, New York, U.S.A. (proposed by R. M. Baum);

Mary Erwin Martin, 16 Rutland Gate, London, S.W.7 (proposed by F. J. M. Stratton); and

Leslie Douglas Scott, County Laboratory, Dorchester, Dorset (proposed by A. F. O'D. Alexander).

The election by the Council of the following Junior Members was duly confirmed :—

Derek John Blundell, Imperial College of Science and Technology, London, S.W.7 (proposed by J. M. Bruckshaw);

Eric Gray Forbes, B.Sc., Imperial College of Science and Technology, London, S.W.7 (proposed by E. Finlay-Freundlich);

Philip James Message, B.A., Gonville and Caius College, Cambridge (proposed by B. G. Tunmore);

Richard Edward Small, University College, London, W.C.1 (proposed by C. W. Allen);

David Edmund Smith, University College, Durham (proposed by F. Sheldrake); and

Malcolm Walsh, University College, London, W.C.1 (proposed by C. W. Allen).

Ninety-four presents were announced as having been received since the last meeting.

MEETING OF 1954 DECEMBER 10

Dr J. Jackson, President, in the Chair

The election by the Council of the following Fellows was duly confirmed :—

Michael Abdulahad, Mesopotamia Observatory, Basrah, Iraq (proposed by A. K. Das);

Christopher Rodney Armstrong, B.Sc., Guy's Hospital, London, S.E.1 (proposed by R. L. Waterfield);

Attia Abd-el-Salam Ashour, Faculty of Science, the University of Cairo, Egypt (proposed by V. C. A. Ferraro);

Ivan Atanasijević, The Physical Laboratory, Faculty of Sciences, Belgrade, Yugoslavia (proposed by M. Ryle);

Sudhir Kumar Dutt, M.Sc., D.I.C., Imperial College of Science and Technology, London, S.W.7 (proposed by J. M. Bruckshaw);

James Fogarty, 20 North Queen Street, Belfast, Northern Ireland (proposed by D. R. Bates);

Kenneth W. Gatland, 431a Chertsey Road, Whitton, Middlesex (proposed by P. A. Moore);

Morley Edwin Good, 18 Wardley Avenue, Little Hulton, Walkden, Manchester (proposed by E. Burgess);

Charles West Graham, M.Inst.B.E., M.I.N., 3 Kathleen Avenue, Cleethorpes, Lincolnshire (proposed by F. E. Townend);

Robert Hardie, Lowell Observatory, Flagstaff, Arizona, U.S.A. (proposed by S. Chandrasekhar);

Leroy Freame Henderson, 70 Park Road, Middle Park, Melbourne, Australia (proposed by C. W. Allen);

Theodore Edwin Houck, Washburn Observatory, University of Wisconsin, Madison, Wisconsin, U.S.A. (proposed by W. H. van den Bos);

Henry George Hughes, M.Sc., F.Inst.P., M.I.E.E., 6 The Dale, Widley, Portsmouth, Hampshire (proposed by C. R. Burch);

George W. Hutchinson, M.A., Ph.D., 12 Morven Road, Bearsden, Glasgow (proposed by T. R. Tannahill);

Alan Maxwell, M.Sc., Ph.D., Jodrell Bank Experimental Station, Lower Withington, Macclesfield, Cheshire (proposed by A. C. B. Lovell);

Sheila Constance Minion, B.Sc., 30 Fairfax Road, Derby (proposed by W. H. McCrea);

Donald Mugglestone, University College of the West Indies, Jamaica, British West Indies (proposed by S. Chandrasekhar);

William Nicholson, B.Sc., Royal Greenwich Observatory, Herstmonceux Castle, Sussex (proposed by D. H. Sadler);

Jagdeo Singh, M.Sc., D.I.C., Imperial College of Science and Technology, London, S.W.7 (proposed by J. M. Bruckshaw);

Henry Joseph Smith, Harvard College Observatory, Cambridge, Massachusetts, U.S.A. (proposed by R. H. Stoy);

Peter Smits, B.Sc., 13 Cluny Road, Forest Town, Johannesburg, South Africa (proposed by A. D. Thackeray);

Gladys Ethel Stone, 5 Belle Vue Road, Rodwell, Weymouth, Dorset (proposed by P. A. Moore);

Antony Geoffrey Strutt, O.B.E., B.Sc., 49 Maintenance Unit, R.A.F., Colerne, Wiltshire (proposed by A. F. Collins);

Jaakko Tuominen, Ph.D., Radio-astronomy Station, Siltavuorenpenger 20, Helsinki, Finland (proposed by F. J. M. Stratton);

Chester B. Watts, U.S. Naval Observatory, Washington 25, D.C., U.S.A. (proposed by R. d'E. Atkinson); and

Roy Bernard Worvill, M.Sc., Innisfree, The Leys, Chipping Norton, Oxfordshire (proposed by H. Wildey).

The election by the Council of the following Junior Members was duly confirmed :—

Charles David Austin, University College, London, W.C.1 (proposed by C. W. Allen);

Michael Gadsden, Imperial College of Science and Technology, London, S.W.7 (proposed by F. J. Hargreaves); and

Michael Guest, 122 Perrywood Road, Great Barr, Birmingham 22 (proposed by P. A. Moore).

Ninety-seven presents were announced as having been received since the last meeting, including :—

B. E. Markaryan, *Atlas of known stellar clusters of varying types* (presented by V. A. Ambartsumyan);

A. W. J. Cousins, *Standard magnitude sequences in the E regions* (presented by the author);

E. G. R. Taylor, *The mathematical practitioners of Tudor and Stuart England* (presented by the Cambridge University Press); and

The Hon. Sir Charles A. Parsons—born 100 years ago on 13th June, 1954 (presented by Messrs C. A. Parsons and Co., Ltd).

SOLUTIONS OF THE NEGATIVE EMDEN POLYTROPES

A. W. Rodgers and D. M. Myers

(Communicated by the Commonwealth Astronomer)

(Received 1954 September 7)

Summary

Tabular and graphical solutions of the negative Emden polytropes arising in the theory of spherical nebulae and clusters are found using a differential analyser.

Models giving the light and density as a function of radius projected against the celestial sphere are constructed for five cases of the assumed mass-function. The results indicate slight dependence of central intensity on this mass-function.

1. *Derivation of the equations.*—A general theory of globular clusters has been presented in a recent paper by Woolley*, taking both dispersion in mass and truncation of velocity into account. The negative Emden polytropes arise as the equations governing the distribution of light and density with radius, and it is the purpose of this present paper to consider the effect on these distributions of arbitrary variations in the assumed mass-function.

Woolley assumed a mass-function of the form $C_m = \text{const.} \times m^a e^{-bm}$ and then showed that the central mass-function $\xi_0(m)$ is related to C_m by the equation

$$\xi_0(m) = C_m \alpha_m^{-3/2} \operatorname{erf}_2(v_0\sqrt{\alpha_m}) \Big/ \int_0^\infty C_m \alpha_m^{-3/2} \operatorname{erf}_2(v_0\sqrt{\alpha_m})\, dm,$$

where $\operatorname{erf}_2(x)$ is written for $\dfrac{4}{\sqrt{\pi}} \displaystyle\int_0^x x^2 e^{-x^2} dx$.

Taking the velocity distribution to be fully Maxwellian, i.e. $v_0 = \infty$, $\xi_0(m)$ then becomes

$$C_m \alpha_m^{-3/2} \Big/ \int_0^\infty C_m \alpha_m^{-3/2}\, dm.$$

Substituting for the assumed C_m, we have $\xi_0(m) \propto m^{a-3/2} e^{-bm}$. The mean mass $\bar{m}$ is defined by $\bar{m} = \displaystyle\int_0^\infty m^{1/2} C_m\, dm \Big/ \int_0^\infty m^{-1/2} C_m\, dm, = (a+\tfrac{1}{2})/b$ and letting $\mu = m/\bar{m}$,

$$C_\mu = \text{const.} \times \mu^a e^{-(a+1/2)\mu}.$$

Assuming, in the general case, equipartition of energy among the low-velocity stars, the density ρ reduces to the form

$$\text{const.} \times \int_0^\infty \mu^{-1/2} C_\mu e^{-\mu\psi} d\mu, \quad \text{where } \psi \text{ is the potential.}$$

* R. v. d. R. Woolley, *M.N.*, **114**, 191, 1954.

Then $\eta=\rho/\rho_0=\text{const.}\times(a+\frac{1}{2}+\psi)^{-(a+1/2)}\int_0^\infty x^{a-1/2}\,e^{-x}\,dx$ and since $\eta=1$ when $\psi=0$ at the centre of the cluster,

$$\eta=\left(\frac{a+\frac{1}{2}}{a+\frac{1}{2}+\psi}\right)^{a+1/2}.$$

If $y=1+\dfrac{\psi}{a+\frac{1}{2}}$, then $\eta=y^{-(a+1/2)}$, which, together with Poisson's equation

$$\frac{1}{r^2}\frac{d}{dr}\left(r^2\frac{d\psi}{dr}\right)=-4\pi\Gamma\rho,$$

gives
$$\frac{1}{z^2}\frac{d}{dz}\left(z^2\frac{d\psi}{dz}\right)=\eta,$$

where
$$z=r\times(8\pi\Gamma\rho_0\beta\overline{m})^{1/2}.$$

Thus, if $x=(a+\frac{1}{2})^{1/2}z$, we find that

$$\frac{d}{dx}\left(x^2\frac{dy}{dx}\right)=x^2y^{-(a+1/2)} \tag{1}$$

with the boundary conditions $y=1$, $\dfrac{dy}{dx}=0$ at $x=0$.

This equation is called the negative Emden polytrope of index $n=a+\frac{1}{2}$ and has been solved numerically for the case $a=2\cdot5$ in Woolley's paper.

In this paper the index n was taken to have the five values, 2, 2·5, 3, 3·5 and 4, and the solutions of equation (1) were found using a differential analyser* constructed by the Mathematical Instruments Section of the (Australian) Council for Scientific and Industrial Research Organization and housed in the Department of Electrical Engineering, University of Sydney.

Letting $y=rx^t$, the asymptotic solutions of these equations are obtained by substituting in (1), giving $r=p^{-1/(1+n)}$, $p=\dfrac{2(n+3)}{(n+1)^2}$ and $t=2/(1+n)$. The asymptotic form of the density is then

$$\rho=y^{-n}=p^{n/(1+n)}\,x^{-2n/(1+n)}. \tag{2}$$

In some cases it may be more convenient to compare the light distribution rather than the density with observation, and in order to obtain the light distribution we need to know the mass-luminosity law for stars in, say, globular clusters.

We will assume that the law is $L\propto M^{3\cdot5}$, though it is open to question whether this is applicable to Baade's Population II stars. Thus, since the relative number of stars per unit volume of a given mass $\dfrac{\nu_\mu(x)}{\nu_\mu(0)}=e^{-n\mu(y-1)}$, the light emitted per unit volume becomes

$$\int_0^\infty \mu^{3\cdot5}\,\nu_\mu(x)\,d\mu=\int_0^\infty \mu^{3\cdot5}\,\nu_\mu(0)\,e^{-n\mu(y-1)}\,d\mu;\quad \nu_\mu(0)=\mu^{n-2}\,e^{-n\mu}.$$

Thus the light is proportional to

$$\int_0^\infty \mu^{3\cdot5}\mu^{n-2}\,e^{-n\mu y}\,d\mu,\quad \text{i.e. to } y^{-(2n+5/2)}.$$

The solution of the equations gives the light and density distributions in space and, for comparison with observations, the projections of these against the celestial

* D. M. Myers and W. R. Blunden, *Journ. I.E. Aust.*, **24**, 10–11, 195, 1952.

sphere must be found. The projection of density is of the form $\int_a^\infty y^{-n}\, d(x^2-a^2)^{1/2}$, where a is the projected central distance. The light projection is similarly

$$\int_a^\infty y^{-(2n+5/2)}\, d(x^2-a^2)^{1/2}.$$

It was found, by a comparison with the numerical solution for case $n=3$, that the asymptotic solution differed from it by less than 0·2 per cent at $x=20$. For $a \geqslant 20$, therefore, the projections were computed from

$$P_\rho = \rho^{n/(1+n)}\, a^{-(n-1)/(n+1)}\, (\pi/2)^{1/2}\, \frac{\Gamma\left(\dfrac{n-1}{2(n+1)}\right)}{\Gamma\left(\dfrac{n}{1+n}\right)} \quad \text{for the density}$$

and

$$P_L = \rho^{(2n+5)/(2n+2)}\, a^{-(n+4)/(n+1)}\, (\pi/2)^{1/2}\, \frac{\Gamma\left(\dfrac{n+4}{2(n+1)}\right)}{\Gamma\left(\dfrac{2n+5}{2n+2}\right)} \quad \text{for the light.}$$

Anticipating a little, another integral which it was found necessary to compute was $\int_{x_0}^\infty (x^2-a^2)^{1/2}\, dy^{-n}$ with $x_0 \gg a$, and $a > 20$. This range of x enables us to use the asymptotic form of y, giving

$$\int_{x_0}^\infty (x^2-a^2)^{1/2}\, dy^{-n} = y_0^{-n}\,(x_0^2-a^2)^{1/2} - \int_{x_0}^\infty y^{-n} d(x^2-a^2)^{1/2},$$

the latter integral being given by

$$\int_{x_0}^\infty y^{-n}\, d(x^2-a^2)^{1/2} = p^{n/(1+n)}\left\{\frac{1+n}{1-n}\, x_0^{-(n-1)/(1+n)} - \frac{na^2}{3n+1}\, x_0^{-(3n+1)/(n+1)} + \frac{na^4(2n+1)}{2(n+1)(5n+3)}\, x_0^{-(5n+3)/(n+1)}\right\}. \tag{3}$$

A fuller discussion of the computational procedures is given in the following section.

It can be seen that the total light $\int_0^\infty P_L\, x\, dx$ and *a fortiori* the total number of stars $\int_0^\infty P_\rho\, x\, dx$ in each of these models is infinite; thus in the comparison of these models with observational data, a method must be found to ascribe to them a finite radius. (Even so, as the projections themselves are finite, comparisons with observation can be made in the inner parts of the models as if there were a finite radius.) Truncation of the Maxwellian velocity distribution is fully equivalent to this both in the physical and analytical aspects of the problem.

2. *Solutions of the equations.*—The solution was carried out in three parts, namely (*a*) determination of y in terms of x for various values of n; (*b*) evaluation of the density projections for various values of a and n; (*c*) evaluation of the light projections for various values of a and n.

(*a*) There is no known analytical solution to equation (1) and a numerical solution for an adequate range of x and for all required values of n would be extremely tedious. It was therefore decided to obtain a set of solutions on the C.S.I.R.O. differential analyser.

It was appreciated that (i) the wide range of y^{-n} makes the equation unsuitable for solution in its present form, and (ii) the singularity at $x=0$ makes it necessary to use an approximate numerical solution, e.g. in series, to get away from the

singularity. The difficulty (i) is easily overcome by putting $u = \ln x$, $w = \ln y$, and the equation reduces to

$$\ddot{w} + \dot{w} + \dot{w}^2 = \exp\{2u - (n+1)w\}. \tag{4}$$

It is clear that the solutions of equation (4) have as asymptotes straight lines whose gradients are given by $\dot{w} = 2/(n+1)$, and substitution of this, with $\ddot{w} = 0$, in (4) gives the equation of the asymptote as

$$2u - (n+1)w = 2(n+3)/(n+1)^2.$$

The machine solution started at $u = 0$, $x = 1$ in each case, the difficulty (ii) being overcome by solving (1) in series for y giving

$$y = 1 + \frac{x^2}{2.3} - \frac{nx^4}{2.3.4.5} + \frac{n(8n+5)x^6}{5.6.7.8.9} - \frac{n(122n^2 - 183n + 70)x^8}{9.9!} + \frac{n(605n^3 - 1947n^2 + 1981n - 630)x^{10}}{9.11!} - \ldots,$$

a result similar to that of von Zeipel.*

The solutions on the differential analyser (see Fig. 2) show that for a small value of x (of the order of $x = 20$), the curves approach their asymptotes to within several parts in a thousand. As the overall accuracy of the differential analyser is of this order, the asymptotes may therefore be taken as the solutions of the equation beyond $x = 20$ without loss of accuracy. This is of considerable importance in evaluating the density projections.

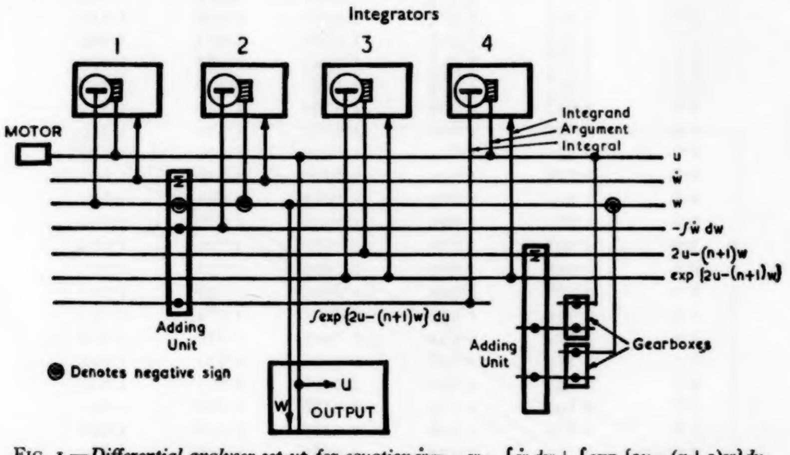

FIG. 1.—*Differential analyser set-up for equation* $\dot{w} = -w - \int \dot{w}\,dw + \int \exp\{2u - (n+1)w\}du$.
(*Scale factors omitted.*)

The set-up of the differential analyser for solving equation (1) in the modified form given in equation (4) is shown in Fig. 1, in which the notation standardized by Bush† is used. It was convenient to integrate each side of the equation, so that it was put on the machine in the form:

$$\dot{w} = -w - \int \dot{w}\,dw + \int \exp\{2u - (n+1)w\}du.$$

Integrator 3 is used to generate the exponential, its argument $2u - (n+1)w$ being obtained from the independent and dependent variables through an adding unit. Otherwise, the set-up is quite straightforward.

* H. von Zeipel, *Kungl. Svenska Vetenskapsakademiens Handlingar*, Band **51**, No. 5.
† V. Bush, *Journ. Franklin Inst.*, **212**, 4, 447, 1931.

The output table was used to plot $-nw(=\log_{10} y^{-n})$ against $u(=\log_{10} x)$ as this gave a convenient scale for each curve and provided suitable input data for evaluating the density projections. These results are shown, together with the corresponding asymptotes, in Fig. 2, and are tabulated also, in the form of y against x, in Table I.

TABLE I

Machine solution of negative Emden polytropes of orders
2, 2·5, 3, 3·5, 4 for $0 \leqslant x \leqslant 20$

x	y_2	$y_{2\cdot5}$	y_3	$y_{3\cdot5}$	y_4
0	1·0	1·0	1·0	1·0	1·0
0·25	1·0103	1·0103	1·0103	1·0103	1·0103
0·5	1·0407	1·0405	1·0402	1·0400	1·0397
0·75	1·0891	1·0880	1·0869	1·0858	1·0847
1·0	1·1522	1·1493	1·1463	1·1433	1·1406
1·1	1·183	1·178	1·1731	1·170	1·169
1·2	1·215	1·208	1·2011	1·198	1·198
1·3	1·247	1·239	1·2301	1·226	1·224
1·4	1·280	1·272	1·2600	1·254	1·258
1·5	1·313	1·306	1·2905	1·283	1·287
1·6	1·348	1·340	1·3216	1·310	1·314
1·7	1·385	1·375	1·3531	1·338	1·340
1·8	1·422	1·409	1·3849	1·365	1·366
1·9	1·459	1·444	1·4170	1·393	1·392
2·0	1·497	1·480	1·4494	1·422	1·417
2·1	1·537	1·515	1·4819	1·451	1·444
2·2	1·577	1·551	1·5143	1·480	1·470
2·3	1·617	1·587	1·5467	1·510	1·496
2·4	1·657	1·622	1·5790	1·540	1·523
2·5	1·697	1·658	1·6113	1·570	1·549
2·6	1·737	1·694	1·6432	1·599	1·575
2·7	1·778	1·730	1·6749	1·626	1·601
2·8	1·819	1·765	1·7065	1·654	1·627
2·9	1·861	1·800	1·7378	1·680	1·652
3·0	1·903	1·835	1·7689	1·706	1·678
3·1	1·945	1·869	1·7997	1·732	1·703
3·2	1·988	1·904	1·8302	1·758	1·728
3·3	2·030	1·939	1·8605	1·784	1·753
3·4	2·072	1·974	1·8905	1·810	1·778
3·5	2·113	2·008	1·9202	1·837	1·802
3·6	2·155	2·042	1·9496	1·863	1·825
3·7	2·197	2·075	1·9788	1·888	1·847
3·8	2·239	2·106	2·0077	1·912	1·868
3·9	2·281	2·135	2·0363	1·936	1·889
4·0	2·322	2·163	2·0646	1·959	1·909
4·2	2·404	2·239	2·1204	2·006	1·950
4·4	2·483	2·305	2·176	2·053	1·995
4·6	2·565	2·367	2·229	2·097	2·035
4·8	2·646	2·432	2·282	2·142	2·074
5·0	2·718	2·493	2·334	2·186	2·115
5·2	2·795	2·559	2·385	2·231	2·154
5·4	2·873	2·620	2·435	2·274	2·190
5·6	2·957	2·679	2·484	2·318	2·222
5·8	3·035	2·733	2·532	2·359	2·257
6·0	3·111	2·791	2·579	2·396	2·292
6·2	3·184	2·856	2·625	2·430	2·325
6·4	3·261	2·916	2·670	2·466	2·356
6·6	3·336	2·967	2·715	2·504	2·388

TABLE I (*cont.*)

x	y_2	$y_{2\cdot5}$	y_3	$y_{3\cdot5}$	y_4
6·8	3·409	3·013	2·759	2·542	2·421
7·0	3·478	3·065	2·803	2·580	2·453
7·2	3·550	3·116	2·846	2·613	2·483
7·4	3·623	3·182	2·888	2·647	2·510
7·6	3·694	3·241	2·930	2·679	2·538
7·8	3·762	3·293	2·971	2·714	2·566
8·0	3·829	3·341	3·012	2·750	2·594
8·2	3·896	3·393	3·052	2·784	2·622
8·4	3·964	3·444	3·091	2·816	2·650
8·6	4·032	3·491	3·130	2·845	2·677
8·8	4·100	3·538	3·168	2·875	2·703
9·0	4·166	3·584	3·206	2·904	2·729
9·2	4·231	3·632	3·244	2·931	2·755
9·4	4·296	3·679	3·281	2·958	2·779
9·6	4·361	3·728	3·317	2·987	2·803
9·8	4·426	3·780	3·353	3·018	2·827
10·0	4·490	3·830	3·389	3·048	2·852
11	4·801	4·055	3·562	3·200	2·972
12	5·105	4·276	3·727	3·336	3·083
13	5·419	4·485	3·884	3·460	3·189
14	5·706	4·680	4·035	3·570	3·289
15	5·986	4·870	4·180	3·686	3·383
16	6·248	5·064	4·319	3·796	3·473
17	6·519	5·256	4·454	3·907	3·562
18	6·769	5·449	4·584	4·009	3·644
19	7·027	5·627	4·711	4·113	3·725
20	7·260	5·777	4·835	4·217	3·806

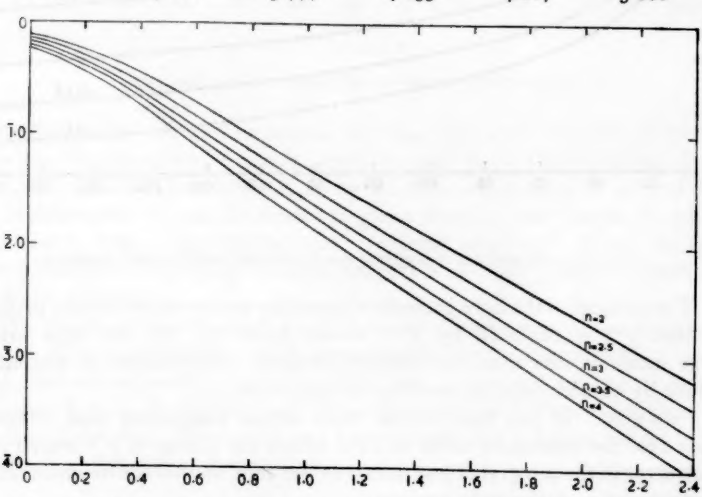

FIG. 2.—*Machine solution of equation* (4); (log y^{-n}) $= w$ *plotted against* $u =$ (log x).

(*b*) The density integrals, defined by

$$P_\rho = a \int_{x=a}^{\infty} (x^2/a^2 - 1)^{1/2} d(y^{-n}), \tag{5}$$

were obtained for various values of n and a. For $a \geqslant 20$ the asymptotic solution was evaluated from the equation (2) and a machine integration was not required.

For $a<20$, the evaluation of the integrals is a matter of simple numerical computation, but for convenience the differential analyser was used, the curve already obtained for $\log y^{-n}$ being fed into the machine from an input table. One integrator was used to evaluate y^{-n} from the input data, whilst another input table was used to feed into the machine the value of $(x^2/a^2-1)^{1/2}$.

However, it was necessary to decide on an upper limit of the integration to provide sufficient accuracy. Assuming that machine integration will proceed at least as far as the apparent coalescence of the input curve and its asymptote, the contribution to the infinite integral for values of x beyond the limit of the machine solution can be readily determined.

This contribution is given by $\int_{x_0}^{\infty}(x^2-a^2)^{1/2}d(y^{-n})$ which is given above in equation (3), where x_0 is the limit to which the machine integration is taken. The density integrals are shown in Fig. 3(*a*).

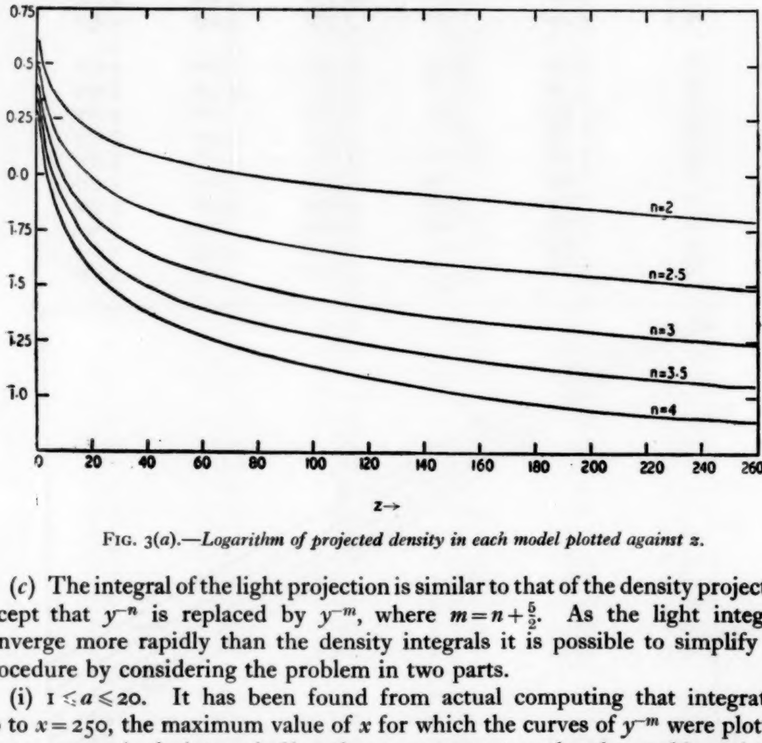

FIG. 3(*a*).—*Logarithm of projected density in each model plotted against z.*

(*c*) The integral of the light projection is similar to that of the density projection except that y^{-n} is replaced by y^{-m}, where $m=n+\frac{5}{2}$. As the light integrals converge more rapidly than the density integrals it is possible to simplify the procedure by considering the problem in two parts.

(i) $1\leqslant a\leqslant 20$. It has been found from actual computing that integration up to $x=250$, the maximum value of x for which the curves of y^{-m} were plotted, leaves an error in the integral of less than 0·01 per cent, so that the machine solution can be accepted as sufficiently accurate.

(ii) $20\leqslant a\leqslant\infty$. The plotted curves of y^{-m} do not differ perceptibly from their asymptotes when $x\geqslant 20$, so that integration of the asymptotes gives a sufficiently accurate result without recourse to the differential analyser.

The required integral is that given above

$$P_L=-a\int_{x=a}^{\infty}(x^2/a^2-1)^{1/2}d(y^{-m}). \tag{6}$$

The central values of the projections of light and density at $a=0$ could not be found using the machine set-up described above (see equations (5) and (6)). Therefore, after having read off $\log y^{-n}$ and $\log x$ from the machine output table, the results were transformed to give y as a function of n. Thus the integrals $P_L|_0^{20}$ and $P_\rho|_0^{20}$ were found by numerical quadrature and the remaining contributions $P_\rho|_{20}^{\infty}$ and $P_L|_{20}^{\infty}$ were found from the asymptotic solutions for y. The curves showing the light projections plotted against z are shown in Fig. 3(*b*).

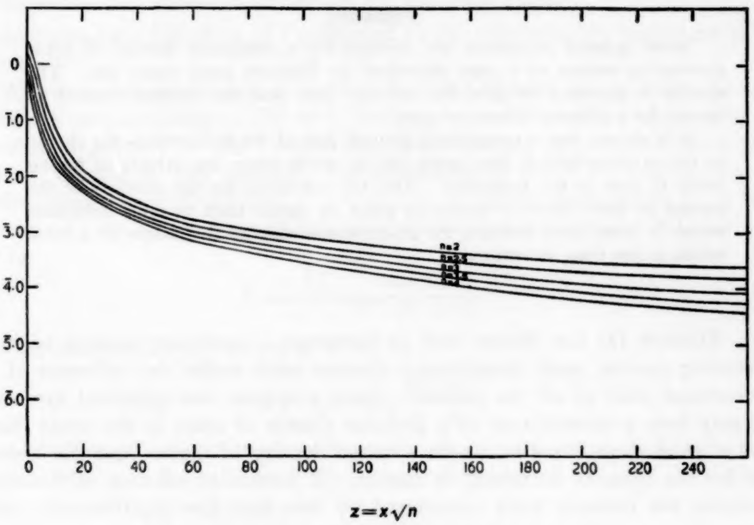

FIG. 3(*b*).—*Logarithm of light projection plotted against z.*

3. *Conclusion*.—It can be shown in Figs. 3(*a*) and 3(*b*) that although for a given set of parameters, e.g. total mass, central density and radius, the curves are rather different for different n, by suitable adjustment of central intensity and radius scale all can be made to agree over a wide range of radius with observations such as de Vaucouleurs' empirical relation.* Thus the quest for more information regarding these parameters is necessary before a discriminating fit can be obtained.

The results demonstrate that a differential analyser can be used satisfactorily for this class of investigation with a reasonable degree of accuracy.

4. *Acknowledgments*.—This problem was attempted at the suggestion of Professor R. v. d. R. Woolley, and the authors are very grateful for his continued advice and interest. We would also like to thank Mr J. Foster for his help in the operation of the differential analyser.

Research School of Physical Sciences,
Australian National University,
Commonwealth Observatory,
Mount Stromlo :

Department of Electrical Engineering,
University of Sydney.

1954 *August* 31.

* G. de Vaucouleurs, *M.N.*, **113**, 2, 1952.

THE STABILITY OF A SPHERICALLY SYMMETRIC CLUSTER OF STARS DESCRIBING CIRCULAR ORBITS

C. Gilbert

(Received 1954 September 27)

Summary

Some general properties are derived for a stationary system of many gravitating masses of a type described by Einstein some years ago. The system is assumed to give the average field and the average density of matter for a globular cluster of stars.

It is shown that a particularly smooth join of the field within the cluster to the exterior field in free space can be made when the density of matter tends to zero at the boundary. Also the condition for the stability of the masses in their orbits is shown to place an upper limit to their velocities, which in most cases restricts the gravitational mass of the cluster to a value which is less than its rest mass.

1. Einstein (1) has shown how to construct a stationary system of many gravitating masses, each describing a circular orbit under the influence of the gravitational field of all the masses. Such a system has spherical symmetry and may bear a resemblance to a globular cluster of stars in the sense that it gives a good approximation to the average density of matter and the average field for the systems occurring in nature. A particular solution of Einstein's equations has recently been considered by Sen and Roy (2) from this point of view.

The object of this paper is to consider, in greater detail than has been done by Einstein, the structure of such a cluster of particles, with particular reference to the stability of the particles in their orbits.

The structure of a cluster depends primarily on the density of matter, which in general is a function of the distance from the centre. When this density function is known the gravitational field and the speed of the particles in their orbits can be determined. The derivation of expressions for these quantities is carried out in polar coordinates, which differ from the isotropic coordinates used by Einstein. These coordinates have a particular advantage over the isotropic coordinates when the density of matter tends to zero at the boundary of the cluster. It is shown in this case that, by suitable choice of the density function, the field within the cluster can be joined to the Schwarzschild field outside so that the field tensors and their derivatives up to any order can be made continuous.

The condition that each particle shall have a stable orbit places an upper limit to the velocities of the particles in the cluster, and it is shown that in most cases this limits the gravitational mass of the cluster to a value which is less than its rest mass.

2. *The material-energy tensor and the field equations.*—We consider a system consisting of particles of rest mass m, each describing a circular orbit about the centre O of the cluster. The gravitational field of the cluster has spherical

symmetry about O and each particle describes its orbit under the influence of this field, the effect of collisions between particles being neglected. In order to have a continuous distribution of matter we make the proper number density of particles $n_0 \to \infty$ and the rest mass of each particle $m \to 0$, in such a manner that the proper density of matter $\rho_0 = mn_0$ is finite at all points of the cluster.

Since we are considering a static system the gravitational field within the cluster is given by

$$ds^2 = -e^{\lambda} dr^2 - r^2 d\theta^2 - r^2 \sin^2\theta \, d\phi^2 + e^{\nu} dt^2, \tag{1}$$

where λ and ν are functions of r only, and $r \leqslant a$, $r = a$ being the boundary of the cluster.

Within a volume element at a point P of the cluster, the particles move in directions perpendicular to OP with the same speed V, and on account of the spherical symmetry of the system the same number of particles have their velocity vectors in any direction perpendicular to OP. Writing g_{ij} for the fundamental tensor of (1), and x^i ($i = 1, 2, 3, 4$) for the coordinates (r, θ, ϕ, t) respectively, the speed of a particle having velocity components dx^α/dt ($\alpha = 1, 2, 3$) will be

$$V = \sqrt{\left(-g_{\alpha\beta} \frac{dx^\alpha}{dt} \frac{dx^\beta}{dt}\right)}. \tag{2}$$

Also the material–energy tensor at P will be

$$T^i_j = n_0 \overline{\quad m g_{ik} \frac{dx^i}{ds} \frac{dx^k}{ds}}, \tag{3}$$

where the barred expression gives the mean value of the energy and momentum of a particle for all the particles in the volume element at P. From (1) and (2) we find for a particle having a velocity V

$$e^{\nu}(dt/ds)^2 = (1 - e^{-\nu} V^2)^{-1}, \tag{4}$$

and consequently dt/ds has the same value for each particle in the volume element.

The mean value in (3) can now be evaluated and gives the components

$$T^2_2 = T^3_3 = -\tfrac{1}{2}\rho_0 V^2 (dt/ds)^2, \tag{5}$$

$$T^4_4 = \rho_0 e^{\nu}(dt/ds)^2 = \rho_{00}, \tag{6}$$

where ρ_{00} is the density of matter referred to axes fixed at P. The other components of T^i_j are zero.

The components (5) and (6) must now be substituted in the field equations

$$8\pi T^i_j = -G^i_j + \tfrac{1}{2} G g^i_j, \tag{7}$$

in which units have been chosen which give the Einstein constant the value 8π. Making use of the well-known components of (7) for the metric (1), as given in (3), we find in a straightforward manner

$$\nu' = (e^{\lambda} - 1)r, \tag{8}$$

$$8\pi\rho_{00} = e^{-\lambda}\left(\frac{\lambda'}{r} - \frac{1}{r^2}\right) + \frac{1}{r^2}, \tag{9}$$

$$e^{-\nu} V^2 = (e^{\lambda} - 1)/2. \tag{10}$$

Since the square of the velocity of light in the transverse direction is e^{ν}, equation (10) gives the square of the ratio of the velocity of a particle to the velocity of light in the same direction. It can be verified from the equations of

the geodesics given in Section 4 that this value of V gives the velocity of a particle in a circular orbit of radius r. Elimination of e^ν from equations (4) and (10) gives

$$V^2\left(\frac{dt}{ds}\right)^2=\frac{e^\lambda-1}{3-e^\lambda}. \tag{11}$$

The information required to discuss the structure of a cluster is contained in the equations (8)–(11).

3. *The gravitational field of the cluster.*—We make the following assumptions concerning the constitution of the cluster.

(i) The density of matter ρ_{00} is finite, continuous and not zero at all points within the cluster, but may be zero at the boundary.

(ii) The particles describe circular orbits about the centre of symmetry, with the exception of particles at the centre, which are at rest.

(iii) The velocity of any particle is less than the velocity of light in the same direction.

We define

$$\mu(r)=4\pi\int_0^r \rho_{00}r^2\,dr \tag{12}$$

for all values of r.

From (i), when $r<a$, $\mu(r)$ is a continuous function of r tending to zero as fast as r^3 at $r=0$. When $r\geqslant a$, $\mu(r)$ has a constant value $\mu(a)$.

The interior field.—From (11), (ii) and (iii),

$$1\leqslant e^\lambda<3. \tag{13}$$

Also, since e^λ is finite at $r=0$, (9) gives, after multiplication by r^2 and integration between $r=0$ and $r=r$,

$$e^{-\lambda}=1-\frac{2\mu(r)}{r}. \tag{14}$$

From (14) and (9), $e^\lambda=1$ and $\lambda'=0$ at $r=0$, and $e^\lambda>1$ for $r>0$. In the interval $0\leqslant r\leqslant a$, e^λ is therefore a bounded positive function of r which may either be a monotonic increasing function of r, or have at least one maximum value in the interval.

We set $\lambda+\nu=0$ at $r=a$, to make the field continuous with the Schwarzschild solution at the boundary. Then from (8) and (14) we find

$$\nu=\int_a^r \frac{2\mu(r)}{r^2(1-2\mu(r)/r)}\,dr+\ln(1-2\mu(a)/a). \tag{15}$$

From (8) $\nu'=0$ at $r=0$ and $\nu'>0$ for $r>0$. From the boundary condition above, ν is finite and negative at $r=a$. Integration of both sides of (8) between $r=0$ and $r=a$ then gives a finite negative value for ν at $r=0$.

From the above it follows that e^ν has a minimum value <1 at $r=0$ and increases monotonically to a value <1 at $r=a$.

The interior field is given by (12), (14) and (15) when the density ρ_{00} is a known function of r. Also the discussion above has shown that the field will be free from singularities.

The exterior field and the boundary conditions.—In order to take the most general static gravitational field for the empty region $r>a$, we assume that the

radial coordinate R is an arbitrary function $f(r)$ of the coordinate r. The Schwarzschild solution may then be written in the form

$$ds^2 = -e^{\xi}\,dR^2 - R^2 d\theta^2 - R^2 \sin^2\theta\, d\phi^2 + e^{\eta} dt^2, \tag{16}$$

where

$$e^{-\xi} = e^{\eta} = 1 - 2\mu/R, \tag{17}$$

μ being the gravitational mass of the cluster.

We write g_{ij} for the fundamental tensor of (16) when ds is expressed in terms of the coordinates x^i and their differentials dx^i, and we assume for the boundary conditions at $r=a$ that the g_{ij} for the interior and exterior fields, as well as their first derivatives, are continuous.

For the g_{22} and g_{33} components these conditions give

$$f(a) = a, \qquad f'(a) = 1, \tag{18}$$

and because we have set $\lambda + \nu = 0$ at $r=a$, the g_{11} and g_{44} components will be continuous if $\mu = \mu(a)$. Their derivatives will also be continuous if

$$\lambda' = \frac{d\xi}{dR} + 2f''(a), \qquad \nu' = \frac{d\eta}{dR} \tag{19}$$

at $r=a$, and from (8), (9), (17) and (18) these conditions will be satisfied if the density at $r=a$ has the value

$$\rho_{00} = f''(a) e^{-\lambda}/4\pi a.$$

If the density vanishes at the boundary of the cluster we must have $f''(a)=0$. This case can be obtained by taking $R=r$. It can then be verified that *in the case when the density of matter tends to zero at the boundary of the cluster both the interior and the exterior fields are given by the same expressions* (14) *and* (15), the value of $\mu(r)$ for the exterior field having the constant value $\mu(a)$ in accordance with (12).

By forming the first n derivatives of the equations (14) and (15) it is clear that in the case $\rho_{00}=0$ at $r=a$, the g_{ij} and their derivatives up to the nth order will be continuous provided $\mu''(r), \mu'''(r) \ldots \mu^n(r)$ are all zero at $r=a$. This will be the case if $d\rho_{00}/dr, d^2\rho_{00}/dr^2 \ldots d^{n-1}\rho_{00}/dr^{n-1}$ are all zero at $r=a$. In particular the Riemann–Christoffel tensor, which depends only on g_{ij} and their first and second derivatives, will be continuous at $r=a$, if $d\rho_{00}/dr=0$ at $r=a$.

The exterior field also will be free from singularities provided $\mu < a/2$, and this condition is satisfied because e^{λ} satisfies the conditions (13) at $r=a$.

4. *The condition for the stability of the particles in the circular orbits.*—To investigate the stability of the particles describing circular orbits, we use the first integrals of the equations for the geodesics. For orbits in the plane $\theta = \pi/2$ these can be written (3)

$$e^{\lambda}\left(\frac{dr}{ds}\right)^2 + r^2\left(\frac{d\phi}{ds}\right)^2 - e^{\nu}\left(\frac{dt}{ds}\right)^2 + 1 = 0, \tag{20}$$

$$\frac{d\phi}{ds} = \frac{h}{r^2}, \tag{21}$$

$$\frac{dt}{ds} = k e^{-\nu}, \tag{22}$$

where h and k are constants of integration.

Substituting from (21) and (22) in (20) we find

$$e^{\lambda}\left(\frac{dr}{ds}\right)^2 = -1 + k^2 e^{-\nu} - \frac{h^2}{r^2} = F(r, h, k). \tag{23}$$

For a circular orbit of radius r, $F(r, h, k)$ and $F'(r, h, k)$ are both zero. Let the particle describing the orbit be subjected to a small perturbation which causes it to follow a geodesic path having constants H and K which differ slightly from h and k respectively. In general there will be a value $r=b$, differing slightly from the value for the circular orbit, such that

$$F'(b, H, K) = -\nu' e^{-\nu} K^2 + 2H^2/b^3 = 0. \tag{24}$$

$F(b, H, K)$ will be a small positive quantity and for $r=b+x$, where x is a small displacement,

$$F(r, H, K) = F(b, H, K) + F''(b, H, K)(x^2/2).$$

The particle will oscillate radially near the circle of radius b if $F''(b, H, K) < 0$, that is, if

$$(-\nu'' + \nu'^2)e^{-\nu}K^2 - 6H^2/b^4 < 0.$$

Substituting from (24) this gives the condition

$$(-\nu'' + \nu'^2 - 3\nu'/b)e^{-\nu} < 0.$$

A *sufficient* condition for the stability of the system is therefore

$$\nu'' - \nu'^2 + 3\nu'/r > 0. \tag{25}$$

The case $F''(r, h, k) = 0$ would require further investigation, otherwise (25) would also be the *necessary* condition for stability.

It is possible that equation (24) cannot be satisfied for a value $r=b$. This will be the case if

$$e^{-\nu} = A + B/r^2,$$

where A and B are constants. In this case the equilibrium will be unstable because (23) then gives only one positive value of r for which $dr/dt = 0$. This value of ν makes the left-hand side of (25) identically zero and does not therefore affect the sufficient condition for stability.

From (8) and (25) the sufficient condition for stability can be stated in the form

$$r\lambda' e^{\lambda} > -(e^{\lambda} - 1)(3 - e^{\lambda}). \tag{26}$$

From (9) and (26) we obtain the condition

$$(e^{\lambda} - 1)(2e^{\lambda} - 3) < 8\pi\rho_{00} r^2 e^{2\lambda}.$$

In a region of space where $\rho_{00} = 0$ we find, from (5) and (6), $T^i_j = 0$. It follows that in free space the condition for stability in a circular orbit is that

$$e^{\lambda} < \tfrac{3}{2}. \tag{27}$$

From (10) and (27) we deduce that the velocity of a particle describing a stable orbit in free space must be less than half the velocity of light. On account of the continuity of the field at $r=a$, the condition (27) must hold at the boundary of the cluster in order to ensure stability for displacements which make $r > a$.

We can also take (27) to be a sufficient condition for stability within the cluster, for then the condition (26) will certainly be satisfied. Since $\lambda' = 0$ when e^{λ} has a maximum value, we then obtain from (9) and (27) the condition

$$8\pi\rho_{00} < \tfrac{1}{3} r^{-2}. \tag{28}$$

For a particle at the centre of the cluster $h=0$, and the stability of the particle can be shown, from (23), to be a consequence of e^{ν} having a minimum value.

5. *Calculation of the proper mass of the cluster.*—The rest mass of the cluster is

$$M=\int \rho_0\, d\Sigma, \tag{29}$$

where $d\Sigma$ is the proper volume element at a point P for an observer moving with speed V, and the integration is taken over the whole cluster.

For the metric (1)

$$d\Sigma=\frac{dt}{ds}\, e^{\frac{1}{2}(\lambda+\nu)} r^2 \sin\theta\, dr\, d\theta\, d\phi, \tag{30}$$

and dt/ds can be found by eliminating V^2 between equations (10) and (11).

Substituting from (6) and (30) in (29) we find

$$\begin{aligned} M &= \int_0^{2\pi}\int_0^{\pi}\int_0^{a} \rho_{00} r^2 \{\tfrac{1}{2}e^{\lambda}(3-e^{\lambda})\}^{\frac{1}{2}} \sin\theta\, dr\, d\theta\, d\phi \\ &= \int_0^a \frac{d\mu(r)}{dr}\{\tfrac{9}{8}-\tfrac{1}{2}(e^{\lambda}-\tfrac{3}{2})^2\}^{1/2}\, dr. \end{aligned}$$

From the definition (12) $d\mu(r)/dr$ is always positive, and therefore, when the condition for stability (27) is satisfied, we find that

$$0<\frac{M-\mu}{M}<0{\cdot}057. \tag{31}$$

The gravitational mass of the cluster is then less than its proper mass by less than 6 per cent of the rest mass. On the other hand, when the only restrictions on e^{λ} are those given by (13), μ can have values which are greater than M.

6. *Discussion of some special cases.*—It will be convenient to distinguish two classes of clusters, called the A and B clusters, which differ in the behaviour of e^{λ} within the cluster.

For the A clusters we assume that e^{λ} is a monotonic increasing function of r. Since $\lambda'>0$ the condition for stability (26) is satisfied within the cluster provided $e^{\lambda}<3$. The condition for stability at the boundary, however, gives the condition $e^{\lambda}<\frac{3}{2}$, according to (27). From (9) at $r=a$, $\rho_{00}>0$ and the proper density ρ_0 cannot be zero. From (10) the velocities of the particles increase with increasing distance from the centre to a value which is less than half the velocity of light at $r=a$. Also, according to (31) the gravitational mass of the cluster is always less than the rest mass of the cluster.

A short calculation has shown that the special cases considered by Einstein and by Sen and Roy are both examples of A clusters, and are therefore stable systems. The restriction placed on the velocities of the particles by the condition for stability, however, restricts these cases to the configurations for which $\mu<M$.

For the B clusters we assume that e^{λ} rises sharply to a maximum value $<\frac{3}{2}$ near $r=0$ and then decreases to the boundary, in such a manner that $\rho_{00}>0$ for $r<a$, and $\rho_{00}=0$ at $r=a$. For these clusters the proper density of matter is zero at the boundary, and the particles having the highest velocities are concentrated near the centre of the cluster. Since the condition (27) is satisfied, these are stable clusters, and according to (31) the gravitational mass is always less than the rest mass of the cluster.

From counts of stellar images on the photographic plates of globular clusters, it is inferred that the number density of stars in general decreases from the centre outwards at first rapidly and then falling gradually to zero near the boundary (4). It would therefore appear that the best approximation to the field for these clusters would be obtained from the B rather than from the A clusters. In addition the B clusters enable a smoother join of the two fields to be made at the boundary of the cluster.

1 *North House,*
Longbenton,
Newcastle upon Tyne :
1954 *September* 25.

References

(1) A. Einstein, *Annals of Math.*, **40,** 922, 1939.
(2) N. R. Sen and T. C. Roy, *Zs. für Astrophysik*, **34,** 84, 1954.
(3) R. C. Tolman, *Relativity, Thermodynamics and Cosmology*, pp. 251, 207, O.U.P., 1934.
(4) H. S. Jones, *General Astronomy*, p. 390, London, 1951.

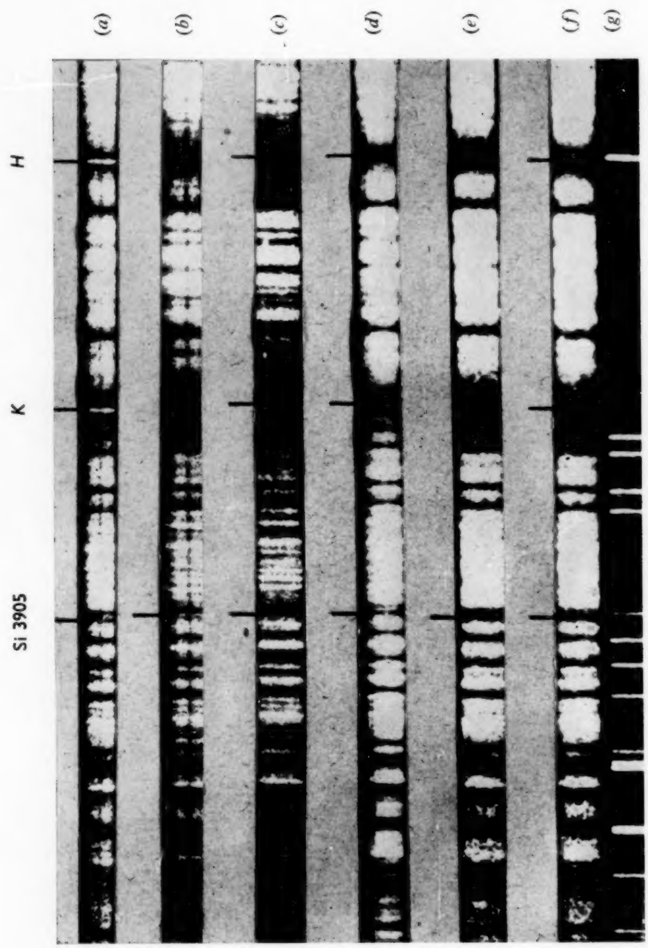

Ca II emission and Si 3905 in K dwarfs and giants.
H and K emission is visible on all original negatives (double in α Tau) except in (e) p Eri A.

(a) ε *Ind* (dK5). (b) α *Tau* (gK5). (c) ε *Peg* (cK0). (d) α *Cen B* (dK1). (e) *p Eri A* (dK2)
(f) *p Eri B* (dK2). (g) *Fe arc.*

Magnification ×21 *original* (a) *to* (d).
×35 *original* (e) *to* (g).

M. W. Feast and A. D. Thackeray, Note on spectra of K-type dwarfs in the region of H and K

NOTE ON SPECTRA OF K-TYPE DWARFS IN THE REGION OF *H* AND *K*

M. W. Feast and A. D. Thackeray

(Received 1954 November 18)

Summary

The line Si 3905 is considerably strengthened in K-type dwarfs compared with giants.

Emission cores to *H* and *K* are recorded on dense exposures as apparently a normal feature in dwarfs of type K2 and later.

The southern stars ϵ Ind ($4^{m}\cdot7$, dK5) and α Cen B ($1^{m}\cdot7$, dK1) have no such bright counterparts among K-type dwarfs in the northern hemisphere. With many bright giants available, their spectra offer the best opportunity for studying absolute magnitude effects at extremes of surface gravity. This note presents two results of interest which have been discovered in the violet region near Ca II *K* on spectra obtained with the two-prism Cassegrain spectrograph attached to the 74-inch Radcliffe reflector.

The line Si 3905.—Comparison of the dwarf ϵ Ind and giant α Tau (both K5) in the region near *K* at a dispersion of 18 A/mm showed immediately one outstanding absolute magnitude effect; the line Si 3905 is considerably stronger in the dwarf (Plate 2*a*, *b*). No other line in the region shows a comparable change, the effect being enhanced by the fact that most lines tend to be somewhat stronger in the giant. The line is well separated from the adjacent line Fe 3906. Wave-lengths measured in the two stars and in a supergiant are as follows:

ϵ Ind (dK5)	α Tau (gK5)	ϵ Peg (cK0)	Identification
3905·51	05·56	05·53	Si I 05·528
3904·78	04·72	04·76	Ti I 04·785
3903·88	03·95	03·84	Fe I 03·900

Microphotometer tracings and visual examination suggest the possible presence of a blending line about 0·2 A to the violet of Si 3905 in the supergiant. We have not been able to identify this feature by consulting laboratory wave-lengths or Miss Davis's measures in β Peg and α Sco (**1**). In ϵ Ind and α Tau at least there is good reason to suppose that the measured line is predominantly due to silicon with negligible blending at the core. Photometric measures of the central intensity of Si 3905 are as follows:

ϵ Ind	α Tau	ϵ Peg
0·233	0·432	0·356

The tracings are unsuitable for measurement of equivalent widths owing to blending in the wings, particularly in the supergiant. Nevertheless it may be

estimated that the ratio of equivalent widths in dwarf and giant is approximately 1·5 : 1. Further measures should be made when coudé dispersion becomes available. The strengthening of Si 3905 is not a peculiarity of ϵ Ind. It has been confirmed in many other dwarfs by visual inspection.

The most complete comparison of spectra of giant (K0) and dwarf (K1) spectra at high dispersion has been undertaken by Miss van Dijke (**2**). It was found in general that the lines below about 2·6 volts E.P. are strengthened in the giant, while lines of higher excitation are strengthened in the dwarf. The present work shows that Si 3905 (E.P. 1·9 volts) clearly violates this empirical rule. No lines due to silicon were included in Miss van Dijke's comparison. Application of Miss van Dijke's values for temperature and pressure in giant and dwarf shows that silicon should be predominantly neutral in both atmospheres; this conclusion should hold good for the cooler stars considered here. The ionization potentials of Si (8·11 eV) and Fe (7·86 eV) are so similar that the marked difference of behaviour of Si 3905 and neighbouring Fe lines of low E.P. constitutes a departure from the predictions of ionization theory on the basis of constant abundances of these elements.

A similar situation exists in the case of Mg 5183 which, as previously shown, is markedly stronger in K dwarfs (**3**).

While this absolute magnitude effect shown by Si 3905 is thus of interest in its bearing on ionization theory, it is not likely to be of practical importance as a luminosity criterion since on low dispersion the line would become severely blended; and, further, it lies in a region of weak radiation. The strengthening of Mg 5183, 5172, 5169 in K dwarfs could however be a useful luminosity criterion on low dispersion.

One possible explanation of the weakness of Si 3905 in giants is that the line may be partly filled in by emission. The line is a prominent emission feature in Me variables and the other lines Fe 4202, 4308, well known as belonging to this category, have been shown by Spitzer (**4**) to have their absorption cores partially filled in by emission in the supergiant α Ori. This explanation can be tested only with higher resolving power than is at present available at the Radcliffe Observatory.

TABLE I

Star	Sp.	M_v	Ca II emission
p Eri A	dK2	6·9	doubtful
p Eri B	dK2	7·0	certain
*ϵ Eri	dK2	6·2	certain
*δ Eri	dK0	3·8	no
*40 Eri A	dK1	6·0	doubtful
γ Lep B	dK3	6·7	certain
λ Vel	cK5		certain
Proxima Cen	dM	15·7	certain
α Cen B	dK1	6·1	certain
HR 7703 A	dK2	6·5	doubtful
*61 Cyg A	dK3	7·7	certain
*61 Cyg B	dK5	8·4	certain
*ϵ Peg	cK0		certain
ϵ Ind	dK5	7·0	certain
*α Tau	gK5		certain

The spectral types and absolute magnitudes of the dwarfs are from Kuiper (*Ap. J.*, **95**, 201, 1942). The Yerkes type for ϵ Peg is K2Ib. The stars marked by an asterisk appear in (**5**).

H and K emission.—It is well known that many late-type stars, dwarfs and giants, show emission cores to the Ca II *H* and *K* lines. In particular, Joy and Wilson (**5**) have listed 445 stars showing such emission lines. The phenomenon becomes increasingly common among the latest types, especially dwarfs. Joy's plates for radial velocity showed that the phenomenon became general at type dM4·5 and later (**6**).

The Radcliffe plates taken to study the behaviour of Si 3905 are sufficiently exposed to show that *H* and *K* emission is a normal feature of dwarfs of type K2 or later. Table I presents our findings concerning Ca II emission in 15 stars.

It is noteworthy that emission was not certainly recorded in p Eri A on the same plate which clearly recorded it in p Eri B, although the two components have practically the same brightness (Plate 2*e*, *f*). Plates of ϵ Ind are available covering two seasons but have not as yet shown any sure signs of variation in the intensity of the emission.

It should be emphasized that the Ca II emission is only recorded by dint of overexposing for the normal region (Hγ to Hδ). Given adequate exposure and resolving power the emission cores could probably be detected in normal stars of still earlier type. By analogy with the Sun the emission probably arises at a chromospheric level.

Radcliffe Observatory,
Pretoria :
1954 *November* 8.

References

(**1**) D. N. Davis, *Ap. J.*, **106,** 28, 1947; *Ap. J.*, **89,** 41, 1939.
(**2**) Suzanne E. A. van Dijke, *Ap. J.*, **104,** 27, 1946.
(**3**) A. D. Thackeray, *M.N.*, **99,** 492, 1939; *M.N.*, **109,** 436, 1949.
(**4**) L. Spitzer, *Ap. J.*, **90,** 494, 1939.
(**5**) A. H. Joy and R. E. Wilson, *Ap. J.*, **109,** 231, 1949.
(**6**) A. H. Joy, *Ap. J.*, **105,** 103, 1947.

ELECTROMAGNETIC FIELD EQUATIONS FOR A MOVING MEDIUM WITH HALL CONDUCTIVITY

J. H. Piddington

(Received 1954 August 17)

Summary

In an isotropically conducting medium the electric field and current density are associated by Ohm's law. This, together with Maxwell's equations, leads to

$$\nabla^2\boldsymbol{H}=4\pi\sigma\left\{\frac{\partial\boldsymbol{H}}{\partial t}-\operatorname{curl}(\boldsymbol{v}\times\boldsymbol{H})\right\}+c^{-2}\frac{\partial^2\boldsymbol{H}}{\partial t^2},$$

where $\boldsymbol{H}$, $\boldsymbol{v}$ and σ are the magnetic field, velocity of the medium and conductivity. This equation describes any electromagnetic field in a moving (or fixed) conductor. It includes the " telegraph equation " of radio waves and also describes any hydromagnetic wave.

Ionized gas in a sufficiently strong magnetic field is anisotropically conducting and σ is replaced by a tensor. An equation analogous to the above is derived for these conditions, allowing the study of electromagnetic disturbances in a medium with Hall conductivity. The equation is used on some simple problems of astrophysical interest, including hydromagnetic waves.

---

1. *Introduction*.—The dynamics of an ionized medium may be studied by considering the *microscopic* motions of individual particles and summing their effects. When a strong magnetic field is present, however, the resulting equations are so complicated as to be insoluble except in some very simple cases.

Numerous more complicated problems are met, particularly in the field of astrophysics, and the most promising approach to these appears to be in the use of "transport equations". These statistically combine individual motions and describe gas movement on a *macroscopic* scale. The transport equation used here is that relating electric current density $\boldsymbol{j}$ to the impressed electric field $\boldsymbol{E}$. In its simplest form, when the conductivity is a scalar quantity σ, when the medium is at rest and when $\boldsymbol{E}$ does not vary rapidly, it is simply Ohm's law

$$\boldsymbol{j}=\sigma\boldsymbol{E}. \qquad (1)$$

When the medium moves with velocity $\boldsymbol{v}$ in the presence of a magnetic field $\boldsymbol{H}$, it takes the form (in electromagnetic units)

$$\boldsymbol{j}=\sigma(\boldsymbol{E}+\boldsymbol{v}\times\boldsymbol{H}). \qquad (2)$$

The current so determined distorts the magnetic field according to the equation

$$\operatorname{curl}\boldsymbol{H}=4\pi\boldsymbol{j}+c^{-2}\frac{\partial\boldsymbol{E}}{\partial t}. \qquad (3)$$

Combining (2) and (3) with Maxwell's other equations

$$\operatorname{curl}\boldsymbol{E}=-\frac{\partial\boldsymbol{H}}{\partial t}\quad\text{and}\quad\operatorname{div}\boldsymbol{H}=0, \qquad (4)$$

an equation is found describing the rates of change of the electro-magnetic (including radiation) field

$$\nabla^2 \boldsymbol{H} = 4\pi\sigma\left\{\frac{\partial \boldsymbol{H}}{\partial t} - \operatorname{curl}(\boldsymbol{v}\times\boldsymbol{H})\right\} + c^{-2}\frac{\partial^2 \boldsymbol{H}}{\partial t^2}. \tag{5}$$

This well-known equation, or one of its simpler forms, is the key to a wide range of problems which fall into two categories. (*a*)—When $\boldsymbol{v}$ is zero or has prescribed values which are independent of the electromagnetic field, if the last term is important it becomes the telegraph equation describing radio waves in conductors which are fixed or moving in a known manner; if the last term is negligible it describes the diffusion of a magnetic field in a rigid conducting medium. (*b*)—When $\boldsymbol{v}$ depends appreciably on the electromagnetic field, the current $\boldsymbol{j}$, as well as influencing the field, also causes a mechanical reaction $\boldsymbol{j}\times\boldsymbol{H}$ on the medium which appears in the hydrodynamic equations. These, together with equation (5), then describe any magneto-hydrodynamic (or hydromagnetic) phenomenon including the type of wave motion first investigated by Alfvén.

Unfortunately this relatively simple situation does not obtain when the magnetic field becomes so powerful that the radius of gyration of the conducting electrons or ions is of the same order as (or smaller than) their mean collision distance. The medium becomes anisotropic, the conductivity being a tensor, and equation (1) is replaced by

$$\boldsymbol{j} = \sigma_0 \boldsymbol{E}_{\parallel} + \sigma_1 \boldsymbol{E}_{\perp} + \sigma_2 \boldsymbol{H}\times\frac{E_{\perp}}{H}, \tag{6}$$

where $\boldsymbol{E}_{\parallel}$ and $\boldsymbol{E}_{\perp}$ are the components of $\boldsymbol{E}$ parallel and perpendicular to $\boldsymbol{H}$. The conductivities σ_0, σ_1 and σ_2 give rise to current components along $\boldsymbol{H}$, parallel to $\boldsymbol{E}_{\perp}$ and perpendicular to both $\boldsymbol{H}$ and $\boldsymbol{E}_{\perp}$ (Hall current).

As for the simple medium, equation (6) is one of a chain of equations linking $\boldsymbol{j}$, $\boldsymbol{H}$, $\boldsymbol{v}$ and $\boldsymbol{E}$ and, in principle at least, allowing all the variables to be simultaneously determined. One approach to this difficult problem is to neglect the space derivative of the magnetic field caused by the current $\boldsymbol{j}$. Then the induced electric field given by equation (4) and the consequent change in $\boldsymbol{j}$ given by equation (6) are both neglected, thus greatly simplifying the problem. This method, valid of course only under certain conditions, has been used elsewhere (1) to find $\boldsymbol{v}$, $\boldsymbol{j}$ and the internal electric field in a medium subjected to external magnetic, electric and mechanical fields of force. The other approach to the problem which does include consideration of induction effects is to derive an equation analogous to (5) and capable of being used like (5).

In the present paper equation (6) is combined with Maxwell's equations to obtain the electromagnetic field equation for a moving, anisotropically conducting medium. The equation resembles (5) and in many problems reduces to an equally simple and almost identical form.

The results are applied to some astrophysical problems including hydromagnetic waves* for which the rate of dissipation of energy may be determined. The results may also be usefully applied to some non-oscillatory problems.

* In private discussion, Dr D. F. Martyn has reported an investigation of wave motions in parts of the ionosphere where Hall conductivity is important. His results seem in general agreement with those given below, referring to the particular geometrical configuration with which he is concerned.

These include further extension of the magnetic storm theory of Chapman and Ferraro, the movement of sunspot magnetic fields in the chromosphere and corona and perhaps the movement of ionized interstellar gas.

Although the examples all refer to gases, the equations developed are equally applicable to liquids or solids and might, for example, have useful application to semi-conductors in strong magnetic fields.

2. *The electromagnetic field equations of a non-isotropic medium.*—Consider a medium permeated by a steady, homogeneous magnetic field of external origin and strength, H_0, such that the Hall conductivity σ_2 is appreciable compared with σ_1. The variable electromagnetic field also present has a magnetic field component much weaker than H_0 so that the total magnetic field $\boldsymbol{H} \simeq \boldsymbol{H}_0$. It is also assumed that the conductivity components are all constant within the region concerned and that changes in the electromagnetic field are slow enough to allow the use of the transport equation. These restrictions are discussed in Section 3.

Choose a right-handed system of axes with the z axis lying along $\boldsymbol{H}_0$ and use the subscripts x, y and z to define the components of the field along those three axes. It is desirable here to introduce a value of conductivity defined by the identity $\sigma_3 \equiv (\sigma_1 + \sigma_2^2/\sigma_1)$; this is discussed in Section 4.

The current components are given by

$$j_x = \sigma_1 F_x - \sigma_2 F_y, \tag{7}$$

$$j_y = \sigma_1 F_y + \sigma_2 F_x, \tag{8}$$

$$j_z = \sigma_0 F_z, \tag{9}$$

where

$$\boldsymbol{F} = \boldsymbol{E} + \boldsymbol{v} \times \boldsymbol{H}. \tag{10}$$

Let us, for the time being, neglect the displacement current term in equation (3) so that

$$\operatorname{curl} \boldsymbol{H} = 4\pi \boldsymbol{j}, \tag{11}$$

from which

$$\nabla^2 \boldsymbol{H} = -4\pi \operatorname{curl} \boldsymbol{j}. \tag{12}$$

The x components of this equation give

$$\begin{aligned} \nabla^2 H_x &= -4\pi \left(\frac{\partial j_z}{\partial y} - \frac{\partial j_y}{\partial z} \right) \\ &= -4\pi \left(\sigma_0 \frac{\partial F_z}{\partial y} - \sigma_1 \frac{\partial F_y}{\partial z} - \sigma_2 \frac{\partial F_x}{\partial z} \right). \end{aligned} \tag{13}$$

Differentiate equation (7) with regard to z, multiply by $4\pi\sigma_2/\sigma_1$ and subtract from (13),

$$\nabla^2 H_x - 4\pi \frac{\sigma_2}{\sigma_1} \frac{\partial j_x}{\partial z} = -4\pi\sigma_3 \left(\frac{\partial F_z}{\partial y} - \frac{\partial F_y}{\partial z} \right) - 4\pi(\sigma_0 - \sigma_3) \frac{\partial F_z}{\partial y}.$$

Using equations (4), (9) and (11) this reduces to

$$\nabla^2 H_x - \frac{\sigma_2}{\sigma_1} \frac{\partial}{\partial z} \operatorname{curl}_x \boldsymbol{H} = 4\pi\sigma_3 \left\{ \frac{\partial H_x}{\partial t} - \operatorname{curl}_x (\boldsymbol{v} \times \boldsymbol{H}) \right\} - \left(1 - \frac{\sigma_3}{\sigma_0} \right) \frac{\partial}{\partial y} \operatorname{curl}_z \boldsymbol{H}. \tag{14}$$

A similar equation in H_y may be derived starting from the y components of equation (12).

Now consider the z components of (12)

$$\nabla^2 H_z = -4\pi\left(\sigma_1 \frac{\partial F_y}{\partial x} + \sigma_2 \frac{\partial F_x}{\partial x} - \sigma_1 \frac{\partial F_x}{\partial y} + \sigma_2 \frac{\partial F_y}{\partial y}\right). \tag{15}$$

Differentiate equation (7) with regard to x, (8) with regard to y and add. For the relatively slow changes in the electromagnetic field (see Section 3) the medium remains everywhere neutral, so that $\operatorname{div} \boldsymbol{j} = 0$. Hence we have

$$\sigma_1\left(\frac{\partial F_x}{\partial x} + \frac{\partial F_y}{\partial y}\right) + \sigma_2\left(\frac{\partial F_x}{\partial y} - \frac{\partial F_y}{\partial x}\right) + \frac{\partial j_z}{\partial z} = 0,$$

which, when multiplied by $4\pi\sigma_2/\sigma_1$ and combined with (15) gives

$$\nabla^2 H_z - \frac{\sigma_2}{\sigma_1}\frac{\partial}{\partial z}\operatorname{curl}_z \boldsymbol{H} = 4\pi\sigma_3\left\{\frac{\partial H_z}{\partial t} - \operatorname{curl}_z(\boldsymbol{v} \times \boldsymbol{H})\right\}. \tag{16}$$

Equations (14), (16) and the corresponding one in H_y, together give the full vector equation of the rates of change of the electromagnetic field. Their generality is subject only to the restrictions mentioned above. However, the additional terms to those in equation (5) (space derivatives of the components of $\operatorname{curl} \boldsymbol{H}$), may add greatly to the difficulty of solving the equation and it is desirable to examine further restrictions which provide simplification.

In the first place, when dealing with a gas for which only electron conductivity is important, $\sigma_3 \simeq \sigma_0$. Such a gas, although it may include substantial proportions of other ions, has the approximate characteristics of the binary gas discussed in Section 4. It is a gas frequently met in astrophysical problems. The equations are simplified for such a gas by omission of the term in $(1 - \sigma_3/\sigma_0)$.

For other types of conductor the same terms are omitted, provided the space derivatives of $\operatorname{curl}_z \boldsymbol{H}$ may be neglected. But $\operatorname{curl}_z \boldsymbol{H}$ indicates a twisting of the magnetic lines of force about the direction of the main part of the magnetic field H_0. Thus the term in question indicates a variation in the xy plane of such a twist. There is no doubt that such effects occur and they may be important, in which case the full equation must be used. In other problems, or for a binary type gas, the field equations reduce to the form

$$\nabla^2 \boldsymbol{H} - \sigma_2/\sigma_1 \frac{\partial}{\partial z}\operatorname{curl} \boldsymbol{H} = 4\pi\sigma_3\left\{\frac{\partial \boldsymbol{H}}{\partial t} - \operatorname{curl}(\boldsymbol{v} \times \boldsymbol{H})\right\}. \tag{17}$$

Finally, for problems where $\partial/\partial z = 0$, that is for disturbances propagated across the magnetic field, the second term in equation (17) may be omitted. When this is done the displacement current term may, if desired, be reintroduced as in equation (5) and we have

$$\nabla^2 \boldsymbol{H} = 4\pi\sigma_3\left\{\frac{\partial \boldsymbol{H}}{\partial t} - \operatorname{curl}(\boldsymbol{v} \times \boldsymbol{H})\right\} + c^{-2}\frac{\partial^2 \boldsymbol{H}}{\partial t^2}. \tag{18}$$

This is of the same form as equation (5), merely having σ_3 substituted for σ, so that problems of this nature have similar solutions to those for an isotropic medium and may be solved by identical procedures. All of the examples given below, admittedly geometrically simple, are solved by the use of equations (17) and (18).

3. *Discussion of the equations.*—A restriction on the use of any of the equations derived above is that the external magnetic field must be steady, homogeneous and large compared with the variable component. This restriction is necessary because the space and time derivatives of the conductivity components have been

neglected. These components depend on the magnitude and direction of the total magnetic field. It is necessary, therefore, that the derivatives of $\boldsymbol{H}/H_0$ should be small compared with the corresponding derivatives of the electromagnetic field components.

Since σ_1 and σ_2 also depend on the density and temperature of the various components of the gas (see Section 4), these must also be stable within the same limits.

These conditions are usually met for oscillatory disturbances, such as hydromagnetic waves of small amplitude or radio waves, because the wave-length is much smaller than the extent of the medium and of the external magnetic field. There is another class of problem, however, in which the gradients of the "external" magnetic field (and perhaps also the gas parameters) are of the same order as those for the electromagnetic field. Such a problem is the large-scale movement of sunspot magnetic fields and their associated gas in the corona. The magnetic field is no longer external but part of the variable electromagnetic field. The equations of Section 2 are not applicable to these problems. Fortunately, however, most such problems met in astrophysics are concerned with a gas in which only electron conductivity is important (see Section 4). For such gases σ_3 depends *only* on gas temperature and if this can be assumed uniform then many problems may be solved as shown in Section 7.

The values of σ_1 and σ_2 are derived on the assumption that the imposed electric and magnetic fields do not vary appreciably in a time necessary to provide a good statistical average of the ion motions. When equation (1) is relevant the time concerned is large compared with the ion collision periods. When the ions and electrons complete one or more rotations in the magnetic field between each collision it is the gyro-period which determines the averaging time necessary. The latter must be long compared with the gyro-period of each ion which contributes appreciably to the conductivity. In the case of a lightly ionized gas (see following section) both electrons and heavy ions may contribute to the conductivity, so that the time must be long compared with the gyro-period of the latter. In a binary gas only electrons contribute appreciably to the conductivity, so that their gyro-period is the deciding factor.

In very tenuous gases another effect may be important in limiting permissible rates of change of the variables. In deriving equation (16) it was assumed that $\operatorname{div}\boldsymbol{j}=0$, which is not strictly true. Disturbances (let us call them waves) propagated across or obliquely to the magnetic field are associated with plasma waves. While the latter may be important and their electric fields substantial, the current required to maintain them is usually insignificant, in fact comparable with displacement current. In the present paper this is assumed so, but criteria for determining the effect of the plasma wave current are given in a paper in preparation.

4. *The conductivity.*—The most complete and detailed account of the derivation of conductivity (and other) transport equations from the Boltzmann equations of gas mixtures is given by Chapman and Cowling (**2**) and Cowling (**3**). With their values of σ_1 and σ_2 the value of σ_3 is found from the identity given in Section 2. Its physical significance was first pointed out by Cowling (**4**)*, who

* While Cowling's proof was not restricted, his paper dealt with a heavily ionized gas. The significance of σ_3 in the case of a lightly ionized gas (when $\sigma_3 \neq \sigma_0$) may first have been realized by Baker and Martyn (**5**).

showed that when Hall current is prevented from flowing, then the conductivity parallel to $\boldsymbol{E}_\perp$ becomes σ_3 instead of σ_1.

For convenience the formulae for σ_0, σ_1, σ_2 and σ_3 for a binary gas and a lightly ionized gas have been summarized in reference (**1**). In general they all depend on the number density of the gas components, on the gas temperature and on H_0, but in the case of a binary gas $\sigma_3 = \sigma_0$ and depends only on gas temperature. This important result is used in Section 7.

In Table I a list of conductivity components is given for some regions of astrophysical interest specified by the electron density n_e and gas temperature T. In interstellar space and most of the solar atmosphere the binary gas formulae

TABLE I

Conductivities in some regions of astrophysical interest

Gas parameters	Region					
	Interstellar H I region	Interstellar H II region	Solar corona	Solar chromosphere	Ionospheric region E (100 km)	Ionospheric region F2
n_e	10^{-2}	10	10^{8}	3×10^{9}	10^{5}	10^{6}
T	100	10^{4}	10^{6}	2×10^{4}	300	10^{3}
H_0	10^{-5}	10^{-3}	30	100	$0{\cdot}3$	$0{\cdot}3$
σ_0	6×10^{-12}	6×10^{-9}	6×10^{-6}	3×10^{-8}	1×10^{-13}	$> 10^{-11}$
σ_1	5×10^{-23}	5×10^{-24}	6×10^{-22}	7×10^{-18}	2×10^{-16}	3×10^{-16}
σ_2	2×10^{-17}	2×10^{-16}	6×10^{-14}	4×10^{-13}	3×10^{-15}	$\ll 10^{-16}$
σ_3	6×10^{-12}	6×10^{-9}	6×10^{-6}	3×10^{-8}	6×10^{-14}	3×10^{-16}

hold closely enough and in the magnetic fields given we have $\sigma_3(=\sigma_0) \gg \sigma_2 \gg \sigma_1$. This means that when equation (18) is applicable the results are the same as for an isotropically conducting medium of conductivity σ_0; that is, the same medium in the absence of a magnetic field. Also the "effective" conductivity σ_3 is much larger than either σ_1 or σ_2. As the value of H_0 is reduced so that the electron gyro-frequency approaches the collision frequency, σ_1 increases continuously and σ_2 increases to a maximum and then decreases. When gyro-angular frequency and collision frequency are equal, $\sigma_2 = \sigma_1$ and $\sigma_3 = 2\sigma_1$; also σ_2 has its maximum value. In yet weaker magnetic fields σ_2/σ_1 becomes small and the main contribution to $\sigma_3 = \sigma_0$ is made by σ_1.

The position is different for a lightly ionized gas, as shown in the last two columns of Table I, calculated by Baker and Martyn (**5**). When the gyro-frequency is large compared with the collision frequency (F2 region), $\sigma_2 \ll \sigma_1 \ll \sigma_0$, so that $\sigma_3 \sim \sigma_1$. This marked difference in the behaviour of tenuous binary and lightly ionized gases is discussed in reference (**1**). For the latter, equation (6) loses its last term and equations (14), (16) and (17) are simplified by losing the terms in σ_2/σ_1.

In the following sections the equations of Section 2 and the data of Table I are used to discuss some problems of electrodynamic disturbances. Such disturbances occur whenever the electromagnetic field and forces acting on

the gas are not in equilibrium, either static or dynamic. They may be roughly divided into small-scale and large-scale disturbances, referring to the extent and not the violence of the disturbance. A small-scale disturbance is one in which the main variations in the electromagnetic field occur in regions small compared with the total extent of the gas and of the steady magnetic field. Hydromagnetic waves usually fall into this category. A large-scale disturbance extends throughout a substantial portion of the magnetic field which now cannot truly be described as either "external" or "steady". The additional difficulties met in such problems are discussed in Section 7.

5. *Disturbances propagated along the magnetic field.*—Consider a transverse, plane wave (either a single disturbance or train of waves) propagated along the magnetic field $\boldsymbol{H}_0$; that is, along the z axis. Then, since $\partial/\partial x = \partial/\partial y = 0$, equation (17) may be used. Neglecting second-order terms the x and y components become

$$s\frac{\partial^2 H_x}{\partial z^2} = \frac{\partial H_x}{\partial t} - H_0\frac{\partial v_x}{\partial z} - \frac{s\sigma_2}{\sigma_1}\frac{\partial^2 H_y}{\partial z^2}, \tag{19}$$

$$s\frac{\partial^2 H_y}{\partial z^2} = \frac{\partial H_y}{\partial t} - H_0\frac{\partial v_y}{\partial z} + \frac{s\sigma_2}{\sigma_1}\frac{\partial^2 H_x}{\partial z^2}. \tag{20}$$

When the conducting medium does not move ($v_x = v_y = 0$), because of adequate rigidity or inertia, the equations reduce to a modified "telegraph equation". For oscillatory disturbances they indicate two waves, circularly polarized in opposite senses. The dispersion equation for solutions of the form $\exp i(pt - kx)$ is

$$\frac{k^2}{p^2} = \frac{4\pi\sigma_3}{p(\pm\sigma_2/\sigma_1 + i)}.$$

This equation should show agreement with the corresponding magneto-ionic equation. Substituting values for the conductivities of a gas having only appreciable electron conductivity (the ions are assumed immobile),

$$\frac{k^2c^2}{p^2} = \frac{-4\pi n_e e^2 c^2}{mp(\mp\omega + i/\tau)},$$

where e, m, ω and τ are the electron charge (e.m.u.), mass, gyro-magnetic frequency and collision period and the other terms have been defined. Agreement is shown with the magneto-ionic theory except for the omission of two terms on the r.h.s. A term unity is missing due to the neglect of the displacement current and a term p inside the brackets is missing because p has been assumed negligibly small compared with ω. The effect of displacement current is not that described in Section 3 above, which occurs only when the gas is compressed (oblique or transverse propagation); it is usually negligible even for frequencies approaching the ion gyro-frequency.

When the medium is moved by the electromagnetic forces, hydromagnetic waves of the kind first investigated by Alfvén (**6**) may occur. Neglecting compression the equations of motion of the medium are

$$\frac{\partial v_x}{\partial t} = \frac{V^2}{H_0}\frac{\partial H_x}{\partial z} \quad \text{and} \quad \frac{\partial v_y}{\partial t} = \frac{V^2}{H_0}\frac{\partial H_y}{\partial z},$$

where $V^2 = H_0^2/4\pi\rho$ and ρ is the mass density. Solving with equations (19) and (20) two hydromagnetic waves are found, circularly polarized in opposite directions. The dispersion equation is

$$\frac{k^2}{p^2} = \left(V^2 \pm \frac{\sigma_2 p}{4\pi\sigma_1\sigma_3} + \frac{ip}{4\pi\sigma_3}\right)^{-1}.$$

In the case of a binary gas (to which the solar corona approximates closely enough) the ratio of the first two terms within the brackets is Ω/p, where Ω is the heavy-ion gyromagnetic frequency. Hence the ratio is very large and the two waves have nearly equal velocities $V \pm \sigma_2 p/8\pi\sigma_1\sigma_3 V$ or $V \pm H_0/4\lambda n_e e$, where λ is the wave-length. The polarization and velocity of these waves are the same as those given previously by Cowling (reference (**9**), p. 582).

In the case of a lightly ionized gas the velocities may differ widely and when $V^2 < \sigma_2 p/4\pi\sigma_1\sigma_3$ one wave will not be propagated. It should be noted that such waves require that each *neutral* molecule should experience many collisions in one wave period. If many wave periods occur within the collision period of a neutral molecule then the hydromagnetic waves are propagated in the electron–ion plasma and not in the gas as a whole.

In all cases the absorption coefficient is $p^2/8\pi\sigma_3 V$, thus depending only on σ_3 among the conductivities.

This result is of considerable significance in astrophysics. It was previously often assumed that σ_1 was the conductivity mainly effective in determining the losses sustained by a hydromagnetic wave.* It is evident from Table I that σ_3 is often very much larger (by factors up to 10^{16}) than σ_1. Even had σ_2 been taken as the relevant conductivity, the error would still be very large. To illustrate this point we refer to a theory of Alfvén (**8**) concerning the propagation of hydromagnetic waves from the solar photosphere to the corona. According to Alfvén such waves would be absorbed in the corona, their energy then being available to maintain the observed high coronal temperature. However, in calculating the absorption coefficient, Alfvén neglects Hall conductivity and assumes σ_1 to be the determining conductivity. For the conditions he assumes (similar to those in Table I) $\sigma_1 \simeq 6\times 10^{-22}$ e.m.u. while $\sigma_3 \simeq 6\times 10^{-6}$ e.m.u. Hence the rate of absorption is overestimated by a factor of $\sim 10^{16}$, the true rate being negligible. This conclusion was anticipated by Cowling (**9**) who pointed out that the Joule loss, which depends on collisions, could not be increased by the presence of a magnetic field.

6. *Disturbances propagated across the magnetic field.*—Consider a plane electromagnetic–hydrodynamic disturbance (including the case of a train of waves) to be propagated across the magnetic field $\boldsymbol{H}_0$, say along the x axis, so that $\partial/\partial y = \partial/\partial z = 0$. Such a disturbance is satisfactorily described by equation (16), which is simplified because the term in $\partial/\partial z \,\mathrm{curl}_z \boldsymbol{H}$ is zero. Also

$$\mathrm{curl}_z(\boldsymbol{v}\times\boldsymbol{H}) = -H_0\,(\partial v_x/\partial x),$$

so that the equation becomes

$$s\frac{\partial^2 H_z}{\partial x^2} = \frac{\partial H_z}{\partial t} + H_0\frac{\partial v_x}{\partial x}. \tag{21}$$

* Schluter (**7**), studying binary gas by a combination of microscopic and macroscopic methods, concluded that σ_0 was the relevant conductivity.

This equation describes any electromagnetic disturbance in an anisotropically conducting medium propagated across the magnetic field and subject to the restrictions of Section 3. It includes the telegraph equation and the equation of hydromagnetic waves. Again σ_3, rather than σ_1, is the conductivity which determines the rate of dissipation of energy.

In order to study the disturbance represented by equation (21) a second relationship between v_x and H_z is required and this is provided by the hydrodynamical equations of momentum and continuity and the gas equation. These are

$$\rho\frac{\partial v_x}{\partial t}+\rho v_x\frac{\partial v_x}{\partial x}+\frac{\partial\theta}{\partial x}=-\frac{H_0}{4\pi}\frac{\partial H_z}{\partial x},$$

$$\frac{\partial}{\partial x}(\rho v_x)+\frac{\partial\rho}{\partial t}=0,$$

$$\theta=f(\rho, T),$$

where θ is the gas pressure, being a function of density and temperature. In general the equations are intractable, but for vanishingly small waves $\partial/\partial t \gg v(\partial/\partial x)$ and $f=\text{const.}\,\rho^\gamma$, where γ is the ratio of specific heats. The three hydrodynamic equations then combine to give

$$\frac{\partial^2 v_x}{\partial t^2}-U^2\frac{\partial^2 v_x}{\partial x^2}+\frac{V^2}{2H_0^2}\frac{\partial^2(H_z^2)}{\partial x\,\partial t}=0, \tag{22}$$

where $U^2=\partial\theta/\partial\rho$ is the square of the velocity of sound waves in the gas (in the absence of a magnetic field). Equations (21) and (22) may be solved simultaneously by assuming a solution of the form $\exp i(pt-kx)$. The dispersion equation is

$$k^4-k^2\left\{p^2/U^2-\frac{ip(U^2+V^2)}{sU^2}\right\}-\frac{ip^3}{sU^2}=0. \tag{23}$$

This equation, not previously derived, allows the study of small transverse hydromagnetic waves in an anisotropically conducting medium. It cannot be compared directly with the corresponding magneto-ionic equation unless it is assumed that $p \ll 4\pi\sigma_1 c^2$. This is due to the effect of displacement current discussed in Section 3. It may be compared with an equation due to Anderson (**10**), derived for an isotropically conducting gas. The only difference is in the value of s which, for a scalar conductivity σ, is $(4\pi\sigma)^{-1}$.

For permissible waves in the gases of Table I (wave-length $\gg$ 1 cm) we have

$$\frac{p(U^2+V^2)}{sU^2}\gg\frac{p^2}{U^2}>\frac{p^3}{sU^2}.$$

The roots of equation (23) are given approximately by

$$k^2=\frac{p^2}{U^2}-\frac{ip(U^2+V^2)}{sU^2}\quad\text{and}\quad k^2=\frac{p^2}{(U^2+V^2)+isp}.$$

The first pair of waves are rapidly damped, the second pair give

$$k=\frac{\pm p}{(U^2+V^2)^{1/2}}\left\{1-\frac{ips}{2(U^2+V^2)}\right\}.$$

This comprises a pair of waves travelling in opposite directions with velocity $(U^2+V^2)^{1/2}$ and absorption coefficient $p^2s/2(U^2+V^2)^{3/2}$. Because the damping has here been assumed small, the expression for the velocity is the same as that

previously determined (**11, 12**) for a perfectly conducting gas. If the damping is large then the velocity will depart from this value.

It is of interest to calculate the rates of attenuation of hydromagnetic waves propagated across the magnetic field for some gases of Table I. In each case the wave frequency is chosen to be as large as possible but still an order of magnitude less than the ion gyro-frequency. In the chromosphere the latter (for protons) is $\sim 10^6$ rad. sec^{-1}, so that a wave of frequency 10^5 rad. sec^{-1} is considered. Its velocity, mainly due to the resilience of the magnetic field ($V \gg U$), is 4×10^8 cm sec^{-1} and it diminishes by a factor $\exp(-1)$ in a distance of about 5×10^4 km or 2×10^5 wave-lengths. Observe that the wave may be propagated only because of the high value of σ_3 and would be damped within a wave-length if it depended on σ_1. Waves of lower frequency will suffer less damping. Waves propagated in the corona will not be damped appreciably in distances large compared with the linear dimensions of the corona.

In the region listed in Table I as interstellar H II, the proton angular gyro-frequency is about 10 rad. sec^{-1}, so that hydromagnetic waves of the type described by equation (23) might have frequencies as high as, say, 1 rad. sec^{-1} (wave-length ~ 4000 km). Such waves would travel about 0·01 parsec before being attenuated by a factor $\exp(-1)$.

Hydromagnetic waves of length short compared with the thickness of ionospheric E or F layers are damped too heavily to allow propagation at all. Longer waves introduce boundary problems with which we have not concerned ourselves here.

7. *Large-scale disturbances.*—A typical large-scale disturbance (according to our definition) occurs when a sunspot magnetic field and its associated gas enters the solar atmosphere. Here the gradients in the electromagnetic field parameters have the same order of magnitude as those of the total magnetic field and of the gas parameters. Hence one of the restrictions listed in Section 3 is not satisfied and the equations are not valid. Another difficulty usually met in these problems is the complicated geometry of the system of magnetic fields and gas distribution. These difficulties are usually insuperable, but an insight into the probable outcome of the disturbances may often be made by assuming a simplified geometry. This method was used with considerable success by Chapman and Ferraro (**13**) in their investigation of a complicated large-scale disturbance: the initiation of a geomagnetic storm by a jet of solar gas.

Let us first consider the simplest possible geometrical configuration of a disturbance, in which the electromagnetic and gas parameters vary in only one direction. Let this be perpendicular to the magnetic field, say along the x axis. It is sufficient to consider the z component of equation (12): $\nabla^2 H_z = -4\pi \,\mathrm{curl}_z \boldsymbol{j}$. Since $\partial/\partial y = \partial/\partial z = 0$ this reduces to (writing H for H_z)

$$\frac{\partial^2 H}{\partial x^2} = -4\pi \frac{\partial j_y}{\partial x}. \tag{24}$$

Now $\mathrm{curl}_x \boldsymbol{H}$ is zero and hence j_x is zero and equation (7) gives $F_x = (\sigma_2/\sigma_1) F_y$. Substituting in equation (8) we have

$$j_y = \sigma_3 F_y,$$

which, with equation (24), gives

$$\frac{\partial^2 H}{\partial x^2} = -4\pi \frac{\partial}{\partial x}(\sigma_3 F_y). \tag{25}$$

In the case of a lightly ionized gas the space derivatives of σ_3 may be important, in which case a solution may be difficult or impossible to obtain. However, in most problems of astrophysical interest, the gas may be considered a binary gas and σ_3 depends only on its temperature. Assuming isothermal conditions, equation (25) reduces to the well-known form

$$\frac{\partial^2 H}{\partial x^2} = 4\pi\sigma_3 \left\{ \frac{\partial H}{\partial t} + \frac{\partial}{\partial x}(v_x H) \right\}. \tag{26}$$

The result indicates that transverse disturbances in an isothermal binary gas show induction effects depending only on the gas temperature. The value of the total magnetic field at any time and place, although it determines σ_1 and σ_2, does not affect the rate of diffusion of the electromagnetic field. It does, however, cause a physical effect not shown in equation (26) but discussed elsewhere (**1, 14**). The gas does not move across the magnetic field in the direction of the mechanical force causing its motion, but at an angle $\tan^{-1}\sigma_2/\sigma_1$ to this force. Thus, while the motion of the gas is determined by the magnetic field strength, the "motion" of the electromagnetic field is not affected.

The next simplest type of disturbance after a plane wave is a cylindrical wave, the magnetic field being parallel to the axis of symmetry. This will not be considered separately but as a special case of a more complex system in which the magnetic field varies in direction as well as intensity. The restriction imposed is that the magnetic field is symmetrical about an axis (say the z axis) and the lines of force all lie in planes through Oz. Such fields include those of dipoles, uniformly magnetized spheres and, with sufficient accuracy for illustrative purposes, sunspot and stellar fields. The mechanical forces associated with such fields will also be symmetrical and lie in planes through Oz. The electric currents will flow in circles with centres on Oz and lying in planes perpendicular to Oz, so that the force $\boldsymbol{j} \times \boldsymbol{H}$ is everywhere in the meridian plane and perpendicular to $\boldsymbol{H}$. There can be no accumulation of electric charge and hence no boundary effects caused by such accumulation.

It is evident that the above electromagnetic field violates the first restriction applying to the equations of Section 2. The magnetic field varies not only in strength but in direction from place to place. Fresh equations must be derived which satisfy the new conditions. It will be assumed, as before, that the space derivatives of σ_3 may be neglected.

It is convenient to use cylindrical coordinates $x = r\cos\alpha$, $y = r\sin\alpha$ and $z = z$, the z axis being so directed that α increases by clockwise rotation when observed along Oz. In these axes we have assumed

$$H_\alpha = \frac{\partial}{\partial \alpha} = j_r = j_z = 0,$$

so that only the α component of equation (3) need be considered. Let us define new components of current and electric force $j_\perp$ and $F_\perp$, perpendicular to $\boldsymbol{H}$ and lying in planes through Oz. Obviously $j_\perp$ is zero and $F_\perp$ and F_α are the only components of electric force, so that equation (6) takes the form

$$j_\alpha = \sigma_1 F_\alpha - \sigma_2 F_\perp,$$
$$0 = \sigma_1 F_\perp + \sigma_2 F_\alpha,$$

from which $j_\alpha = \sigma_3 F_\alpha$. With equation (3) (neglecting displacement current) this gives

$$\frac{\partial H_r}{\partial z} - \frac{\partial H_z}{\partial r} = 4\pi\sigma_3 F_\alpha. \tag{27}$$

Multiply both sides by r and differentiate with regard to r:

$$\frac{\partial}{\partial r}\left(r\frac{\partial H_r}{\partial z} - r\frac{\partial H_z}{\partial r}\right) = 4\pi\sigma_3 \frac{\partial}{\partial r}(rF_\alpha)$$

$$= 4\pi\sigma_3 r \operatorname{curl}_z \boldsymbol{F}.$$

Together with equations (10) and (14) this gives

$$\frac{\partial}{\partial r}\left(r\frac{\partial H_z}{\partial r} - r\frac{\partial H_r}{\partial z}\right) = 4\pi\sigma_3\left\{r\frac{\partial H_z}{\partial t} + \frac{\partial}{\partial r}(rv_r H_z - rv_z H_r)\right\}. \tag{28}$$

This equation (apart from the omitted displacement current term) is simply one of the component equations of equation (18). The second may be similarly derived by differentiating equation (27) with regard to z and proceeding as before; it is

$$\frac{\partial}{\partial z}\left(\frac{\partial H_z}{\partial r} - \frac{\partial H_r}{\partial z}\right) = 4\pi\sigma_3\left\{\frac{\partial H_r}{\partial t} + \frac{\partial}{\partial z}(v_z H_r - v_r H_z)\right\}.$$

Thus for the much more complex magnetic field system we have

$$\nabla^2 \boldsymbol{H} = 4\pi\sigma_0\left\{\frac{\partial H}{\partial t} - \operatorname{curl}(\boldsymbol{v}\times\boldsymbol{H})\right\}. \tag{29}$$

Only the meridian plane components of this equation are applicable, but these are sufficient for the solution of many problems. In such cases the gas behaves, as far as electrical induction effects are concerned, as though the gas were entirely unaffected by the presence of the magnetic field, its conductivity remaining σ_0.

A special case of the above configuration of magnetic field occurs when the magnetic field is everywhere parallel to the axis Oz and conditions are uniform along Oz. The electromagnetic field is sufficiently well described by equation (28), which simplifies to

$$\frac{\partial}{\partial r}\left(r\frac{\partial H}{\partial r}\right) = 4\pi\sigma_3\left\{r\frac{\partial H}{\partial t} + \frac{\partial}{\partial r}(rv_r H)\right\},$$

where H is now written for H_z.

These results, summarized in equation (29), will only be applied to one relatively simple problem: the degree to which solar and interstellar magnetic fields are "frozen into" the conducting gas. The degree is generally assumed to be very high, although the reason is not clear. In fact, if the Hall conductivity is neglected, the assumption is usually not justified.

When the meridian plane component of $\boldsymbol{v}$ vanishes, the meridian plane component of equation (29) reduces to $\nabla^2\boldsymbol{H} = 4\pi\sigma_3(\partial\boldsymbol{H}/\partial t)$. Cowling (**15**) has derived a similar equation relating to the decay of a sunspot field at photospheric levels where σ_2 may be neglected, so that $\sigma_3 = \sigma_0 = \sigma_1 = \sigma$. He points out that the time of decay is of the order σl^2, where l is the radius of the spot field. For a field of radius 10^9 cm and $\sigma = 10^{-8}$ e.m.u., the time is about 300 years, so that the field is effectively frozen in. If Hall conductivity were negligible in the chromosphere and corona (as at lower levels) the times of decay of fields of similar dimensions would be of the order 7 sec and 0·005 sec respectively.

The much shorter times are due to the greatly reduced value of σ_1 ($=\sigma_3$ when Hall current is neglected) at these higher levels. The effect of Hall current is to increase these times to about 10^3 years and 2×10^5 years respectively. It should be noted that the increase is much greater than if σ_2 itself replaced σ_1 in equation (29).

For interstellar H II regions (as in Table I) a field of dimensions (say) 10^{-3} parsecs would have decay times of about 1 year and 10^{15} years depending on the absence or presence of Hall conductivity. The time remains at 10^{15} years even if Hall current is prevented from flowing, for the direct conductivity then rises from σ_1 to σ_3. It is evident that the magnetic fields concerned are frozen in mainly because of Hall conductivity.

The problem of axially symmetric poloidal fields with Hall conductivity has been considered previously by Ferraro and Unthank (**16**) and by Sweet (**17**).

Acknowledgments.—I should like to thank Dr J. A. Roberts, Dr D. F. Martyn and Mr W. L. Price for helpful discussions and the former for help with the manuscript.

Division of Radiophysics,
Commonwealth Scientific and Industrial Research Organization,
Sydney, Australia :
1954 *August.*

References

(1) Piddington, J. H., *M.N.*, **114**, 651, 1954.
(2) Chapman, S. and Cowling, T. G., *The mathematical theory of non-uniform gases*, Cambridge, 1939.
(3) Cowling, T. G., *Proc. Roy. Soc.* A, **183**, 453, 1945.
(4) Cowling, T. G., *M.N.*, **93**, 90, 1933.
(5) Baker, W. G. and Martyn, D. F., *Phil. Trans.* A, **246**, 36, 1953.
(6) Alfvén, H., *Cosmical electrodynamics*, Oxford, 1950.
(7) Schlüter, A., *Zeit. f. Naturforsch.*, **5A**, 72, 1950.
(8) Alfvén, H., *M.N.*, **107**, 209, 1947.
(9) Cowling, T. G., *The Solar System : vol.* 1, *The Sun*, edited by G. P. Kuiper, Chicago University Press, 1953.
(10) Anderson, N. S., *J. Acoust. Soc. Amer.*, **25**, 529, 1953.
(11) Herlofson, N., *Nature*, **165**, 1020, 1950.
(12) de Hoffman, F. and Teller, E., *Phys. Rev.*, **80**, 692, 1950.
(13) Chapman, S. and Ferraro, V. C. A., *Terr. Mag.*, **45**, 245, 1940.
(14) Piddington, J. H., *M.N.*, **113**, 188, 1953.
(15) Cowling, T. G., *M.N.*, **106**, 218, 1946.
(16) Ferraro, V. C. A. and Unthank, H. W., *M.N.*, **109**, 462, 1949.
(17) Sweet, P. A., *M.N.*, **109**, 507, 1949.

THE MOTION OF IONIZED GAS IN COMBINED MAGNETIC, ELECTRIC AND MECHANICAL FIELDS OF FORCE

J. H. Piddington

(Received 1954 September 13)

Summary

Transient electric and mechanical forces uniform in space are applied to a gas in the presence of a steady magnetic field. The current transport equation for the anisotropically conducting medium is used to determine the subsequent motion of the gas, the internal electric field and the current density. These are damped oscillatory functions leading to a steady state.

There is a close connection between the effects of the electric and mechanical forces: a steady internal electric field perpendicular to the magnetic field cannot exist unless accompanied by a mechanical force. The relationship between the two is examined. Neglect of this relationship has already proved fatal to many astrophysical theories. On the other hand, there seems little justification for treating mechanical forces as " equivalent electric fields ", as is often done.

This and a companion paper appear to provide, for the first time, a satisfactory system for using transport equations in the study of dynamical problems in nearly uniform, anisotropically conducting gases. Such problems are proving increasingly numerous and important in astrophysics.

---

1. *Introduction.*—The motion of ionized gas in fields of force may be studied by summing individual ion motions or by the use of transport equations. The latter method has many advantages and is used here.

The transport equation of interest is the relationship between an applied electric field represented by the vector $\boldsymbol{E}'$ and the resulting current density $\boldsymbol{j}$. In an isotropically conducting medium and for slow changes in $\boldsymbol{E}'$ this is simply Ohm's law. When a magnetic field $\boldsymbol{H}$ is present it takes the form:

$$\boldsymbol{j}=\sigma_0\boldsymbol{E}'_{\parallel}+\sigma_1\boldsymbol{E}'_{\perp}+\sigma_2\boldsymbol{H}\times\boldsymbol{E}'_{\perp}/H, \tag{1}$$

where $\boldsymbol{E}'_{\parallel}$ and $\boldsymbol{E}'_{\perp}$ are the components of $\boldsymbol{E}'$ parallel and perpendicular to $\boldsymbol{H}$ and σ_0, σ_1 and σ_2 are the the components of the conductivity tensor. The current component $\sigma_0\boldsymbol{E}'_{\parallel}$ is not influenced by the presence of the magnetic field and it provides no mechanical reaction on the gas. Without loss of generality it is neglected in the present paper. The other current components are the " direct " and Hall currents in that order.

The current given by equation (1) causes a whole chain of associated events: first a distortion of the magnetic field according to the equation:

$$\text{curl}\ \boldsymbol{H}=4\pi\boldsymbol{j}. \tag{2}$$

Electromagnetic units are used throughout and the displacement current neglected. The current also provides a mechanical reaction $\boldsymbol{j}\times\boldsymbol{H}$ on the gas and this, with hydrodynamic parameters, determines the gas velocity $\boldsymbol{v}$. The distortion of the magnetic field and the gas movement in their turn help determine $\boldsymbol{E}'$, which is the electric field *experienced by the gas:*

$$\boldsymbol{E}'=\boldsymbol{E}+\boldsymbol{E}_i+\boldsymbol{v}\times\boldsymbol{H}. \tag{3}$$

Here $\boldsymbol{E}$ is a potential field due to a distribution of external electric charge, $\boldsymbol{E}_i$ is an induction field due to changes in the distribution of $\boldsymbol{H}$ and the last term is the electric force per unit charge due to movement of the gas. The parameters $\boldsymbol{j}$, $\boldsymbol{H}$, $\boldsymbol{v}$ and $\boldsymbol{E}'$ are thus linked in a complete chain of cause and effect; for example, a steady electric field $\boldsymbol{E}'$ cannot be maintained in an ionized gas unless accompanied by a mechanical force of appropriate magnitude and direction.

Failure to consider every link in this chain has proved disastrous for many astrophysical theories, some of which have been discussed (1) already.

Although in principle $\boldsymbol{j}$, $\boldsymbol{H}$, $\boldsymbol{v}$ and $\boldsymbol{E}'$ may be determined simultaneously, this is often difficult or impossible. The problem may be greatly simplified, while reality is still retained, by neglecting the effect of $\boldsymbol{j}$ on the magnetic field. In a separate paper (2) this effect is discussed, but at present it is neglected so that equation (3) reduces to

$$\boldsymbol{E}' = \boldsymbol{E} + \boldsymbol{v} \times \boldsymbol{H}. \tag{4}$$

This procedure has been used by Cowling (3, 4) in studying the motion of solar gas across a magnetic field. The results only apply when dealing with regions with linear dimensions small compared with $H/4\pi j$. In larger regions induction shielding is effective.

The values of $\boldsymbol{v}$, $\boldsymbol{j}$ and $\boldsymbol{E}'$ are determined for a gas in combined magnetic, electric and mechanical fields of force. A transient treatment is used so that conditions prior to the steady state may be studied. The results are discussed in connection with different types of ionized gas which show marked and, at first sight, surprising differences in dynamical properties. The similarity between the effects of mechanical and electric forces applied to an ionized gas have led some workers to treat the former as " equivalent electric fields " (see reference (4) for example). This approach has led to some confusion and seems neither necessary nor desirable.

This paper and its companion (2) appear to provide, for the first time, a complete and self-consistent system for using transport equations to study dynamical problems in nearly uniform, anisotropically conducting gas. Such problems are profuse in the field of astrophysics. Most of the groundwork was already available, of course, due in very large part to Cowling (3, 4, 5). The required degree of uniformity of the gas is discussed in the companion paper and below; departure from uniformity may introduce boundary problems, which will be discussed elsewhere.

2. *The motion of ionized gas in a steady magnetic field and transient electric and mechanical fields.*—Consider a uniform ionized gas permeated by a steady, homogeneous magnetic field of strength H. We confine our attention to electrical and mechanical fields and motions perpendicular to H. Take rectangular right-handed coordinates with the z axis parallel to the magnetic field. At time $t=0$ apply an external (potential) electric field with components E_x and E_y and also a mechanical force F dynes cm^{-3} along Ox. This constitutes the most general arrangement of (uniform) fields of force.

A transient treatment is necessary to study conditions prior to the steady state; this study is necessary for a full understanding of the gas dynamics involved. It might well be asked whether there is any physical significance in the transient treatment. This is because of the statistical nature of σ_1 and σ_2 which do not determine the current at an instant but only over a period long enough to average

random-ion motions. The question is answered in Section 5 where it is shown that the treatment is permissible provided time $t=0$ really represents a short *interval* of time commencing slightly after the application of the electric field.

At time t the gas velocity components are v_x and v_y and the electric field components (as experienced by the gas) are (E_x+v_yH) and (E_y-v_xH). Hence, from equation (1), the current components are :

$$j_x=\sigma_1(E_x+v_yH)-\sigma_2(E_y-v_xH), \tag{5}$$

$$j_y=\sigma_1(E_y-v_xH)+\sigma_2(E_x+v_yH). \tag{6}$$

Under the influence of the force F and the electromagnetic force $\boldsymbol{j}\times\boldsymbol{H}$ the gas, of mass density ρ, moves according to:

$$\rho\dot{v}_x=j_yH+F=H\sigma_1(E_y-v_xH)+H\sigma_2(E_x+v_yH)+F,$$

$$\rho\dot{v}_y=-j_xH=-H\sigma_1(E_x+v_yH)+H\sigma_2(E_y-v_xH).$$

These may be rearranged and solved to give:

$$v_x=E_y/H+F/H^2\sigma_3+e^{-\alpha t}(A_1\cos\beta t+\beta_1\sin\beta t), \tag{7}$$

$$v_y=-E_x/H-F\sigma_2/H^2\sigma_1\sigma_3+e^{-\alpha t}(A_2\cos\beta t+B_2\sin\beta t), \tag{8}$$

where $\alpha=H^2\sigma_1/\rho$, $\beta=H^2\sigma_2/\rho$ and $\sigma_3\equiv\sigma_1+\sigma_2{}^2/\sigma_1$, being the value assumed by the direct conductivity (normally σ_1) when Hall current is prevented from flowing (5).

The constants A_1 and A_2 are chosen so that $v_x=v_y=0$ when $t=0$, so that $A_1=-E_y/H-F/H^2\sigma_3$ and $A_2=E_x/H+F\sigma_2/H^2\sigma_1\sigma_3$. The constants B_1 and B_2 are found by differentiating equations (7) and (8) with respect to time and comparing with equations (5) and (6) at zero time. This gives $B_1=A_2$ and $B_2=-A_1$, so that:

$$v_x=A(1-e^{-\alpha t}\cos\beta t)+Be^{-\alpha t}\sin\beta t, \tag{9}$$

$$v_y=-B(1-e^{-\alpha t}\cos\beta t)+Ae^{-\alpha t}\sin\beta t, \tag{10}$$

where $A=E_y/H+F/H^2\sigma_3$ and $B=E_x/H+F\sigma_2/H^2\sigma_1\sigma_3$.

The electric field (or force) experienced by the gas is given by equation (4):

$$E'_x=-F\sigma_2/H\sigma_1\sigma_3+He^{-\alpha t}(B\cos\beta t+A\sin\beta t), \tag{11}$$

$$E'_y=-F/H\sigma_3+He^{-\alpha t}(A\cos\beta t-B\sin\beta t). \tag{12}$$

The currents are given by equations (5), (6), (9) and (10):

$$j_x=(\sigma_1E_x-\sigma_2E_y)e^{-\alpha t}\cos\beta t+(\sigma_2E_x+\sigma_1E_y+F/H)e^{-\alpha t}\sin\beta t, \tag{13}$$

$$j_y=-F/H+(\sigma_2E_x+\sigma_1E_y+F/H)e^{-\alpha t}\cos\beta t-(\sigma_1E_x-\sigma_2E_y)e^{-\alpha t}\sin\beta t. \tag{14}$$

The dynamic behaviour of an ionized gas in the fields of force may be illustrated graphically. The various parameters are represented by lightly damped oscillations when $\beta\gg\alpha$ and are non-oscillatory when $\beta\ll\alpha$. An intermediate condition best illustrates the effects and we choose $\beta/\alpha=\sigma_2/\sigma_1=5$, so that $\sigma_3/\sigma_2=5{\cdot}2$. The units used are chosen more or less arbitrarily: the time unit is such that $\beta=1$ and $\alpha=0{\cdot}2$. The effect is first studied of a force F of magnitude such that $F/H^2\sigma_3=1$ ($E_x=E_y=0$) suddenly applied along Ox. In Fig. 1(*a*) the locus of the end of the velocity vector $\boldsymbol{v}$ is shown moving in the xy plane in a spiral towards its steady state position S. In Fig. 1(*b*) the path traced by a small volume of the gas is plotted in the xy plane, the position being found by integrating equations (9) and (10). Both of these diagrams apply equally well for an electric field which gives the same values of A and B. That is, for $E_x=F\sigma_2/H\sigma_1\sigma_3=5H$ and $E_y=F/H^2\sigma_3=H$. This equivalent electric field is called $\boldsymbol{E}_F$ and is shown as a vector in Figs. 1(*a*) and 1(*b*).

In Fig. 2(*a*) are shown the internal electric field components E'_x and E'_y due to the force $\boldsymbol{F}$ (along Ox) ; these are plotted against time and denoted $E'_x(F)$ and $E'_y(F)$. The corresponding curves for the equivalent electric field $\boldsymbol{E}_F$ are denoted by $E'_x(E_F)$ and $E'_y(E_F)$. Their steady state values are zero. In Fig. 2(*b*) the two sets of current density components are plotted similarly, being denoted by $j_x(F)$, $j_y(F)$ and $j_x(E_F)$, $j_y(E_F)$ for the applied fields $\boldsymbol{F}$ and $\boldsymbol{E}_F$ respectively. The steady states of all but $j_y(F)$ are zero.

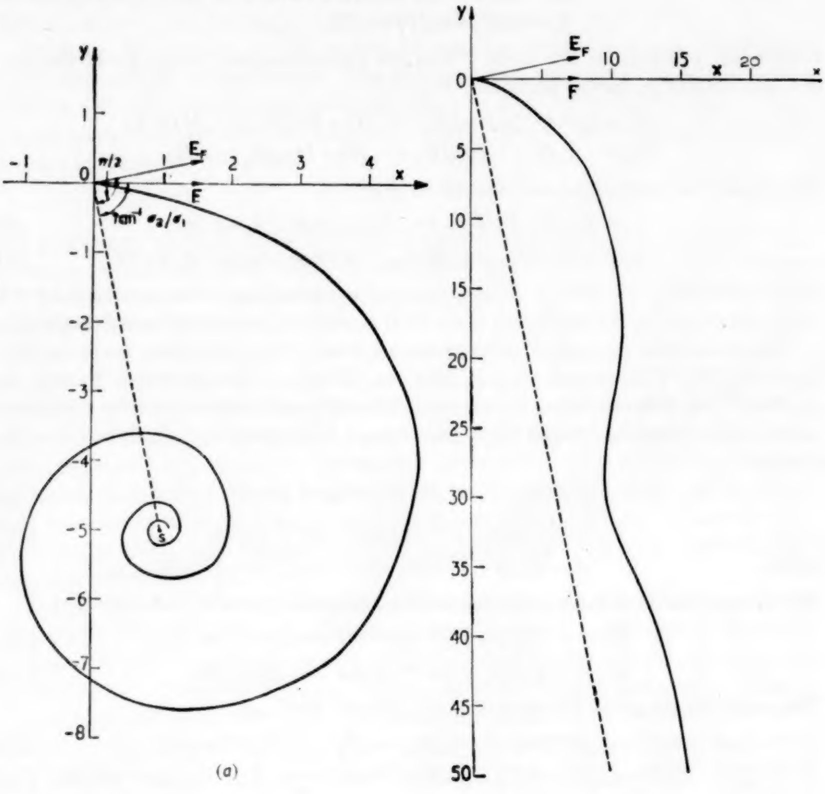

FIG. 1.—*The movement of ionized gas under the influence of a steady magnetic field (vertically outward from the paper) and either a suddenly applied mechanical force* $\boldsymbol{F}$ *or a suddenly applied electric field* $\boldsymbol{E}_F$ *as shown.*

(*a*) *The locus of the end of the velocity vector* $\boldsymbol{v}$. (*b*) *The path traced by a small volume of the gas.*

It has been assumed above that conditions are everywhere uniform. If this is not the case, then attention must be paid to the possible effects of variation of $\boldsymbol{v}$ and $\boldsymbol{j}$ throughout the medium. In some problems such variation is not important; in others, however, it results in accumulations of one or more types of particle (charged or uncharged) in certain regions. This is a boundary problem and may add greatly to the difficulty of solution. Boundary effects must be considered in relation to each individual problem. For example, if the conductivity changes at a plane, there will be a tendency for space charge to collect on that plane and the values of E_x and E_y in equations (5) to (14) would be functions

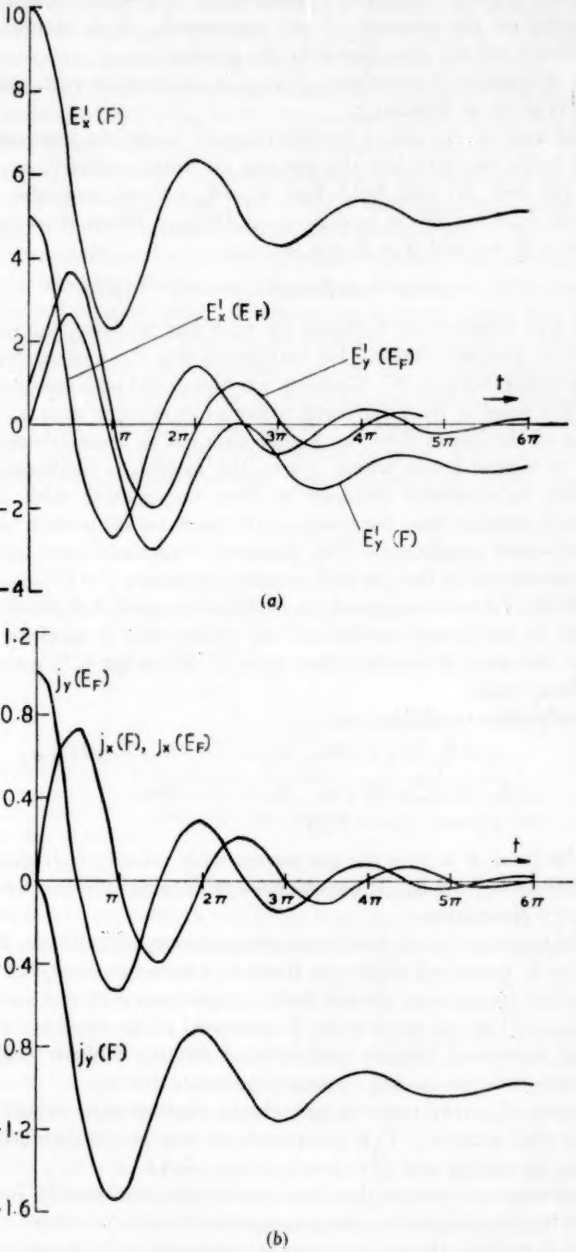

FIG. 2.—*(a) Internal electric field components $E'_x(F)$ and $E'_y(F)$ due to a suddenly applied force* **F** *and internal electric field components $E'_x(E_F)$ and $E'_y(E_F)$ due to the equivalent electric field* $\mathbf{E_F}$. *All plotted against time. (b) Electric current density components $j_x(F)$ and $j_y(F)$ due to a suddenly applied force* **F** *and electric current density components $j_x(E_F)$ and $j_y(E_F)$ due to the equivalent electric field* $\mathbf{E_F}$. *All plotted against time.*

of j_x and j_y and of time. Mention is made below of pressure gradient as one type of force acting on the element of gas concerned. It is tacitly assumed that boundary effects are not introduced by the gradient.

Further discussion of equations (9)–(14) in connection with specific types of ionized gas is given in Section 5.

A special case of the above problem occurs when the external electric and mechanical fields are zero but the gas has an initial velocity, say v along Ox. Equations (5) and (6) still hold but $E_x = E_y = F = 0$ and also when $t = 0$: $v_x = v$, $v_y = 0$, $\dot{v}_x = -\sigma_1 H^2 v/\rho$ and $\dot{v}_y = -\sigma_2 H^2 v/\rho$. From these boundary conditions $A_1 = -B_2 = v$ and $A_2 = B_1 = 0$, so that:

$$v_x = ve^{-\alpha t}\cos\beta t \text{ and } v_y = -ve^{-\alpha t}\sin\beta t.$$

This result was obtained by Cowling (5) who was studying the motion of solar material across magnetic fields. He concluded that the motion decays in a time comparable with α^{-1} or $\rho/\sigma_1 H^2$. Cowling was concerned with gas near the reversing layer at which level σ_2 is of the same order as or smaller than σ_1, so that $\beta \leqslant \alpha$. The motion of the gas is then too highly damped to be oscillatory. It may be noted that at higher levels where $\sigma_2 \gg \sigma_1$ the motion is oscillatory, the *forward* motion being substantially changed in time comparable with β^{-1} or $\rho/\sigma_2 H^2$ which is much smaller than the time $\rho/\sigma_1 H^2$ taken for *all* motion to disappear.

3. *Steady-state conditions.*—The transient treatment used above indicates oscillatory movement of the gas with angular frequency $\beta = H^2\sigma_2/\rho$. It is evident that if the fields of force are applied gradually over a period of about $2\pi/\beta$ or more, there will be no oscillatory motion and the steady state is assumed immediately. In any case this state is reached after time of the order α^{-1}, owing to the exponential decay term.

The steady-state conditions are:

$$v_x = E_y/H + F/H^2\sigma_3, \quad v_y = -E_x/H - F\sigma_2/H^2\sigma_1\sigma_3, \tag{15}$$

$$E_x' = -F\sigma_2/H\sigma_1\sigma_3, \quad E'_y = -F/H\sigma_3, \tag{16}$$

$$j_x = 0, \quad j_y = -F/H. \tag{17}$$

When the force F is zero the gas moves with velocity E/H perpendicular to the applied electric field E. It experiences no internal electric field, no current and no energy dissipation.

When the external electric field is zero the gas moves with velocity $F/\{H^2(\sigma_1\sigma_3)^{1/2}\}$ in a direction ϕ, measured clockwise from F, where $\tan\phi = \sigma_2/\sigma_1$. At the same time an internal (induction) electric field is experienced by the gas of magnitude $E' = F/\{H(\sigma_1\sigma_3)^{1/2}\}$ at an angle $\pi/2 + \phi$ measured clockwise from F. The components and vectors of velocity and internal electric field are shown in Fig. 3. which is drawn for a gas having σ_2 somewhat larger than σ_1.

In the case of a very tenuous gas when collisions may almost be neglected $\sigma_2/\sigma_1 \gg 1$, so that $\phi \simeq \pi/2$. The gas moves almost perpendicularly to the force which causes its motion and E' is nearly antiparallel to F.

It is important to observe the close connection between the internal electric field and the mechanical force: one cannot exist without the other. If an external electric field is applied, the gas moves so as to neutralize this by an induction field. In so doing it may experience a force due, say, to the development of a pressure gradient. The steady condition is shown in Fig. 3 by the vectors F and E'. If no steady force opposes gas motion, then the internal electric field dwindles to

zero. Again, if a mechanical force is applied without an electric field the gas moves until an induction field provides a balance as in Fig. 3. Failure to observe these interdependent factors has led to much confusion in the past.

To complete Fig. 3 an electric field vector $\boldsymbol{E}_F$ is drawn equal and opposite to $\boldsymbol{E}'$ and so at an angle $\tan^{-1} \sigma_1/\sigma_2$ to $\boldsymbol{F}$. This electric field is exactly equivalent to $\boldsymbol{F}$ in determining gas velocity, both transient and steady state. They are not, however, equivalent in other respects and should not be treated as such. Thus from equations (16) and (17) and Figs. 1 and 2 they are clearly not equivalent in determining the values of internal electric field and current.

Steady-state conditions for the case of a lightly ionized gas have been discussed by Martyn (**6**) who has determined the ion and electron drift-velocity vectors due to an applied electric field. He finds an internal force due to collisions between the ion-electric gas and the neutral gas. This force bears the same relationship to the electric vector as that given in Fig. 3 (when allowance is made for the different assumed directions of the magnetic field). Following the procedure used here of considering the gas as a whole (neutral as well as charged particles), an external force of the same magnitude must be exerted on the neutral particles to prevent them from moving. This corresponds to $\boldsymbol{F}$ in Fig. 3.

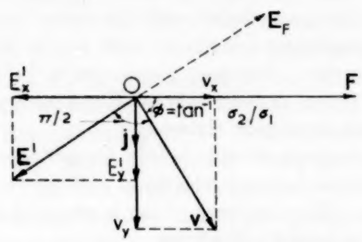

FIG. 3.—*Vector diagram of steady-state gas velocity* $\boldsymbol{v}$, *internal electric field* $\boldsymbol{E}'$ *and current* $\boldsymbol{j}$ *for a gas in a magnetic field (vertically outward from the paper) and subject to a mechanical force* $\boldsymbol{F}$ *cm*$^{-3}$ *as shown. The electric field* $\boldsymbol{E_F}$ *shown causes the same movement of gas but no internal electric field or current.*

The rate at which the force F does work on the gas is Fv_x or $F(E_y/H+F/H^2\sigma_3)$. The second term corresponds to the Joule heat dissipation $F^2/H^2\sigma_3=j^2/\sigma_3=jE'_y$ and shows that σ_3 is the conductivity which determines rate of energy dissipation, an important conclusion reached elsewhere (**2**). The first term, $FE_y/H=-j_yE_y$, corresponds to the energy supplied by the force F and transmitted by the gas to the external electrical system responsible for supplying the electric field E_y. This energy may result in a build-up of electric polarization at boundaries or in the dissipation of Joule heat in external circuits.

A case which may have some astrophysical interest is that of a gas moving with velocity $v_x=E_y/H$ under the influence of E_y. If this velocity is destroyed by a sufficiently powerful force antiparallel to Ox, the gas develops a velocity $v_y=(\sigma_2/\sigma_1)v_x$. The value of σ_2/σ_1 is often large, being 10^5–10^8 in the Sun's atmosphere and in interstellar H II regions, so that even relatively small values of v_x and therefore of E_y may result in values of v_y approaching the velocity of light. In practical problems close consideration must be given to the build-up of electric polarization at boundaries. This effect tends to prevent the gas moving as above.

Before proceeding with, and in order to facilitate the discussion of the equations of Section 2, expressions for the conductivity coefficients of some gases will be introduced.

4. *Ionized gas conductivity.*—The conductivity coefficients of equation (1) have been determined for various gas mixtures by Chapman and Cowling (**7**) and Cowling (**3**). It is proposed to discuss two extreme types: a binary gas consisting of electrons and one type of heavy ion, and a lightly ionized gas containing the same two ingredients with a much larger number of neutral atoms or molecules.

In a binary gas:

$$\sigma_0 = n_e e^2 \tau/m, \quad \sigma_1 = \sigma_0/(1+\omega^2\tau^2), \quad \sigma_2 = \sigma_0 \omega\tau/(1+\omega^2\tau^2) \quad \text{and} \quad \sigma_3 = \sigma_0$$

in electromagnetic units, where n_e, e, m and τ are the electron density, charge, mass and mean interval between collisions with ions and $\omega = He/m$. It was first shown by Cowling (**5**) that $\sigma_3 \equiv \sigma_1 + \sigma_2^2/\sigma_1$ was the value assumed by the direct conductivity (normally σ_1) when the Hall current was prevented from flowing by electric polarization. Although Cowling was discussing a binary gas there is nothing restrictive in his argument which applies for any gas. The importance of σ_3 in some ionospheric problems has been shown by Baker and Martyn (**8**) and others.

The important identity $\sigma_0 = \sigma_3$ holds only for binary and other gases in which collisions by a single component (electrons) with one or more other components determines the conductivity. For such gases $\tau \propto n_e^{-1} T^{3/2}$, where T is the gas temperature, so that σ_0 and σ_3 depend only on T and not on n_e or H. This greatly simplifies many problems as already shown (**2**).

The conductivity components of a lightly ionized gas each have two terms corresponding to collisions between electrons and neutral atoms and between ions and neutral atoms. Only one type of ion is assumed and collisions between electrons and ions are neglected. We have:

$$\sigma_0 = \sigma_e + \sigma_i = n_e e^2 \tau_e/m + n_i Z^2 e^2 \tau_i/M,$$

$$\sigma_1 = \sigma_e/(1+\omega^2\tau_e^2) + \sigma_i/(1+\Omega^2\tau_i^2),$$

$$\sigma_2 = \sigma_e \omega\tau_e/(1+\omega^2\tau_e^2) - \sigma_1 \Omega_1 \tau_i/(1+\Omega^2\tau_i^2),$$

where τ_e and τ_i are the collision periods of electrons and ions with the neutral molecules and n_i, Ze and Ω are the ion density, charge and gyro-frequency respectively.

A difference of fundamental importance occurs in the values of σ_2 and σ_3 for the above gases when they are very tenuous or the magnetic field very strong, that is when $\omega\tau$, $\omega\tau_e$ and $\Omega\tau_i$ are all large. For the binary gas σ_1, σ_2 and σ_3 may be written $n_e e/H \,.\, 1/\omega\tau$, $n_e e/H$ and $n_e e/H \,.\, \omega\tau$, so that $\sigma_3/\sigma_2 = \sigma_2/\sigma_1 = \omega\tau$ which is large compared to unity. For the lightly ionized gas, which is neutral so that $n_e e = n_i Ze$, we have:

$$\sigma_1 = \frac{n_e e}{H}\left(\frac{1}{\omega\tau_e} + \frac{1}{\Omega\tau_i}\right) \text{and } \sigma^2 = 0, \text{ so that } \sigma_3 = \sigma_1.$$

Thus $\quad \sigma_3/\sigma_2 \to \infty$ and $\sigma_2/\sigma_1 \to 0$ and $\sigma_3/\sigma_0 = \sigma_1/\sigma_0 = 1/(\omega\tau_e \Omega\tau_i)$,

which is very small instead of unity for the binary gas. This profound, and at first sight surprising, difference in behaviour of the two gases is discussed in Section 6.

Because of their great importance in astrophysics " impure binary gases " also require discussion. One such gas comprises electrons and ions together with some neutral particles (called atoms for brevity), but in which the electrons collide much more frequently with ions than with atoms. Because of the smaller collision cross-section of atoms they may be much more numerous than ions while still satisfying this condition. The conductivity components of such a gas are the same as for binary gas provided one vital condition is satisfied; this is discussed in the following section.

Another gas which might be called impure binary comprises electrons and two or more types of ion, in which the contribution to conductivity due to collisions between ions is negligible. This gas has the same conductivity as a binary gas.

5. *Discussion of equations* (9)–(14).—The quantities σ_1 and σ_2 determine the average current which flows when an electric field is applied to a medium for a sufficiently long period. Generally this period is taken as long compared with both the gyro-period and the collision period. In Section 2 this rule was not observed and the physical significance of the treatment needs discussion.

5.1. *Binary gas.*—Consider first a binary gas in which $\omega\tau \gg 1$; the conductivity is provided by the electrons and the correct values of σ_1 and σ_2 are established in a period during which the electrons have made several gyrations. In this period the ions will hardly have moved and may be considered at rest. Subsequent movement of the ions constitutes movement of the gas as a whole and introduces the term $\boldsymbol{v} \times \boldsymbol{H}$ into the equations, thus changing $\boldsymbol{j}$ but not σ_1 or σ_2. It is not necessary that the period during which $\boldsymbol{j}$ is averaged should be long compared with the collision period. Each collision by any electron contributes to $\boldsymbol{j}$ and it is only necessary that the total number of collisions of all the electrons in a volume small compared with the total volume of the gas should be statistically large. Hence when $\omega\tau \gg 1$, σ_1 and σ_2 determine the average current flowing in a period short compared with the gyro-period of the ions.

A better understanding of the result above may be obtained by assuming a force F applied to the gas simultaneously with the electric field. Let F be a gravitational force acting almost entirely on the ions and of such strength that it exactly neutralizes the electric force due to the applied electric field. Neglecting thermal motion the ions remain stationary while the electrons move under the influence of the electric field. Stable conditions are established within a few electron gyro-periods, the electrons conducting current of density $\boldsymbol{j}$ such that $\boldsymbol{j} \times \boldsymbol{H} = \boldsymbol{F}$. When $\boldsymbol{F}$ is not present the conditions are only changed in so far as $\boldsymbol{F}$ is replaced by the force necessary to overcome inertia of the protons.

When the collision period is not long compared with the electron gyro-period, the necessary averaging period is not increased although it may be decreased if $\omega\tau < 1$. It is concluded that for a binary gas the treatment of Section 2 is valid provided " zero time " really means a time interval during which the electrons may perform several gyrations.

The binary gas equations show that $\sigma_2/\sigma_1 = \omega\tau$, so that $\beta = \alpha\omega\tau$, and when $\omega\tau$ is substantially greater than unity equations (11)–(16) represent an oscillatory condition. The angular frequency β is found from the conductivity equations to be equal to the angular frequency of rotation of the heavy ions in the magnetic field, HZe/M. The amplitude of the oscillation is found for the case where $F = E_x = 0$, so that $A = E_y/H$ and $B = 0$. Since we have shown the correspondence between a mechanical force and an electric field, this example is sufficiently general.

The amplitude of oscillation (found by integrating equations (9) and (10)) is $A/\beta = E_yM/H^2Ze$ along both x and y axes. There is also a steady drift with velocity E_y/H along Ox. The oscillations are damped by a factor $\exp(-1)$ in time $\alpha^{-1} = \rho/H^2\sigma_1$.

When the collision period is equal to or smaller than the electron gyro-period $\beta \leqslant \alpha$ and no oscillations occur. Steady-state motion is acquired, as before, in time of the order α^{-1}.

5.2. *Impure binary gas.*—A binary gas to which some atoms have been added may be considered as a pure binary gas moving freely within an atomic gas. All the considerations above regarding a binary gas are equally applicable, the value of ρ corresponding to the binary gas only and not the whole gas, and $\boldsymbol{F}$ being the force acting on the binary gas. However, when the steady state given by equations (15)–(17) has been attained, a further process takes place. The collisions between the binary and the atomic gas, although few, must sometimes be taken into account. This is done by calculating the rate of transfer of momentum from the binary to the atomic gas, namely $(n_em/\tau_e + n_iM/\tau_i)(\boldsymbol{v} - \boldsymbol{u})$, where $\boldsymbol{v}$ and $\boldsymbol{u}$ are the velocities of the binary and atomic gases and τ_e and τ_i are defined as for a lightly ionized gas. Although the electrons and ions have drift components other than $\boldsymbol{v}$, these components make no contribution to momentum transfer. This has been demonstrated by Martyn (**6**) for a lightly ionized gas and is equally applicable here. The importance of the frictional force between the gases depends on the relative values of τ_e and τ_i and the time during which the fields of force are applied. Thus for oscillatory fields of period $\ll \tau_{i,e}$ it may be neglected. If the period is comparable with or greater than $\tau_{i,e}$ it may be important.

Gas containing two types of heavy ion but having no appreciable ion conductivity is really a mixture of two binary gases. In the oscillatory stage each gas moves approximately independently with the gyro-frequency of its heavy ions. In the steady state the gas may be considered as a single binary gas with appropriate mean mass density.

5.3. *Lightly ionized gas.*—In a lightly ionized gas, electrons sometimes contribute nearly all of the conductivity, in which case the treatment used in Section 2 is valid. If, on the other hand, ions contribute appreciably, then the treatment is not valid. In this case ion transient movement may be studied by a consideration of the electrons and ions as constituting a binary gas with infinite collision period, moving within an atomic gas. The conductivity components of the binary gas are:

$$\sigma_1 = 0, \quad \sigma_2 = n_ee/H, \quad \sigma_3 = \sigma_0 = \infty.$$

The constants A and B of equations (9) to (13) become E_y/H and $(E_x/H + F/H^2\sigma_2)$ and $\alpha = 0$. If $\omega\tau_e$ and $\Omega\tau_i$ is both much greater than unity then the binary gas oscillates according to the equations, F being the force on the binary gas only.

If $\omega\tau_e$ or $\Omega\tau_i$ is comparable with or smaller than unity the binary gas does not oscillate. In any case after a time of order $\omega\tau_e/\Omega$ or τ_i, whichever is the smaller, the steady state is attained. The motion is then described by equations (15), the electric field experienced by the binary gas and the current flowing are given by equations (16) and (17). The force $\boldsymbol{F}$ is the frictional force $-(\boldsymbol{v} - \boldsymbol{u})(n_em/\tau_e + n_iM/\tau_i)$ between the binary and atomic gases. The latter moves under the influence of a force $-\boldsymbol{F}$ together with any other forces acting directly on the atoms.

For steady-state conditions a lightly ionized gas is best considered as a whole, relative internal movement of the binary gas being ignored. The value of $\boldsymbol{v}$ then refers very nearly to the atomic gas (this is discussed further in the next section) and $\boldsymbol{E}'$ and $\boldsymbol{F}$ also refer to this gas. The conductivity components are those of a lightly ionized and not a binary gas.

6. *Dynamics of ionized gas.*—There is as yet no complete and self-consistent system of using the conductivity equation to solve gas dynamical problems. The reason is that different workers have developed different methods of approach which are difficult to reconcile with one another and in some cases are faulty. Methods tend to differ when dealing with different kinds of gas or different combinations of mechanical and electrical forces. Three aspects of the problem require discussion in which the present approach is compared with some others.

6.1. *The gas velocity.*—A point which has caused some confusion is the definition of $\boldsymbol{v}$ in the equation $\boldsymbol{j}=[\sigma](\boldsymbol{E}+\boldsymbol{v}\times\boldsymbol{H})$, $[\sigma]$ being the conductivity tensor and $\boldsymbol{E}$ the electric force experienced by unit charge at rest. The concept of conductivity was introduced as a property of solids and it was evident that $\boldsymbol{v}$ should refer to the solid itself, even though charged particles moving within the solid had different velocities and so, individually, experienced different electric forces. In the case of gases and, in particular, of a fully ionized gas, the position is not so clear because then all the particles are electrically charged and each type of particle moves with a different average velocity. However, the value of $\boldsymbol{v}$, as pointed out by Cowling (**4**) is the " velocity of the mass as a whole". It might help to be even more specific and define $\boldsymbol{v}$ as the net momentum per unit mass of the medium. The different drift velocities of the components are cared for in the derivation of the conductivity.

It is the definition of $\boldsymbol{v}$ which accounts for the extreme difference in $[\sigma]$ of very tenuous binary and lightly ionized gases mentioned in Section 4. Students of lightly ionized gases sometimes tend to regard binary gases as extreme cases of lightly ionized gases, from which most of the neutral atoms have been removed. This is not so, because of the different definition of $\boldsymbol{v}$ for the two gases. In the lightly ionized gases $\boldsymbol{v}$ is (very nearly) the velocity of the neutral atoms, while in a binary gas it is (very nearly) the velocity of the heavy ions. Thus in a lightly ionized gas, in which the atoms remain at rest, movement of ions modifies $\boldsymbol{j}$ without changing $\boldsymbol{v}$—hence it must affect the value of $[\sigma]$. In a binary gas, on the other hand, a velocity $\boldsymbol{v}$ of the ions corresponds almost exactly to a velocity $\boldsymbol{v}$ of the whole medium and thus determines the electric force experienced by the medium but not its conductivity. The apparent anomaly is now easily explained. When an electric field $\boldsymbol{E}_\perp$ is applied perpendicular to $\boldsymbol{H}$ in a lightly ionized gas in which collisions may be neglected, the ions and electrons move separately as a binary gas and assume a velocity such that $\boldsymbol{E}_\perp+\boldsymbol{v}\times\boldsymbol{H}$ is zero and $\boldsymbol{j}$ is zero. Since the electric field $\boldsymbol{E}_\perp$ experienced by the *gas as a whole* (the neutral atoms) is not diminished it follows that σ_1 and σ_2 must be zero. In the case of a binary gas, when $\boldsymbol{E}_\perp$ is applied without a mechanical force, the electric force $\boldsymbol{E}_\perp+\boldsymbol{v}\times\boldsymbol{H}$ experienced by the *whole* gas falls to zero. Hence $\boldsymbol{j}$ is zero, not because σ_1 and σ_2 are zero but because the total electric force is zero. If a mechanical force restrains the ions from moving, a (Hall) current flows, indicating a finite value of σ_2.

6.2. *Pressure gradients.*—The results of Sections 2 and 3 are derived for a uniform gas. However, provided conditions do not change appreciably in the

region considered, they may be applied where pressure and density gradients exist. The various parameters are then given by the equations of Sections 2 and 3 in which $\boldsymbol{F}$ may now contain a term in grad p, where p is the total gas pressure.

If $\boldsymbol{F}$ includes other forces, say gravitational, these may be lumped together with grad p. It may seem surprising that a gravitational force which acts almost exclusively on the heavy ions (in the case of a fully ionized gas) is equivalent to a pressure gradient which acts on both ions and electrons. The reason is that a space-charge electric field is set up which effectively links the two gases. If there is a pressure gradient there is, in general, a density gradient, and as the electrons have less inertia they are pushed ahead of the heavy ions in the direction of decreasing density. Only a small movement is generally sufficient to create a space-charge field sufficient to transfer the necessary momentum from the electron to the ion gas. The space-charge electric field may be considered as an internal part of the whole mechanism and need not appear in the gas-dynamical equations unless it is of interest in its own right.

In the case of a partially ionized gas there may be very different forces acting not only on electrons and heavy ions but also on neutral particles. Thus radiation pressure might act exclusively on the latter while electric forces acted only on the charged particles. This would seem to necessitate great complexity in the gas-dynamical equations. However, only in the transient stage need the separate motions of the gas components be considered. In the steady state an appropriate drift of neutral particles relative to ions provides a frictional force between them which allows a suitable transfer of momentum as in the case of the space-charge field. The relative motion and frictional force may remain an internal matter not considered in dynamical problems.

It is seen that whenever possible any ionized gas should be considered dynamically as a single gas, relative motions of its components being ignored as well as internal electrostatic fields. In the case of a partially ionized gas this can only be done provided changes are slow enough to allow a steady drift to be attained.

6.3. *Equivalent electric fields.*—Cowling (**4**), Schlüter (**9**) and others have developed gas-dynamical equations from the individual equations of motion of the electron gas or the positive ion gas or both. Cowling finds the total force on the electron gas to be

$$\operatorname{grad} p_e - n_e e[\boldsymbol{E} + (\boldsymbol{v} + \boldsymbol{V}) \times \boldsymbol{H}] + n_e \nu m \boldsymbol{V},$$

where p_e and $\boldsymbol{V}$ are the partial pressure of the electron gas and its velocity relative to the heavy ion gas (a binary gas is being considered), ν is the collision frequency of the electrons, and the other terms have been defined above. He then deduces a total " effective " electric intensity on the moving gas

$$\boldsymbol{E}' = \boldsymbol{E} + \boldsymbol{v} \times \boldsymbol{H} + \operatorname{grad} p_e/n_e e. \tag{18}$$

If $\boldsymbol{E}'$ is perpendicular to $\boldsymbol{H}$, then it is the field which determines the total current density according to the equation:

$$\boldsymbol{j} = \sigma_1 \boldsymbol{E}' + \sigma_2 \boldsymbol{H} \times \frac{\boldsymbol{E}'}{H}, \tag{19}$$

Thus the " effective " electric intensity includes a force term grad p_e/n which is termed an " equivalent " electric field.

In subsection 6.2 above it was stated that a pressure gradient could be lumped with a gravitational (or any other) force in determining the gas motion and electric

current density. In Section 3 it was shown that a force F caused an internal electric field of magnitude $F/H(\sigma_1\sigma_3)^{1/2}$ which would be effective in causing current flow according to equation (19). For low values of collision frequency in a binary gas:

$$H(\sigma_1\sigma_3)^{1/2} \simeq n_e e,$$

so that the "equivalent" electric field is approximately $F/n_e e$ or grad $p/n_e e$ when F comprises a pressure gradient. This appears inconsistent with Cowling's result in which only the partial pressure of the electron gas is introduced.

To resolve this inconsistency it is necessary to consider the actual physical effects of the pressure gradient. That part of the pressure gradient which acts on the electron gas causes this gas to move slightly away from the heavy ion gas and so creates a space-charge field which may be included in the term $\boldsymbol{E}$ of equation (18) or kept separate and called an equivalent electric field. This electric field is present when the steady magnetic field is zero. That part of the pressure gradient which acts on the heavy ions may be considered as acting on the gas as a whole (as would a gravitational force), dragging it across the magnetic field. The motion induces an electric field which may be included in the term $\boldsymbol{v} \times \boldsymbol{H}$ or kept separate and called an equivalent electric field. This component occurs only when there is a steady magnetic field with a component perpendicular to grad p. The two electric fields due to the pressure gradient may be kept separate if desired, or combined to give a total equivalent electric field grad $p/n_e e$.

Schlüter (9) also found an "equivalent" electric field which differed from that of Cowling and from the value given above.

The concept of "equivalent" electric forces may be useful but it may also introduce some confusion. The alternative approach used above is to deal only with real electric fields, all of which are included in the terms of equation (4), and with mechanical forces which help determine these fields as well as the values of gas velocity and current density.

Acknowledgments.—The writer wishes to thank Dr D. F. Martyn and Mr R. C. Mullaly for helpful discussions and the latter for assistance with the manuscript.

Division of Radiophysics, C.S.I.R.O.,
Sydney,
Australia :
1954 *September.*

References

(1) J. H. Piddington, *M.N.*, **113**, 188, 1953.
(2) J. H. Piddington, *M.N.*, **114**, 638, 1954.
(3) T. G. Cowling, *Proc. Roy. Soc.* A, **183**, 453, 1945.
(4) T. G. Cowling, "*The Sun*", ed. G. P. Kuiper, Chicago U.P., 1953.
(5) T. G. Cowling, *M.N.*, **93**, 90, 1933.
(6) D. F. Martyn, *Phil. Trans.* A, **246**, 306, 1953.
(7) S. Chapman and T. G. Cowling, "*The mathematical theory of non-uniform gases*", Cambridge University Press, 1939.
(8) W. G. Baker and D. F. Martyn, *Phil. Trans.* A, **246**, 281, 1953.
(9) A. Schlüter, *Z. f. Naturforschung* **5A**, 72, 1950; **6A**, 73, 1951.

A POSSIBLE MECHANISM FOR BINARY STAR FORMATION

K. N. Dodd

(Communicated by W. H. McCrea)

(Received 1954 July 1)

Summary

The possibility is examined of a pair of originally single stars becoming gravitationally bound together as a result of their interaction with interstellar material. In the first instance, a special model is considered in which it is assumed that this interaction is in accordance with the Bondi–Hoyle–Lyttleton accretion theory. It is found that in this model such binary star formations are possible, but under certain conditions which could have existed only at an early stage in the evolution of the stars. In the light of the results of this preliminary examination, a more realistic model is considered and this leads to a very effective process for binary formation when the same properties of the interstellar material are assumed as in the accretion theory.

---

1. *Introduction.*—There appear to be only three logically possible theories of the origin of binary stars: the binary systems may have been formed by the disintegration of originally single stars, they may have been born or created as double stars, or they may have been formed by the coming together of two originally single stars.

We shall consider briefly the three types of theory. The first or fission theory was for some time the accepted one. However, later examination (**1, 2**) indicated that it is inadequate to explain the formation of binaries. According to the second theory, which is the one now receiving most attention, binary stars were formed by the condensation of two stars within each other's gravitational influence. In the third theory, two originally independent stars are considered to come together and remain together. It can be shown that if two stars approach from a great distance, they must necessarily separate again to a great distance in the absence of forces other than their gravitational attraction. The most obvious way to introduce another force is by the presence of a third star. Thus, if three stars approach from a great distance, it is possible for one to recede to infinity leaving the other two gravitationally bound together.

The first theory we wish to consider here is of the third type but the place of the third star is taken by interstellar material. In other words, two stars are considered to approach from a great distance apart in a region containing interstellar material. During the approach and subsequent encounter, each star will experience a resistance to its motion and so will lose energy. If this energy loss is sufficient, the stars will not again recede to a great distance apart but will remain gravitationally bound together. Once the binary has formed in this way, its orbital elements may be subsequently affected by the interstellar material, but it is not proposed to consider this in the present paper.

If we examine more closely the second type of theory of binary formation, we see that some similar process must occur, because after the stars have condensed their subsequent motions must for some time be influenced by the star-forming medium. It was during this early stage that we consider the mechanisms here put forward to have been of most importance.

In Section 2 of this paper an elementary mathematical treatment of such a binary-forming encounter is given. This treatment is based on the assumption that the stars experience a mass increase in accordance with the Bondi–Hoyle–Lyttleton accretion theory. In Section 3 the result of this treatment is discussed and its implications are considered. In Section 4 a limitation of the elementary treatment is considered and a different model is suggested that can be treated more realistically. This leads to a mechanism which appears to be an efficient agency for the formation of binary stars.

2. *Elementary mathematical treatment.*—In considering the dynamics of a binary-forming encounter between two stars, as outlined above, we must imagine the stars to approach from a separation of the order of the local mean interstellar distance, since at greater separations each star is more likely to be influenced by other neighbouring stars. The maximum initial velocities of the stars necessary to produce a capture will depend on the initial directions of motion and on the masses of the stars. A full investigation of the binary-forming encounter would be quite difficult in view of the numerous parameters involved. However, a simple example has been investigated in order to find the order of magnitude of the initial velocities. The case considered is that of two stars of equal mass approaching with equal speeds in almost opposite directions. The word "almost" in the last sentence is intended to mean that from the mathematical point of view the motion of the star can be considered rectilinear, but on the other hand the stars must miss a collision at the point of minimum separation. The centre of mass of the stars is taken to be at rest in the medium which has density ρ. Starting with an initial separation d, the initial speeds are found, so that stars never again separate to a distance of more than $\frac{1}{2}d$. The choice of this maximum subsequent separation is arbitrary but it must be such that the probability is low that the stars will be torn apart again by gravitational interaction with neighbouring stars.

We must next consider the interaction between the interstellar material and the stars. It is proposed to assume the mechanism which has been developed in the accretion theory of Bondi, Hoyle and Lyttleton. For details of this, see for example (3) and the references therein. For our purpose, however, we only need to know that the theory implies that each star "accretes" or captures the interstellar material lying within a distance σ from the star as it moves through the material. As shown in (4),

$$\sigma = 2\mu/v^2, \tag{1}$$

where μ = mass of star × constant of gravitation and v = velocity of star relative to the interstellar material. For very small velocities it is seen that the value of σ becomes very large. There is however a limit set by the presence of neighbouring stars. These limit the capture radius σ to about one-half of the distance of the star from its nearest neighbour, because it is only within this distance that a star can be considered to have a predominating gravitational effect on the interstellar material. We are going to suppose that the velocities are so small that this maximum capture radius applies. The rate of capture of material by the star is

therefore $\pi\sigma^2\rho v$, where σ is half the distance of the star from its nearest neighbour, which in our case will be the other star partaking in the encounter. We must remember however that this capture rate applies subject to the condition that the velocity does not exceed the value given by (1), i.e. $v<(2\mu/\sigma)^{1/2}$.

Let a frame of reference be placed such that the origin O is at the mass centre of the stars and let the axis Ox pass through the starting points of the stars. Then the motion of either star will be almost rectilinear and coincident with Ox. Let x be the position, v the velocity along Ox and m the mass at time t of the star which started on the negative part of the axis Ox. Then

$$\frac{dx}{dt}=v. \tag{2}$$

The equation of motion is

$$\frac{d(mv)}{dt}=\frac{Gm^2}{4x^2} \tag{3}$$

when the stars are approaching, where G is the constant of gravitation. The rate of accretion is

$$\frac{dm}{dt}=\pi x^2\rho\,|\,v\,|. \tag{4}$$

The velocity of the star under consideration is positive, so dividing (4) by (2) gives

$$\frac{dm}{dx}=\pi\rho x^2,$$

whence

$$m=\tfrac{1}{3}\pi\rho x^3+M \tag{5}$$

where M is the mass of the star when it reaches the origin. From (3),

$$m\frac{dv}{dt}+v\frac{dm}{dt}=\frac{Gm^2}{4x^2}$$

and using (2), (4) and (5), this becomes

$$\frac{dv^2}{dx}+\frac{2\pi\rho x^2v^2}{M+\frac{1}{3}\pi\rho x^3}=\frac{G(M+\frac{1}{3}\pi\rho x^3)}{2x^2},$$

of which the solution is

$$v^2=\frac{1}{(M+\frac{1}{3}\pi\rho x^3)^2}\left[G\left(-\frac{M^3}{2x}+\frac{\pi\rho M^2x^2}{4}+\frac{\pi^2\rho^2Mx^5}{30}+\frac{\pi^3\rho^3x^8}{432}\right)+A\right], \tag{6}$$

A being a constant of integration. Now (5) implies that as the stars approach each other, they accrete the material lying within the cone whose vertex is at O and whose semi-angle is $\pi/4$. The stars narrowly miss a collision at O and then proceed and come to rest at $x=\pm\frac{1}{4}d$. Since after passing O each star will be entering a region which has just been cleared of material by the other star, we assume that the stars do not accrete between O and their first position of rest. Thus, in this part of the motion, we have from elementary considerations (or else by putting $\rho=0$ and changing the sign of G in (6)),

$$v^2=\frac{GM}{2x}+B, \tag{7}$$

B being a constant which is determined by the fact that $v=0$ at $x=\frac{1}{4}d$. So $B=-2GM/d$. The condition at the origin is that at $x=\delta$ (where δ is a small positive quantity), v^2 given by (7) must be the same as v^2 at $x=-\delta$ given by (6).

From this it follows that $A=-2GM^3/d$. To obtain the maximum initial velocity of a star we put $x=-\frac{1}{2}d$ in (6). We obtain

$$v^2=\frac{G\rho d^2}{\left(\alpha-\frac{\pi}{24}\right)^2}\left[-\alpha^3+\frac{\pi}{16}\alpha^2-\frac{\pi^2}{960}\alpha+\frac{\pi^3}{110592}\right], \tag{8}$$

where $\alpha=M/\rho d^3$, which determines v for various values of M. It will be noted that when α is large enough, v^2 will be negative owing to the negative coefficient of α^3 in (8). Thus there is a limit above which α must not go. This limit is obtained by equating to zero the cubic expression in (8). The solution is approximately $\alpha=0{\cdot}135$. The physical significance is that stars with $\alpha>0{\cdot}135$ cannot be brought to rest at a separation of $\frac{1}{2}d$ even if their initial velocities (at separation d) are zero.

TABLE I

Masses of stars resulting from the binary-forming encounter of stars of initial separation ½ parsec and of given initial masses in a medium of given density

ρ g/cm³	Initial masses (in solar masses) 0·00069	0·0069	0·069	0·69
10^{-22}	0·023*	(0·029)	(0·091)	(0·712)
10^{-21}	0·222	0·230*	(0·290)	(0·91)
10^{-20}	2·21	2·22	2·30*	(2·90)
10^{-19}	22·1	22·1	22·2	23·0*

TABLE II

Maximum initial velocities (km/sec) of stars in the binary-forming encounter (initial separation ½ parsec)

ρ g/cm³	Initial masses (in solar masses) 0·00069	0·0069	0·069	0·69
10^{-22}	0·0299* (0·0035)	...	...	...
10^{-21}	2·13 (0·0035)	0·0945* (0·011)	...	...
10^{-20}	70·1 (0·0035)	6·75 (0·011)	0·299* (0·035)	...
10^{-19}	2240 (0·0035)	222 (0·011)	21·3 (0·035)	0·945* (0·11)

3. *Discussion of the results.*—For stated values of the initial masses and of the density of the interstellar material, Tables I and II give the maximum initial velocities and resulting masses M of the stars undergoing such a binary-forming encounter. The initial masses are such that the diagonal figures in the tables (marked with an asterisk) correspond to $\alpha=0{\cdot}135$. For these tables the value of d was taken to be half a parsec. This value was taken because although the present mean interstellar distance in the neighbourhood of the Sun is about one parsec, if the binary stars were formed by the method suggested then the mean interstellar distance of the original single stars must have been rather less.

The initial velocities given in Table II are unfortunately too large for the assumption about the accretion rate to be satisfied. The maximum velocity for this assumption to hold is given by the condition (1). Applying this condition at the point $x=-\frac{1}{2}d$ (i.e. putting $\sigma=\frac{1}{2}d$ in (1)) we obtain the velocities given in brackets in the table. We must therefore look upon these as representing the order of magnitude of the maximum velocities. It may be thought that by using the appropriate accretion formula for higher velocities, a higher maximum could be obtained. But it is unlikely that the maximum velocities could be appreciably increased in this way because as the velocity increases beyond the value determined by (1), the accretion rate falls off very rapidly.

The bracketed velocities are very small and consequently this binary-forming process can only be considered to apply to stars which are almost at rest initially. This is one reason for thinking that this process could only have been of importance at the stage when the stars were condensing from the original medium. Another reason is the fact shown at the end of the last section, that the initial masses of the stars in the encounter have an upper limit. Another point arising from the fact that the initial velocities must be small is that in all cases the binary-forming encounter must be an almost rectilinear motion, since the small initial velocities will soon become negligible compared with the velocities developed by the attraction of the two stars. It follows that the treatment given in Section 2 is not such a special case as at first it appeared to be.

The next point to note is that the resulting masses of the stars are almost independent of the initial masses. This is because the mass of material accreted by each star is much greater than its original mass. The resulting masses are therefore only dependent on the density ρ and also on d, being proportional to d^3. To obtain a binary consisting of two components of solar mass we would require a density of between 10^{-21} and 10^{-22} g/cm^3 (with $d=\frac{1}{2}$ parsec). This is high compared with the densities of most clouds observed at present, for which ρ does not exceed 10^{-22} g/cm^3, but it must be remembered that when the binaries were formed, considerably different conditions of the interstellar material must have prevailed. Of course, for a given value of ρ, any desired resulting mass can be obtained by a suitable choice of d. The importance of the present calculations is that the masses of observable binaries can be obtained with quite reasonable values of ρ and d.

In Table I the bracketed figures are included for the cases which do not result in captures. It is seen, of course, that in all cases the masses of the stars are increased. It follows that if a star does not form a binary in its first encounter with another star, then it can never again do so by this process in a medium of the same density because if we re-enter the table at an initial mass equal to the new mass of the star, we shall be even further removed from the region of the table where binary-formation is possible. It also follows that if a binary forms, it cannot subsequently pick up a third star to form a tertiary system under the influence of the medium alone. It is however possible for three or more initial condensations to become mutually attracted and form a multiple system. To investigate the case of three condensations, we may consider three equal condensations at the corners of an equilateral triangle and examine their motions as they approach their common centre of mass through the medium. If we do this, we obtain the expression (8), except that the G is increased by a factor $4/\sqrt{3}$. Thus, the initial velocities of approach v, as given by (8), are no smaller than for a binary-forming encounter. Similarly for four condensations originally at the corners of a regular tetrahedron.

3.1. *Amount of interstellar material remaining.*—When a binary-forming encounter of the type discussed above occurs, the mass of material accreted by the two stars is about one-half of that originally contained within a sphere of diameter d. Consequently there will still be sufficient interstellar material left to form a resistive medium for further accretion effects to occur. The formation of multiple systems leaves somewhat less unaccreted material.

3.2. *Time required for the encounter.*—In any particular case (i.e. for given initial masses and velocities of the stars), the time required for the stars to reach the origin is

$$\int_{-d/2}^{0} \frac{dx}{v},$$

where v is given by (6). This integral was evaluated numerically for the case of initial masses corresponding to $\alpha = 0 \cdot 135$ and for zero initial velocities. This integration was performed with the help of the initial approximation for the velocity

$$v^2 = 2Gm_0(x + \tfrac{1}{2}d)/d^2,$$

where m_0 is the initial mass of the star, which from (5) is $\rho d^3(\alpha - \pi/24)$. The resulting time was found to be $9 \cdot 12(G\rho)^{-1/2}$. For $\rho = 10^{-22}$ g/cm^3 this is $1 \cdot 12 \times 10^8$ years and for $\rho = 10^{-20}$ g/cm^3 it is $1 \cdot 12 \times 10^7$ years.

3.3. *Effect of unequal initial masses.*—If the masses of the condensations are not equal initially, let the masses at any instant be m_1, m_2, the positions x_1, x_2 and the inward directed velocities relative to the interstellar material v_1, v_2 respectively. Then (3) becomes

$$\frac{d(m_1 v_1)}{dt} = \frac{Gm_1 m_2}{(x_1 - x_2)^2} = \frac{d(m_2 v_2)}{dt},$$

from which it follows that at any instant

$$m_1 v_1 = m_2 v_2 + \text{constant}. \tag{9}$$

If, in this case, we consider the stars to tunnel out regions of radii equal to their distances from the neutral point of the gravitational field (i.e. the point where the gravitational attractions of m_1 and m_2 are equal and opposite) then the accretion rate for m_1 is given by

$$\frac{dm_1}{dt} = \pi \rho v_1 \left[\frac{m_1^{1/2} | x_1 - x_2 |}{m_1^{1/2} + m_2^{1/2}} \right]^2. \tag{10}$$

If the condensations start from rest, the constant in (9) is zero and so (10) and the corresponding expression for dm_2/dt are equal. Thus, during the encounter, both masses accrete equally and since the total mass of the accreted material greatly exceeds the masses of the initial condensations, it follows that the masses of the stars after the encounter are practically equal. If, however, the initial velocities are not zero, the accretion rates will be unequal and so some difference may be expected in the resulting masses. It is not possible to estimate the extent of this difference in general but a numerical integration of the equations for unequal initial masses with velocities of the required order has given resulting stars of mass-ratio 1 : 2. It is difficult without further investigation to say whether larger mass-ratios could be obtained, but this process can at any rate account for some differences between the masses of the components of the resulting binaries.

3.4. *Effect of initial lateral velocities.*—In the above treatment of the binary-forming encounter, the stars subsequently form a binary star whose components have highly elongated orbits. If the stars originally have slight lateral velocities off Ox, then the stars will follow paths which are curved but nevertheless close to Ox, so that the above treatment may still be expected to hold approximately and the resulting binary will have approximately the same energy in each case. However, the orbits of the resulting binaries will be elliptic or, in the extreme case, circular. It is important to find the maximum separation in such cases and this can be done by equating the energies of the different orbits. Consider a binary with an elongated orbit and one with a circular orbit. Let the stars be of equal mass m, and in the elongated orbit let the maximum separation be $2R$. Then the energy of the binary is $-Gm^2/2R$. In the circular orbit the energy is

$$\tfrac{1}{2}mv^2+\tfrac{1}{2}mv^2-\tfrac{1}{2}Gm^2/r,$$

where v is the velocity of each star and r is the radius of the orbit. But $v=(Gm/4r)^{1/2}$, as can be shown from the equation of motion for either star, so the energy is $-Gm^2/4r$. Equating these energies we have $R=2r$ so that in a binary-forming encounter, if the stars separate to $\frac{1}{2}d$ in the elongated case, they would separate to about $\frac{1}{4}d$ in the circular case and to intermediate distances in the elliptic case.

It is of interest to note that the angular momentum of the binary depends on the small initial velocities of the stars and on the inclination of these velocities to the line joining the stars. If inclinations up to 10° are permitted (and this seems reasonable), then the angular momentum can be shown to be of the same order as that of observed binaries. For example, if we let both stars (having the initial mass stated in the nth column of Tables I and II) have the maximum allowable initial velocities, and these are both inclined at 6° to the joining line, then the angular momentum of the resulting binary is

$$1\cdot 02\times 10^{48\cdot 5}\times 10^{1\cdot 5n}\,\mathrm{cm^2\,g\,sec^{-1}}\,(n=1,2,3,4),$$

i.e. in the range 10^{50} to 10^{54} cm^2 g sec^{-1}.

It is to be expected that the binary will interact further with the remaining interstellar material, with a consequent reduction in the separation of the components and in the eccentricity of their orbits; but it is not proposed to consider this subject here.

3.5. *Limitation of the elementary treatment.*—The principal weakness of the above elementary treatment is that the mass of accreted material is very much greater than the masses of the original stars. This means that the gravitational effects of the material which is to be accreted may well be greater to start with than the gravitation of the stars which is alone taken into account. In fact, the reason for giving the elementary treatment was to show that a straightforward application of the accretion theory to our model does not give a reliable picture of the situation and to indicate in which direction improvement should be sought.

4. *A more realistic model.*—We may now consider a more realistic model of this situation.

We suppose that stars are condensing at various points in the star-forming medium which is initially at rest. We do not propose to study the reasons why a star should form at any one point rather than at another, nor indeed why they should form at all. These are problems connected with the formation of single

stars. We merely take for granted that stars are in fact forming around various " centres of condensation ". In a completely homogeneous medium there are no (local) variations in the gravitational field. It is only when condensations begin to occur that these local variations develop and these variations in turn produce movements of the interstellar material which we shall now consider. Let two neighbouring centres of condensation A and B be situated a distance d apart. The magnitude of d is to be considered as of the same order as the average distance between condensations in the neighbourhood, but the distance from A to B is to be less than the distances of either of these points from any other centre of condensation. We shall first briefly describe the process we envisage and then we shall discuss its various aspects.

The material within the spheres EIHK and FLGJ (Fig. 1), which have centres at A and B, collapses under its self-gravitation to form stars at A and B. At the same time, the material in the cylinder EFGH collapses on to the axis AB, partly

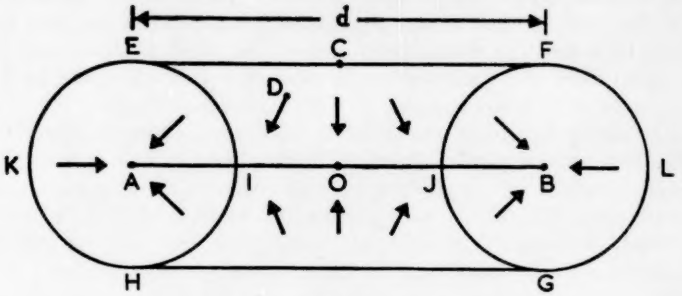

Fig. 1.

under its own gravitation but mainly under the gravitational influence of the condensations which are formed at A and B. As the material collapses on to the axis, collisions between the particles of the material occur and heat is generated and radiated away. In this way, energy is removed from the material along the axis and so it remains as a column of comparatively small section extending between the stars at A and B. The second stage of the process then occurs in which the stars at A and B move towards one another under their gravitational attraction. In so doing they move through the column of material and sweep it up. We shall show in the calculations below that this column offers substantial resistance to the motions of the stars which can easily remove sufficient energy from the stars to form them into a binary. The motion of A towards B will not quite be rectilinear due to the disturbing gravitational influence of the neighbouring stars. This influence makes the probability very small of a collision between A and B.

The first point which requires consideration is the size of the spheres EIHK and FLGJ. These are to be sufficiently small so that at points within one sphere the gravitational attraction of the material in the other is small. If the material inside EIHK collapsed purely under its self-gravitation, it would all arrive (as we shall see) at the centre A at the same time. This will not occur in reality because the particles at points like I on the surface of the sphere will be retarded due to the attraction of the material condensing at B. The size of the sphere is arbitrary but it is taken so that all the material in it will arrive at A at approximately the same

time in spite of the retardation of some of the material due to other centres of condensation. The sizes of the spheres need not be the same and they will depend on the number, sizes and proximity of neighbouring condensations.

A few words may be said on the behaviour of the material in the region EFJGHI. The process of collapse on to the axis is the same as the process established in the Bondi–Hoyle–Lyttleton accretion theory for the capture of interstellar material by stars. The difference in this case is that the column of material forms *ahead* of the stars instead of *behind* as in the accretion theory. The main point is that if the accretion process is possible, then so is this process, since it uses the same assumptions about the physical condition of the medium. In fact the column produced in this process is more stable than that of the accretion theory for if a particle strays from the axis, it immediately experiences a net force (due to A and B) tending to bring it back. The process by which each star sweeps up the material in the column is precisely the mechanism of Bondi and Hoyle as for a single star (i.e. the star " accretes " the material). It follows from this that the width of the column of material lying between the stars need not necessarily be as small as the diameter of the stars. It also follows that the stars can sweep up most of the material in the column, even if (as would be the case) the paths of the stars do not coincide with the axis of the column.

In considering the pair of stars A and B, we have seen how the material within ECFLGHK is predominantly influenced by the condensations at A and B. The neighbouring condensations produce a cut-off effect which determines the shape of the region which we have ideally represented by ECFLGHK, i.e. the region within which the material all collapses towards the axis AB. As regards the condensations and material beyond the immediate neighbourhood, we may expect their joint gravitational field to be negligible near AB if the condensations have formed from an originally uniform medium. If the medium was not originally uniform we may still expect this gravitational field to *vary* only slightly over the region ECFLGHK and it will therefore have a negligible effect on the processes outlined above.

For the purpose of the calculations, the radii of the spheres EIHK and FLGJ have both been taken as $\frac{1}{4}d$. It is quite possible that material outside the region EFLGHK also is attracted and is involved in the process. It will be shown, however, that such material will not to any extent reduce the likelihood of binary formation.

4.1. *Time of collapse of a sphere of material.*—Our first calculation is to determine the time the material in the sphere EIHK takes to collapse assuming a free fall of the material under its self-gravitation. If we consider a particle originally at rest at a distance R from A, then it is attracted towards A by a force which is the same as if all the material within a sphere of radius R were concentrated at A. This force, when the particle is at a distance r from A, is $\frac{4}{3}G\pi R^3\rho/r^2$. By integrating the equation of motion we obtain the velocity v of the particle,

$$\tfrac{1}{2}v^2 = \tfrac{4}{3}G\pi R^2\rho(R/r-1),$$

then the total time for the fall of the particle to A is

$$\begin{aligned}\int_0^R \frac{dr}{v} &= (3\pi/32)^{1/2}(G\rho)^{-1/2}\\ &= 0{\cdot}543(G\rho)^{-1/2}, \qquad (11)\end{aligned}$$

which is independent of R, so that all the particles reach A at the same time.

In our initial statement of the process it was implied that the stars condense at A and B and then begin to attract each other. In fact, of course, the attraction begins as soon as any sort of condensation occurs at A and B. We can show, however, that the condensations move a negligible distance in the time (11). The distance moved from rest by A in time t is $\frac{1}{2}ft^2$, where f is the acceleration. If all the material in the sphere FLGJ is considered concentrated at B, then $f=\frac{4}{3}G\pi(d/4)^3\rho/d^2$, and putting t equal to (11), we have $\frac{1}{2}ft^2=0\cdot0096d$.

4.2. *Time of collapse of cylindrical region.*—In order to obtain an estimate of the time required for the region EFJGHI to collapse we shall calculate the time required for a particle at C to fall to the centre O under the influence of the material in the spheres EIHK and FLGJ on the assumption that this material attracts as if it were all concentrated at A and B respectively. At any time t let y be the distance from AB of the particle, originally at C, and let v be its velocity. The acceleration of the particle at this time, due to the attraction of A and B, is

$$\frac{2G.\frac{4}{3}\pi(\frac{1}{4}d)^3\rho}{y^2+(\frac{1}{2}d)^2}\cdot\frac{y}{(y^2+(\frac{1}{2}d)^2)^{1/2}}.$$

Integration of the equation of motion gives

$$\tfrac{1}{2}v^2=2G\,.\,\tfrac{4}{3}\pi(\tfrac{1}{4}d)^3\rho[(\tfrac{1}{4}d^2+y^2)^{-1/2}-(\tfrac{1}{4}d^2+y_0^2)^{-1/2}],$$

y_0 being the initial value of y, i.e. $\frac{1}{4}d$. The time for the particle to fall from C to O is

$$\int_0^{d/4}\frac{dy}{v}.$$

This was evaluated numerically and was found to be

$$1\cdot74(G\rho)^{-1/2}. \tag{12}$$

This must be compared with the time required for the star A or B to fall to O. We can obtain a lower limit of this by assuming that these stars experience no resistance. It can easily be shown that the time required for two particles each of mass $\frac{4}{3}\pi(\frac{1}{4}d)^3\rho$ to come together from rest at a separation d is

$$(3\pi)^{1/2}(G\rho)^{-1/2}=3\cdot07(G\rho)^{-1/2}. \tag{13}$$

So, as (12) is little more than half (13), it is seen that the cylindrical region EFJGHI has adequate time to collapse before the separation of the stars is appreciably reduced. If we had taken the self-gravitation of the cylindrical region into account, the time of collapse would have been even shorter.

4.3. *The approach of the stars.*—We must now consider what happens when the stars approach one another and encounter the column of material. We shall assume that the stars move under their mutual attraction and that they capture all the material in the column as they move through it. To start with, we shall assume that the material is uniformly distributed in the column which extends from A to B. We shall suppose the mass of material per unit length of column is a. Then considering the axis Ox to be coincident with AB, the coordinate of B is $+\frac{1}{2}d$. Writing down the equations for the star B we obtain equation (2) as in Section 2. We also have

$$\frac{d(mv)}{dt}=-\frac{Gm^2}{4x^2},\quad \frac{dm}{dt}=a\,|\,v\,|.$$

Since v is negative

$$\frac{dm}{dx} = -a$$

and so
$$m = -ax + M, \tag{14}$$
where M is the mass of the star when it reaches the origin. The equation for v^2 becomes

$$\frac{dv^2}{dx} - \frac{2av^2}{M-ax} = -\frac{G(M-ax)}{2x^2},$$

of which the solution is

$$v^2 = \frac{G}{2(M-ax)^2}\left[\left(\frac{M^3}{x} + 3M^2a\ln x - 3Ma^2x + \tfrac{1}{2}a^3x^2\right) + A\right], \tag{15}$$

the constant A being determined by the fact that $v=0$ when $x=\frac{1}{2}d$. Now the total energy (kinetic + potential) of the two stars at any instant is

$$(M-ax)v^2 - G(M-ax)^2/2x,$$

and using (15) this becomes

$$\frac{G}{2(M-ax)}[3M^2a\ln x + \tfrac{3}{2}a^3x^2 - 6Ma^2x + 3M^2a + A].$$

In this, as $x \to 0$, the logarithmic term predominates and becomes large and negative. Consequently, the total energy of the pair of stars becomes greatly reduced so that they cannot again separate. If the stars were to continue to collect material until they get right to O, then $\ln x \to -\infty$ and the stars would be unable to separate at all. Furthermore, this would occur however small is a. We suppose in reality that the process breaks down before O is reached. This could be caused by the stars being slightly deflected off Ox by the gravitational field of neighbouring stars. To take a particular example, suppose the process discontinues when the stars are $\frac{1}{8}d$ apart, then their subsequent separation would not exceed $0{\cdot}39d$. (In making this calculation, we used $a = M/d$, which is what it would be if the material in EFJGHI were uniformly distributed along AB.)

The above analysis is based on the assumption that the material in the column remains at rest until it is collected by one of the stars. This assumption is invalid for two reasons. In the first place, when the material first collapses on to the axis, most of it (e.g. particle D in Fig. 1) will have a velocity component along the axis away from O. The effect of this is that the stars will be encountering material moving against them. They will therefore lose more momentum than in our treatment and consequently this treatment does not overestimate the resistive effect of the material column. In the second place, we have ignored the gravitational interaction between the stars and the unaccreted parts of the column. This is a difficult factor to assess, but it seems to be an effect which would largely cancel itself. For, consider the star A: at the beginning of its approach towards O, it will be attracted by the material in the column and this will cause its momentum to be increased. However, the material in the column (to the left of O) will be attracted by A and will begin to move towards A. Consequently, when the material collides with A, the momentum which A originally gained will largely be lost in destroying the momentum of the material.

A close examination of the above analysis shows that the occurrence of the logarithmic term depends on the assumption of a uniform column. However,

this is not essential to the process; all that is necessary is that material is captured by the stars sufficiently close to the origin O. This explains why material from outside EFLGHK cannot appreciably affect the process. The physical principle involved is simple: it is that if a mass L moving with velocity U collides with and captures a mass l at rest, then the energy loss is $\frac{1}{2}LlU^2/(L+l)$, which is large if U is large. The velocities of the stars $\rightarrow \infty$ as they approach O.

4.4. *Comparison with the previous process.*—In comparison with the binary-forming encounter considered in Sections 2 and 3, in this process there is no limit on the initial masses of the stars which condense at A and B. Also, the mass of material subsequently captured is of the same order as the initial masses of the stars so that the possibility of a star having a second chance to form a binary is not ruled out. Nevertheless it seems likely that a process of the type here considered could only have been important at a very early stage in the evolution of the stars. In this process it seems quite possible that any reasonable mass ratio of the binary components could be obtained. Although more of the interstellar material is used up in the process, a good percentage is left for further effects.

5. *Conclusion.*—In putting forward this mechanism for binary star formation it is hoped that it will indicate a way by which binary stars can be formed from the star-forming medium without the postulation of very close initial condensations.

It remains for me to express my thanks to Professor W. H. McCrea for his help and encouragement during the development of the work contained in this paper. The idea of binary stars being produced as a result of the resisted motion of single stars through interstellar material was first conceived by Professor McCrea and it was this idea that led to the present work.

Royal Holloway College,
Englefield Green, Surrey:
1954 *June* 28.

References

(1) J. Jeans, *The Universe Around Us*, fourth edition, p. 232, Cambridge, 1945.
(2) R. A. Lyttleton, *The Stability of Rotating Liquid Masses*, Cambridge, 1953.
(3) K. N. Dodd, *Proc. Camb. Phil. Soc.*, **49**, 486, 1953.
(4) F. Hoyle and R. A. Lyttleton, *Proc. Camb. Phil. Soc.*, **35**, 410, 1939.

TOPOCENTRIC LIBRATIONS FOR AN ECLIPSE STATION

C. A. Murray

(Communicated by the Astronomer Royal)

(Received 1954 November 12)

Summary

The selenographic coordinates of an observer who is instantaneously on the axis of the Moon's shadow during a solar eclipse are diametrically opposite to those of the Sun. The latter, and hence the former, may be obtained directly from the *Nautical Almanac*. The present paper gives a short method for computing differential corrections to these coordinates, giving the topocentric librations for any eclipse station. The method makes use of computations which will have been made in any case for the prediction of the local circumstances of an eclipse.

In a recent paper (1), Atkinson has given a simple method for computing the topocentric librations and the position angle of the Moon's axis appropriate to any lunar observation. His method is to apply parallactic corrections to the geocentric librations (" Earth's selenographic longitude and latitude ") which are tabulated in the *Nautical Almanac*.

In the case of solar eclipse observations the computation may be shortened by making use of the selenographic coordinates of the Sun instead of those of the Earth. The former are readily obtainable from the *Almanac* by linear interpolation, whereas the latter require second differences at least. For an observer who is instantaneously on the axis of the shadow, i.e. one for whom the eclipse is central at the instant of the observation, the topocentric librations are diametrically opposite to the selenographic longitude and latitude of the Sun. Accordingly if l_0, b_0 are the topocentric librations for this observer,

$$l_0 = 270^\circ - \text{Sun's selenographic colongitude,}$$
$$b_0 = \quad - \text{Sun's selenographic latitude.}$$

The topocentric position angle of the Moon's axis may be obtained from the general formulae, given in the N.A. " Explanation " from 1931 to 1941, modified to take account of the circumstances peculiar to eclipses. The most suitable form of the general formula for C', the position angle of the Moon's axis without physical libration, is

$$\sin C' = -\sin i \cos(\alpha - \Omega')\sec b', \tag{1}$$

where α is the topocentric R.A. of the Moon, b' the optical libration in latitude, and i, Ω', are mean elements of the Moon's equator tabulated in the *Almanac* at ten-day intervals. No sensible error is caused by writing $\sec b' = 1$ in computing C_0', the value of C' for the observer on the axis of the shadow. Also, for this observer,

$$\alpha = \text{Greenwich sidereal time} - \mu,$$

where μ, the Greenwich hour angle of the point on the celestial sphere toward which the axis of the shadow is directed, is tabulated at ten-minute intervals throughout the eclipse. Accordingly we compute C_0' from

$$\sin C_0' = -\sin i \cos (\text{G.S.T.} - \mu - \Omega'). \tag{2}$$

The formula for the physical libration of the Moon's axis reduces in the present case to

$$C'' = -0^\circ{\cdot}020 \cos (\Gamma' - \Omega + 2l') \mp 0^\circ{\cdot}003, \tag{3}$$

since the libration in latitude must be nearly zero and the Moon near one of its nodes. Γ', Ω are mean elements of the Moon's orbit tabulated at ten-day intervals in the *Almanac* and l' is the optical libration in longitude. It is sufficient to substitute l_0 for l' in (3). The upper or lower sign in (3) is to be taken according as the Moon is near the ascending or descending node. The topocentric position angle of the Moon's axis for the observer on the axis of the shadow is then

$$C_0 = C_0' + C'', \tag{4}$$

where C_0' and C'' are computed from (2) and (3) respectively.

The topocentric librations and position angle of the Moon's axis for an observer who is situated at any point where the eclipse is visible may be obtained by the application of differential corrections to l_0, b_0 and C_0.

Let
$$l = l_0 + \Delta l',$$
$$b = b_0 + \Delta b'$$

be the topocentric librations for this general observer; $(\Delta l', \Delta b')$ are then the coordinates of the centre of the apparent lunar disk, with respect to the point on the lunar surface which is on the axis of the shadow (i.e. the centre of the apparent disk for the observer on the axis of the shadow).

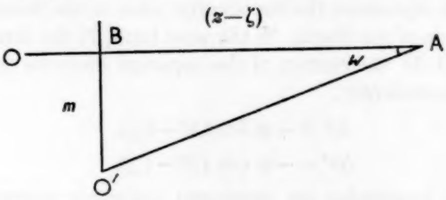

FIG. 1.

In Fig. 1, let O be the observer on the axis of the shadow, O′ the general observer, A the Moon's centre, and B the intersection of the axis of the shadow OA with the plane through O′ perpendicular to OA. In the usual Besselian coordinate system and notation,

$$x - \xi = m \sin M,$$
$$y - \eta = m \cos M \tag{5}$$

are the coordinates of B with respect to O′, and the distance AB is $(z - \zeta)$. Let w be the angle O′AO, then

$$\tan w = \frac{m}{z - \zeta} \tag{6}$$

and the total change in optical libration in moving from O to O′ is w in position angle $M + 180^\circ$. With an error not exceeding 4 parts in 10^4 we may write

$$z = \operatorname{cosec} \pi_{\text{☾}}$$

where $\pi_{☾}$ is strictly the Moon's equatorial horizontal parallax at the instant of observation, but may be taken as the value for the time of conjunction in R.A. of the Sun and Moon which is given under " Elements of the Eclipse " in the *Almanac*. Also, since $z \simeq 60$, $|\zeta| \leqslant 1$ and $m < 0{\cdot}6$ we may write (6) as

$$w = m\pi_{☾} \tag{7}$$

with a maximum error of $0^{\circ}{\cdot}01$. This is sufficiently accurate for all purposes at the present time. (See Atkinson, *loc. cit.* p. 452.)

Since the libration in latitude is nearly zero the extremities of the Moon's axis of rotation are for all practical purposes on the apparent limb.

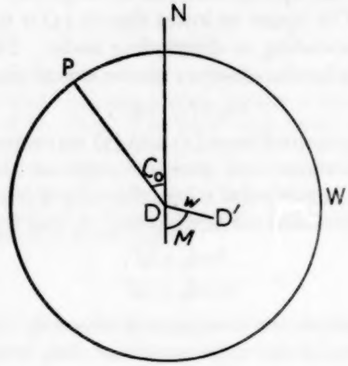

FIG. 2.

In Fig. 2, which represents the topocentric view of the Moon for the observer O, P is the north pole of the Moon, W the west limb, N the direction of the north celestial pole, and D, D′ the centres of the apparent disks for the observers O, O′ respectively. Then evidently,

$$\begin{aligned} \Delta l' &= +w \sin (M - C_0), \\ \Delta b' &= -w \cos (M - C_0), \end{aligned} \tag{8}$$

since selenographic longitudes are measured positively towards the west limb and latitudes towards the north. Combining (5) and (7) with (8) we have

$$\begin{aligned} \Delta l' &= +\pi_{☾} \{(x-\xi) \cos C_0 - (y-\eta) \sin C_0\}, \\ \Delta b' &= -\pi_{☾} \{(x-\xi) \sin C_0 + (y-\eta) \cos C_0\}. \end{aligned} \tag{9}$$

The change in the topocentric R.A. of the Moon in moving from O to O′ is evidently

$$\Delta\alpha = \pi_{☾} (x-\xi) \sec d,$$

where d is the declination of the point on the celestial sphere toward which the axis of the shadow is directed. Hence, logarithmic differentiation of (1) gives the change in the topocentric position angle of the Moon's axis

$$\Delta C' = -\pi_{☾} (x-\xi) \sec d \tan (\text{G.S.T.} - \mu - ☊') \tan C_0' \tag{10}$$

neglecting a small term in $\Delta b' \tan b'$.

The main disadvantage of the above method is the necessity for computing C_0 from first principles. If this were tabulated in the *Almanac* at intervals during the eclipse the work would be considerably shortened.

The method has advantages over Atkinson's method even when C_0 has to be computed. It makes use of quantities derived in the course of the prediction of the local circumstances, instead of requiring the computation of the apparent zenith distance, parallax and parallactic angle of the Moon. Although it requires the same number of interpolations from the *Nautical Almanac* (in addition to those needed in the course of the prediction), these are all linear, whereas at least three of the quantities in Atkinson's method, the geocentric librations and position angle of the Moon's axis, require second differences.

In conclusion I wish to thank Mr D. H. Sadler for his helpful criticisms of this paper.

Royal Greenwich Observatory,
Herstmonceux Castle,
Hailsham,
Sussex:
1954 *November* 10.

Reference

(1) R. d'E. Atkinson, "The Computation of Topocentric Librations", *M.N.*, 111, 448, 1951.

A PHOTOELECTRIC STUDY OF EARLY-TYPE SUPERGIANTS AROUND h AND χ PERSEI

M. K. Vainu Bappu

(Communicated by the Director, Nizamiah Observatory)

(Received 1954 November 29)

Summary

Photoelectric colours and magnitudes for thirty early-type stars, classified as supergiants belonging to the double cluster in Perseus, have been determined with the aid of the Lick 12-inch refractor. Measures of four stars in Harvard Standard Region C12 were used for the tie-in to the (P, V) system.

A general increase of absorption is found as one passes from h to χ Persei, in accordance with the earlier conclusions of Miss Pismis. A considerable non-uniformity of interstellar absorption exists around the cluster.

The supergiants of type B2 and the B0, B0·5, B1 and B2 stars of luminosity class III yield a distance modulus of $11^{m}{\cdot}7$ for the cluster of supergiants, corresponding to a distance of 2·2 kps. Using the new value of the distance modulus, absolute magnitudes have been calculated for supergiants of other spectral classes. The number of stars used in this investigation is too few to give an estimate of the dispersion in M_v for these early-type supergiants.

Highly luminous early-type stars are generally too far away from the Sun to give a reliable determination of their absolute magnitudes from parallax data. We therefore resort to the study of magnitudes and colours of objects of this kind that form part of large stellar aggregates with known distance moduli. The double cluster in Perseus, the Orion aggregate and NGC 6231 have, more or less, a fair sample of such supergiants. The double cluster in Perseus, however, contains a larger number of B and A type supergiants than the other two. It also contains a few very luminous stars of type M. It is natural, therefore, that our knowledge of the absolute magnitudes of these objects, and their dispersion in luminosity, should rest heavily on the results that can be derived from this cluster.

Much of our knowledge concerning the remarkable cluster of supergiants around h and χ Persei depends on a thorough investigation by Bidelman (**1**). He employed the MKK system of classification and separated the likely cluster members from the field supergiants. More recently Morgan, Whitford and Code (**2**) have provided more accurate classes on the MK system for some of the cluster members sorted out by Bidelman.

It is the purpose of this investigation to determine accurate magnitudes and colours for those supergiants belonging to h and χ Persei which can be " resolved " by a photoelectric photometer on a visual refractor of medium focal length.

The photoelectric observations of colours and magnitudes for 30 supergiants in and around the double cluster were carried out on four nights in 1952 September using the 12-inch refractor of Lick Observatory. The photometer employed a

1P21 photomultiplier tube, the output of which was amplified by a d.c. amplifier, designed by Kron, and fed into a Brown recorder. The filters used were Corning 5562 and 3385 giving effective wave-lengths of approximately 4200 A and 5200 A respectively. The deflections were obtained in the order blue, yellow, blue, followed by readings on the sky in the two colours. Also, deflections caused by a standard source provided a check on the stability of the overall response of the system. Mean extinction coefficients determined from Mount Hamilton extinction data gathered over several years were utilized in the reductions. Nightly extinction coefficients were also derived by Eggen's method (3) for three of the four nights, and these proved to be very close to the mean coefficients used. The reductions were carried out using the mean extinction coefficients as well as the values determined observationally for the night under consideration. No sensibly different values were obtained for magnitudes or colours, and hence the mean extinction values were used throughout finally.

The instrumental magnitudes m_L and colours C_L were transformed to the (P, V) system by means of nightly comparisons with stars A, C, D, F of Eggen's photoelectric sequence (4) in the Harvard Standard Region C12. While the V magnitudes used were those of Eggen, the $P-V$ values used were revised values, kindly supplied by Dr Kron in advance of publication. The transfers were made every night when C12 and the double cluster had nearly the same zenith distance. The transformation equations used are the following:—

$$P-V=A+BC_L, \qquad (1)$$

$$V=m_L+D+F(P-V), \qquad (2)$$

where

$$A=0\cdot417\pm0\cdot012,$$

$$B=1\cdot055\pm0\cdot005,$$

$$D=6\cdot494\pm0\cdot003,$$

$$F=-0\cdot116\pm0\cdot006.$$

From the individual values of V and $P-V$ obtained each night for the stars under observation the probable errors for one observation were found to be

$$P-V\ :\ \text{p.e.}=\pm0^{\text{m}}\cdot009,$$

$$V:\ \text{p.e.}=\pm0^{\text{m}}\cdot012.$$

In Table I are listed the relevant data for the stars included in this investigation. The first column contains the HD number, the BD number being given for one star not listed in the *Henry Draper Catalogue*. The second and third columns list the observed magnitudes V and colours $P-V$, these being means of three or four observations (rarely only two) on separate nights. Column 4 contains information on the spectral types; those with asterisks are due to Bidelman, the rest have been recently classified by Morgan (2) on the MK system. Finally in column 5 we have the colour excesses derived from the intrinsic colours of unreddened stars, on the (P, V) scale, as transformed from the (B, V) values given by Morgan, Harris and Johnson (5).

The available sources of reliable magnitudes or colours in the h and χ Persei region are the investigations of Wallenquist (6), Oosterhoff (7), and Stebbins, Huffer and Whitford (8). Fourteen stars in Table I have also been included in Wallenquist's photoelectric studies. Assuming that Wallenquist's system of

TABLE I

Colours and magnitudes of early-type supergiants around the double cluster

HD Number or BD Number	*V*	*P−V*	Spectral type	Colour excess	Remarks
12856	8·61	+0·08	*B0·5 ne	0·56	MWC 25
12953	6·73	+0·45	A1 Ia	0·59	
13051	8·75	−0·01	*B0·5	0·47	MWC 27
13267	6·42	+0·17	B5 Ia	0·52	
13476	6·49	+0·46	A3 Iab	0·54	
13744	7·65	+0·60	A0 Iab	0·77	
13621	8·17	−0·09	*B0·5	0·57	ADS 1714
13745	7·94	+0·01	B0 III	0·51	
13841	7·46	+0·08	B2 Ib	0·52	
13854	6·54	+0·13	B1 Iab	0·59	MWC 31
56° 473	9·13	+0·09	*B1n	0·55	MWC 441
13866	7·57	+0·05	B2 Ib	0·49	
13900	9·26	+0·02	*B1n	0·48	
13969	8·86	+0·15	*B1	0·61	
14250	9·01	+0·20	*B2n	0·64	
14322	6·82	+0·18	B8 Ib	0·45	
14321	9·31	+0·15	*B2	0·59	
14422	8·96	+0·36	*B1ne	0·82	MWC 37
14433	6·45	+0·42	A1 Ia	0·56	
14434	8·57	+0·04	*O7n	0·56	
14476	8·79	+0·25	*B0·5	0·73	
14520	9·23	+0·10	*B1	0·56	ADS 1810
14535	7·56	+0·57	A1 Ia	0·71	
14542	7·03	+0·47	B8 Ia	0·74	
14818	6·28	+0·15	B2 Ia	0·59	
14899	7·47	+0·29	*A0	0·46	
14956	7·26	+0·58	B2 Ia	1·02	
15316	7·29	+0·64	A3 Iab	0·72	
15497	7·08	+0·63	B6 Ia	0·96	
14143	6·70	+0·34	B2 Ia	0·78	

* Spectral classification by Bidelman. Those not starred are due to Morgan (2).

magnitudes and colours can be converted to the (P, V) system by a linear transformation, we get the following relations, by least squares, using stars fainter than $9^{\mathrm{m}}{\cdot}0$ for the purpose:

$$P = m_{\mathrm{pe}} + 0{\cdot}037 - 0{\cdot}140\ (P - V), \tag{3}$$

$$P - V = 0{\cdot}119 + 0{\cdot}966\ C_{\mathrm{pe}}. \tag{4}$$

A similar procedure for Oosterhoff's photographic magnitudes gives the relation

$$P = m_{\mathrm{pg}} + 0{\cdot}051 + 0{\cdot}163\ (P - V). \tag{5}$$

The values derived from equations (3), (4) and (5) are compared with those from Table I in Fig. 1. The central diagram of Fig. 1 shows that equation (4) is a good approximation, as the colour differences between the two photoelectric systems are negligibly small over the range of magnitudes observed. Below magnitude 9·0 a randomness sets in in the measures that might be considered to indicate the rapid approach of the limiting magnitude for accurate measurement with Wallenquist's experimental arrangement. The two magnitude systems, on the other hand, are not completely described by equations (3) and (5). The

similarity between the trends in the upper and lower diagrams of Fig. 1 is probably due to the heavy weighting of Wallenquist's scale and zero point with the aid of Oosterhoff's magnitudes.

Twenty-two stars in Table I have colours on the C_1 scale measured by Stebbins, Huffer and Whitford. These colours can be transformed to the (P, V) system by the linear relation

$$P-V=0.199+1.722\ C_1. \tag{6}$$

There is, however, a large scatter among the points. A better fit is obtained by the curve

$$P-V=0.208+1.833\ C_1-1.042\ C_1^2. \tag{7}$$

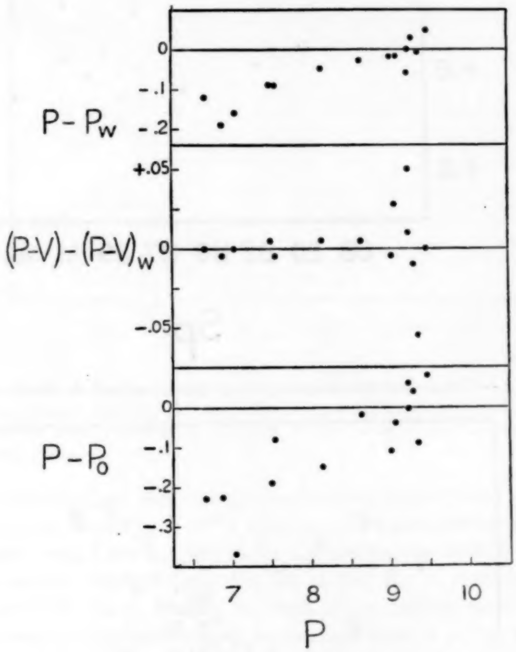

FIG. 1.—*Comparison of the photoelectric observations with the results of Wallenquist and Oosterhoff.* P_W, $(P-V)_W$ *and* P_O *are calculated values using equations* (3), (4) *and* (5) *respectively.*

A plot of observed colours against spectral type, as seen in Fig. 2, shows the non-uniformity of interstellar absorption around the double cluster. Fig. 3 shows the variation of colour excess (100× colour excess is plotted) over the region containing the two clusters. There is a general increase of absorption as one passes from h to χ Persei, in agreement with the results of Miss Pismis (**9**); and superimposed on this is the irregular variation caused by a patchy distribution of the absorbing clouds. Consequently, any observed colour-magnitude array would show a large dispersion in values along any of the sequences of interest.

In Fig. 4, I have plotted apparent visual magnitudes corrected for interstellar absorption (2·8× colour excess) against spectral type for the stars listed in Table I.

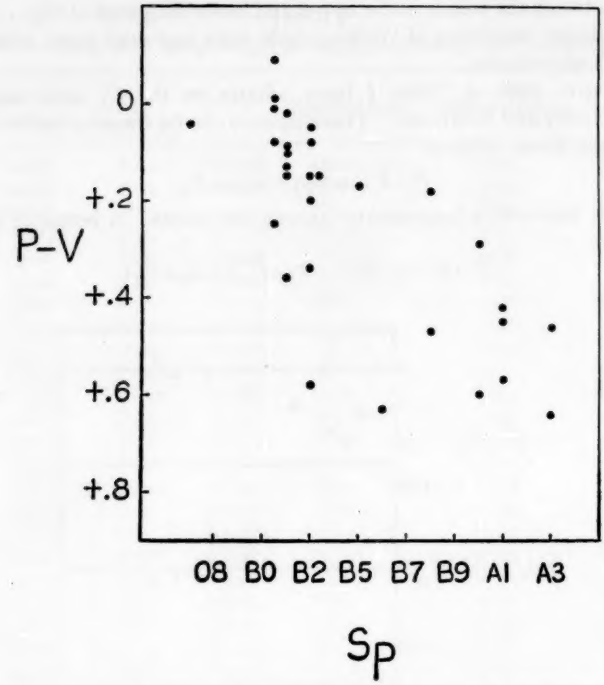

FIG. 2.—*Colour-spectrum diagram for supergiants around the double cluster.*

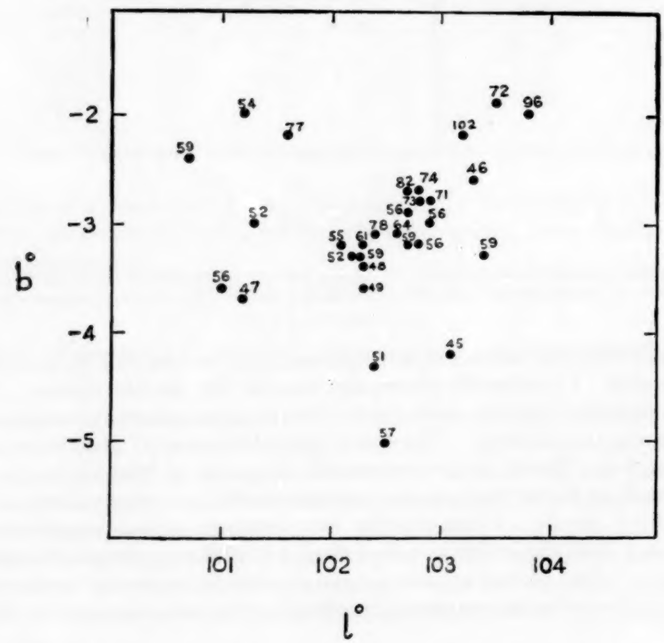

FIG. 3.—*Variation of colour excesses in the region around h and χ Persei. The figures shown are* 100 × *colour excess.*

The solid dots represent stars classified by Morgan, while the circles indicate the remaining stars having Bidelman spectral types. The trend followed by the stars of luminosity class I clearly shows that it may be reasonable to assume some of the stars classified by Bidelman to fall in the category of luminosity class III.

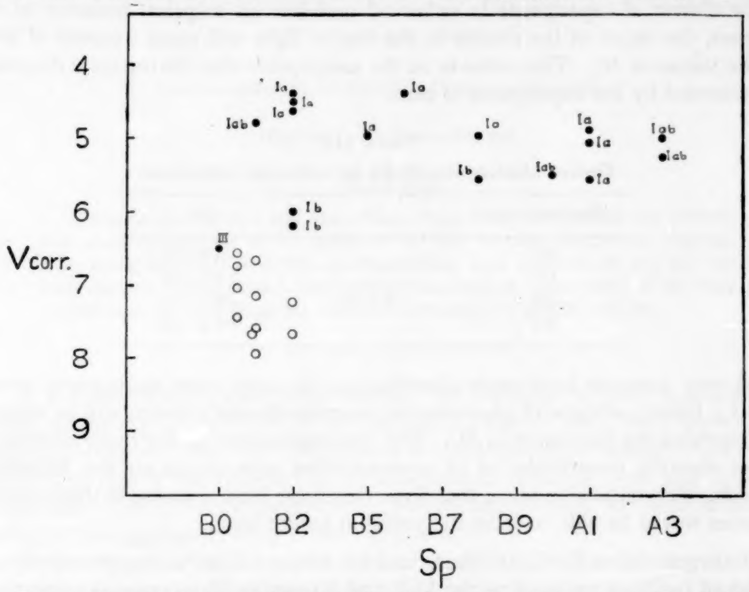

FIG. 4—*V magnitudes, corrected for interstellar absorption, for supergiants around h and χ Persei. Filled circles are for stars classified by Morgan, while the open circles represent stars having Bidelman spectral classes.*

Adopting this assumption, and using the absolute magnitudes given by Keenan and Morgan (**10**) corrected by $-0^{m}\cdot 1$ to bring them in accordance with the visual magnitudes used here, I get the values for the distance moduli given in Table II. The distance moduli derived from the B2 Ia and B2 Ib stars agree remarkably well with those of B0, B0·5, B1 and B2 stars of luminosity class III. Assuming then that the distance modulus of the B-star aggregate is $11^{m}\cdot 7$, we get the values of absolute magnitudes given in Table III for the other spectral types. The quantity in parentheses after each value of M_v indicates the number of stars used for its determination. It becomes apparent from Table III as well as from Fig. 4 that the absolute magnitudes of the super-giants of class Ia do not possess the

TABLE II

Determination of distance modulus of the cluster of supergiants around h and χ Persei

Spectral type	$\overline{m}_v$	M_v	$\overline{m}_v - M$
B0·5 III	6·95	−4·5	11·45
B1 III	7·40	−4·4	11·80
B2 III	7·44	−4·2	11·64
B2 Ia	4·51	−7·1	11·61
B2 Ib	6·10	−5·8	11·90
		Mean $\overline{m}_v - M = 11\cdot 7$	

same values for all spectral types. A decrease in M_v from B2 to A2 is quite noticeable. This cluster contains very few stars to permit a reliable study of the dispersion in M_v among the early-type supergiants. Nevertheless it does appear that the intrinsic dispersion may be much smaller than is generally assumed. If the cluster of supergiants is spherical and has an angular diameter of four degrees, the depth of the cluster in the line of sight will cause a scatter of $0^m\cdot 15$ in the values of M_v. This value is on the assumption that the intrinsic dispersion experienced by the supergiants is zero.

TABLE III

Derived absolute magnitudes for early-type supergiants

Spectral type	Ib	Ia
B5		−6·7 (1)
B6		−7·3 (1)
B8	−6·1 (1)	−6·7 (1)
A1		−6·5 (3)

A very accurate luminosity classification of many more supergiants around h and χ Persei, along with photoelectric magnitudes and colours, will be required to determine the dispersion in M_v. The ideal regions for getting more information about absolute magnitudes of all representative supergiants are the Magellanic Clouds. It is natural to hope, therefore, that those having access to these external galaxies would be able to solve the problem before long.

I am grateful to Dr C. D. Shane and Dr Akbar Ali for having generously provided all facilities for work at the Lick and Nizamiah Observatories respectively. It is a pleasure to acknowledge indebtedness to Drs Kron, Bok and Miczaika for critical discussions, and to Mr M. Ramanathan of the Nizamiah Observatory for having carried out a major portion of the reductions.

Nizamiah Observatory,
Begampet, Hyderabad,
Deccan, India:
1954 *October* 1.

References

(1) W. Bidelman, *Ap. J.*, **98**, 61, 1943.
(2) W. Morgan, A. Whitford and A. Code, *Ap. J.*, **118**, 318, 1953.
(3) Olin J. Eggen, *Ap. J.*, **111**, 65, 1950.
(4) O. J. Eggen, *Ap. J.*, **114**, 141, 1951.
(5) W. Morgan, D. Harris and H. L. Johnson, *Ap. J.*, **118**, 92, 1953.
(6) Ake Wallenquist, *Uppsala Astronomiska Observatoriums Annaler*, **3**, No. 2, 1949.
(7) P. Th. Oosterhoff, *Leiden Annals*, **17**, 5, 1937.
(8) J. Stebbins, C. M. Huffer, and A. Whitford, *Ap. J.*, **91**, 20, 1939.
(9) Paris Pismis, *Harv. Bull.*, No. 915, 1941.
(10) P. C. Keenan and W. Morgan, *Astrophysics* (ed. J. A. Hynek), p. 23, McGraw-Hill, 1951.

MAGNITUDES AND COLOURS OF SOME MEMBERS OF THE PERSEUS CLUSTER

M. K. Vainu Bappu

(Communicated by the Director, Nizamiah Observatory)

(Received 1954 November 29)

Summary

Photoelectric colours and magnitudes have been determined for twenty-five stars considered to be members of the moving cluster in Perseus. A distance modulus of $6^{m}.83$, corresponding to a distance of 230 ps, has been derived. This value is nearly twice the value of 120 ps derived by Miss Roman and Morgan from the upsilon component of proper motion.

In a recent investigation, Miss Roman and Morgan (1) have examined the visual clustering around the F5 supergiant α Persei. They have shown that twenty-five stars of types B3 to A2 appear to share the space motion of the supergiant, and that a fair correlation exists between spectral type and apparent magnitude. The evidence provided by Roman and Morgan seems to favour the reality of this aggregate being a moving cluster.

Earlier, Smart and Ali (2) examined a list of 48 stars spread out over a large area of the sky and which had been ascribed to the moving cluster. They concluded " (*a*) that a considerable proportion of the stars in the so-called Perseus cluster cannot belong to a moving cluster, and (*b*) that a nucleus of stars remains which may possibly be regarded as a cluster formation ". Roman and Morgan comment that if α Persei, or some B stars of the visual clustering around the supergiant, had been considered as representatives of the group by Smart and Ali, the reality of this smaller group would have been easily noticed.

To settle the question of the existence of the Perseus moving cluster definitely, one would need reliable radial velocities and a homogeneous set of proper motions, which do not exist at present. Establishment of an accurate colour-magnitude array would decide whether the stars form part of a cluster. Whether they are members of a moving cluster can be determined only if a distance modulus (easily derivable from the colour-magnitude array) agrees, within the usual limits of tolerance, with that determined dynamically. In this paper a magnitude-spectral type diagram plotted from photoelectric data gives us a distance modulus for the cluster.

Twenty-five stars that were shown to be definite cluster members by Roman and Morgan have been included in this study. The photoelectric observations were made on three nights in 1952 September with the 12-inch refractor of Lick Observatory. The observational procedure and method of reduction are similar to those described in an earlier paper (3). Thirteen stars of this list have only one observation each. The consistency of the $P-V$ and V values derived for the remaining twelve stars indicates that there is no lack of observational accuracy in the colour and magnitude values derived from a single observation. One source

of error, however, may exist, and that is the recording of the sensitivity of the amplifier for the single observation. The Lick 12-inch photometer has gain-switch positions which change in steps of half a magnitude and, consequently, a mistake in recording will tend to alter the star's V value by $\pm 0^m \cdot 5$, while $P-V$ value remains unchanged. The magnitudes obtained in this paper agree with those derived by Roman and Morgan without any serious discordances; thus such a source of error can scarcely exist. The tie-in with the (P, V) system was effected by nightly comparisons with C12, where the V values were those given by Eggen (4) and the $P-V$ values were revised values kindly supplied by Dr Kron in advance of publication. The probable errors for a final value of V and $P-V$ are the following:

$$P-V : \text{p.e.} = \pm 0^m \cdot 008,$$
$$V : \text{p.e.} = \pm 0^m \cdot 011.$$

Table I gives the magnitudes and colours of the cluster members investigated. The colour excesses have been computed by using the intrinsic $B-V$ colours of

TABLE I

Magnitudes and colours of members of the moving cluster in Perseus

Star	V	$P-V$	No. of obs.	Spectral type	E	V_{corr}	M
HD 20365	5·20	−0·20	2	B3 V	0·19	4·69	−2·1
HD 20418	5·08	−0·19	2	B5 V	0·16	4·63	−2·2
HD 20391	8·01	0·00	3	A1 V	0·14	7·62	+0·8
HR 1011	5·38	−0·20	2	B5 V	0·15	4·96	−1·8
HR 1029	6·13	−0·21	2	B6 V	0·12	5·79	−1·0
HR 1034	5·03	−0·22	3	B3 V	0·17	4·55	−2·2
HD 21375	7·55	−0·03	3	A1 V	0·11	7·24	+0·4
HD 21479	7·36	−0·05	2	A2 V	0·06	7·19	+0·4
34 Per	4·72	−0·24	2	B3 IV	0·15	4·30	−2·5
HR 1037	5·65	−0·19	2	B6 V	0·14	5·26	−1·5
HD 21481	7·70	−0·00	2	A0 V	0·17	7·22	+0·4
HR 1051	5·87	−0·17	2	B8 IV	0·10	5·59	−1·2
HD 20701	8·43	−0·03	1	A1 V	0·11	8·12	+1·3
HD 22401	7·50	−0·12	1	A0 V	0·05	7·36	+0·6
HD 20961	7·74	−0·03	1	A0 V	0·14	7·35	+0·6
HD 21091	7·60	−0·11	1	A0 V	0·06	7·43	+0·6
HD 21181	6·88	−0·13	1	B9 V	0·11	6·57	−0·2
HD 21398	7·44	−0·12	1	B9 V	0·12	7·10	+0·3
HR 1047	6·27	−0·01	1	B5 V	0·34	5·32	−1·5
HD 21641	6·77	−0·13	1	B9 V	0·11	6·46	−0·3
HD 21672	6·61	−0·16	1	B8 V	0·11	6·30	−0·5
HR 1063	5·53	−0·22	1	B8 III	0·05	5·39	−1·4
HD 21931	7·41	−0·11	1	B9 V	0·13	7·05	+0·3
ψ Per	4·27	−0·20	1	B5 e	0·15	3·85	−2·9
HD 22136	6·92	−0·15	1	B8 V	0·12	6·58	−0·2

Morgan, Harris and Johnson (5), converted to the $(P-V)$ scale. Fig. 1 is a plot of spectral type against observed colour. The absorption is non-uniform. In particular HR 1047 is highly reddened. But its membership in the cluster can scarcely be disputed, as will be seen from the colour-magnitude array in Fig. 2. Fig. 3 is a plot of spectral type against V, now corrected for absorption by subtracting $2 \cdot 8 \times$ the colour excess (see col. 7 of Table I). The scatter among the stars in Fig. 3 is what we would expect for the main-sequence stars of early type. Most of the stars, therefore, do form a cluster.

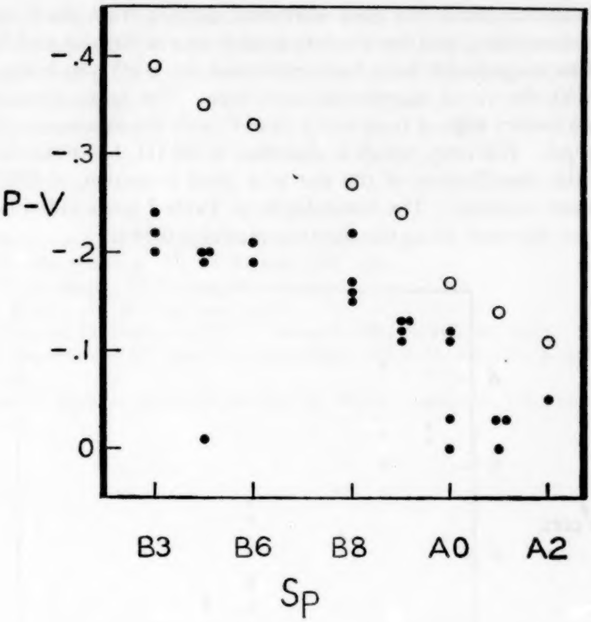

FIG. 1.—*Colour-spectral type diagram for members of the Perseus cluster. Open circles are intrinsic colours, while the observed colours are represented by filled circles.*

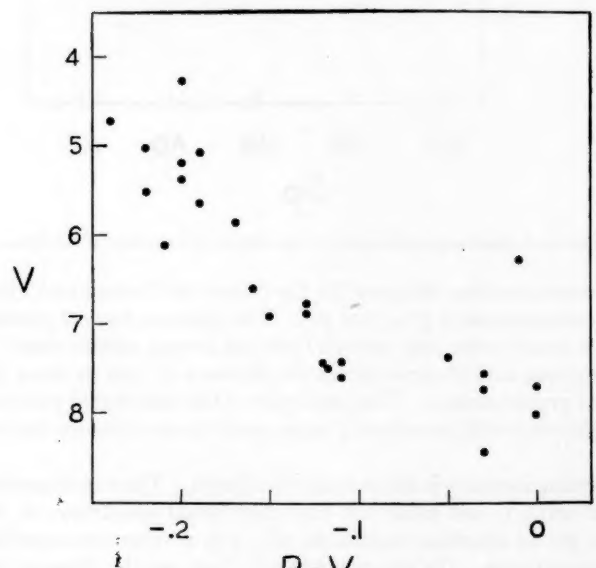

FIG. 2.—*Colour-magnitude array for members of the Perseus cluster.*

The distance moduli of the stars were next derived from the *V* magnitudes, corrected for absorption, and the absolute magnitudes of Keenan and Morgan (**6**). These absolute magnitudes have been corrected by $-0^{m}\cdot1$ to bring them into accordance with the visual magnitudes used here. The mean distance modulus obtained from twenty stars of luminosity class V, with the exception of HD 20701, is $6^{m}\cdot83$ (239 ps). HR 1063, which is classified as B8 III, has a distance modulus of $8^{m}\cdot4$. If the classification of the star as a giant is correct, it cannot be considered a cluster member. The last column of Table I gives individual absolute magnitudes for the stars using the distance modulus $6^{m}\cdot83$.

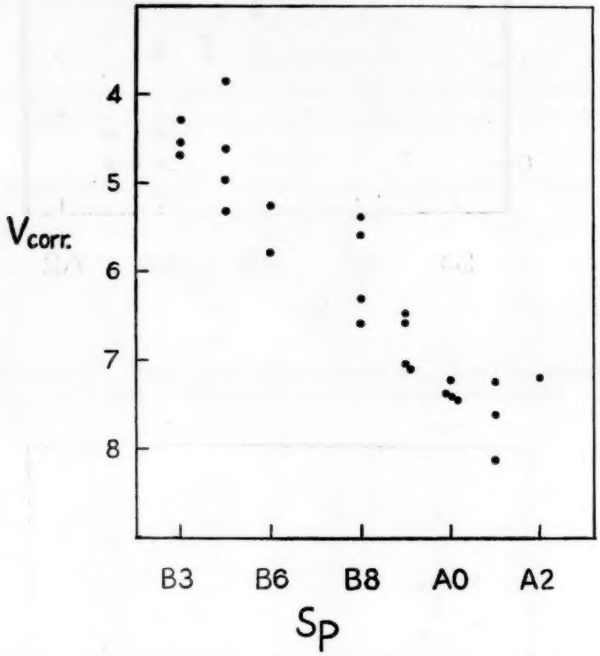

FIG. 3.—*Corrected visual magnitude-spectral type diagram for members of the Perseus cluster.*

The distance modulus obtained for the cluster by Roman and Morgan from dynamical considerations is $5^{m}\cdot4$ (120 ps). The distance derived photometrically by me is thus nearly twice that derived from the proper motion data. It may be noted that Roman and Morgan derive the distance of 120 ps from the upsilon component of proper motion. The proximity of the convergent point to the solar antapex might very well introduce a large error in any distance derived by this means.

An interesting anomaly is the parallax of α Persei. The trigonometric parallax is $0''\cdot029 \pm 0''\cdot005$ (7) and using the corrected visual magnitude of Roman and Morgan, we get an absolute magnitude of $-1\cdot3$, a value incompatible with its spectral characteristics. On the other hand, if we use the distance modulus as obtained in this study, the apparent magnitude, corrected for absorption, would have the low value of magnitude 2·2.

I am indebted to the Directors of the Lick and Nizamiah Observatories for providing me with all necessary facilities at their respective institutions, and to Mr M. Ramanathan for his help in the reduction of the observations.

Nizamiah Observatory,
Begampet, Hyderabad,
Deccan, India :
1954 *October* 5.

References

(1) N. Roman and W. Morgan, *Ap. J.*, **111,** 426, 1950.
(2) W. M. Smart and A. Ali, *M.N.*, **100,** 560, 1940.
(3) M. K. V. Bappu, *M.N.*, **114,** 680, 1954.
(4) O. J. Eggen, *Ap. J.*, **114,** 141, 1951.
(5) W. Morgan, D. Harris and H. L. Johnson, *Ap. J.*, **118,** 92, 1953.
(6) P. C. Keenan and W. Morgan, *Astrophysics* (ed. J. A. Hynek), p. 23, McGraw-Hill, 1951.
(7) Louise F. Jenkins, *General Catalogue of Stellar Parallaxes*, Yale, 1952.

ENERGY LEVELS IN Ca xv

David Layzer

(Communicated by Donald H. Menzel)

(Received 1954 December 3)

Summary

A discussion of the structure of term spectra in isoelectronic sequences shows that spectral terms fall naturally into certain groups, which we call "complexes". A complex is completely specified by the set of principal quantum numbers (n) and the parity p, and contains one or more entire configurations. The interval between terms that belong to the same complex varies asymptotically as the nuclear charge Z for large values of Z, while the interval between terms that belong to complexes with different sets of principal quantum numbers (n) varies asymptotically as Z^2. The electrostatic coupling between configurations whose terms belong to different complexes tends to vanish with increasing Z; but the coupling between configurations whose terms belong to the same complex approaches constancy. This circumstance greatly simplifies the discussion of configuration mixing in highly ionized atoms.

In Ca xv the configurations $(1s^2)$ $(2s^2)$ $(2p^2)$ and $(1s^2)$ $(2p^4)$ are strongly coupled, but the complex $(1^2 2^4)$ is weakly coupled with higher complexes. On the approximation of zero coupling between $(1^2 2^4)$ and higher complexes, the energy levels of $(1^2 2^4)$ are the eigenvalues of a tenth-order matrix, which reduces to two fourth-order matrices and a second-order matrix. We have evaluated the matrix elements partly by extrapolation along the isoelectronic sequence and partly by theoretical considerations. The predicted wave-lengths for the transitions $2p^2\,{}^3P_{2\to1}$, ${}^3P_{1\to0}$ are 5456 A and 5650 A respectively. These agree with the observed wave-lengths of the coronal lines λλ 5445, 5694 to within the uncertainty of the calculation, thus confirming the identifications of Edlén and Waldmeier.

1. *Introduction*

In 1942 Edlén (1) published an epoch-making paper in which he identified twenty-three coronal emission lines with transitions from metastable levels in the ground configurations of very highly ionized atoms. Only two of the identifications were listed as doubtful. One of these, the identification of the yellow line λ 5694 with the magnetic-dipole transition $p^2\,{}^3P_{1\to0}$ in Ca xv, has aroused considerable controversy and stimulated several investigations because of the fact that no ion definitely known to produce coronal emission lines has an ionization energy approaching that of Ca xv (814 eV).

In 1947 Waldmeier (2) discovered a faint emission line in the coronal spectrum at λ 5445, which he subsequently (3) identified with the magnetic-dipole transition $p^2\,{}^3P_{2\to1}$ in Ca xv.

Shklovsky (4) rejected the identifications of λλ 5694, 5445 on the ground that the intensity ratio $I(5694)/I(5445)=6$ observed by Waldmeier is incompatible with any known mechanism for exciting the levels $2p^2\,{}^3P_{2,\,1}$ in Ca xv. However, Mme Pecker, Billings and Roberts (5) have since discovered that λ 5445 is blended with a Fraunhofer line. Making allowance for the blending, they derived an intensity ratio of 1·6, in satisfactory agreement with theoretical expectations.

These writers also measured the Doppler widths of the red (Fe X, λ 6374), green (Fe XIV, λ 5303), and yellow (λ 5694) lines on two occasions when all three lines appeared simultaneously in the same (projected) region of the corona. By assuming that the three lines originated on each occasion in a single region, characterized by a unique kinetic temperature, they derived the atomic weight 40 ± 2 for the ion producing the yellow line. This result tends to confirm the identifications of Edlén and Waldmeier, though it does not exclude the possibility that argon (atomic weight 39·9) may be responsible for the yellow line.

The most serious objection to the identifications of Edlén and Waldmeier rests on a very thorough semi-empirical study by Garstang (6) of the configuration $(1s^2)(2s^2)(2p^2)$ in the isoelectronic sequence headed by C I. On the theory employed by Garstang, the five energy levels of this configuration are expressed in terms of five atomic parameters. Garstang determined the values of these parameters empirically in the first ten members of the isoelectronic sequence, for which the experimental data are nearly complete. He then (7) extrapolated these values to Ca XV, and used the extrapolated parameters to calculate the positions of the energy levels. The wave-lengths predicted for the transitions $^3P_{1\to 0}$, $^3P_{2\to 1}$ were 5480 A and 5380 A respectively. On account of the high internal consistency of the calculations, Garstang concluded that the identifications of Edlén and Waldmeier were incompatible with these results.

Now the theory underlying Garstang's calculations is imperfect in one respect. It takes into account only approximately, and in an indirect way, the effects of configuration mixing, which are known to be large in the configuration $(1s^2)(2s^2)(2p^2)$. In the present paper I have redone the calculation for Ca XV, using an improved theory that explicitly takes account of the major effects of configuration mixing. The results tend to support the identifications of Edlén and Waldmeier.

The chief difficulty one ordinarily encounters in estimating the effects of configuration mixing stems from the multiplicity of perturbing configurations. In Section 2 we shall derive some elementary properties of term spectra in isoelectronic sequences. We shall find that in highly ionized atoms the problem of configuration mixing simplifies considerably. Thus, in Ca XV the only perturbing configuration that needs to be taken into account is $(1s^2)(2p^4)$.

2. *Theoretical considerations*

2.1. *Term energies and complexes.*—The term energies of an N-electron atom of nuclear charge Z are defined as the eigenvalues of the Hamiltonian

$$H(N,Z)=\sum_{i=1}^{N}\left(-\frac{\hbar^2}{2m}\nabla_i^2-\frac{Ze^2}{r_i}\right)+\sum_{i\neq j}\frac{e^2}{r_{ij}}. \tag{2.1}$$

We shall find it convenient to take as the units of energy and length

$$\epsilon=\frac{mZ^2e^4}{2\hbar^2}, \qquad \lambda=\frac{\hbar^2}{mZe^2}. \tag{2.2}$$

In these units

$$H(N,Z)=\sum_{i=1}^{N}\left(-\nabla_i^2-\frac{2}{r_i}\right)+Z^{-1}\sum_{i\neq j}\frac{2}{r_{ij}}. \tag{2.3}$$

Ordinarily one treats Z as a numerical constant. In the present discussion, however, we shall assume that all radial wave functions and matrix elements are explicit functions of Z. This will enable us to survey certain regularities in the

structure of isoelectronic sequences that are not apparent in the spectra of individual atoms.

For a fixed value of N the eigenvalues of $H(N, Z)$ depend on Z in a definite way. We shall now determine the nature of this dependence.

When $Z^{-1}=0$ the right-hand side of (2.3) reduces to a sum of one-electron Hamiltonians. The eigenfunctions are antisymmetrized products of hydrogenic wave functions and certain linear combinations of these products. Let the symbol (n) denote the set of principal quantum numbers $(n_a, n_b, \ldots, n_N)$, taken in any order. Then any linear combination of antisymmetrized products, each of which has the same set of principal quantum numbers (n), is an eigenfunction of (2.3) with $Z^{-1}=0$ belonging to the eigenvalue

$$E^{(0)} = -\sum_{n_i \text{ in } (n)} n_i^{-2}. \tag{2.4}$$

From these well-known facts it follows that the eigenfunctions of $H(N, Z)$ and the corresponding eigenvalues can be written as power series in Z^{-1}:

$$E = \left(\frac{mZ^2e^4}{2\hbar^2}\right)\{E^{(0)} + E^{(1)}Z^{-1} + E^{(2)}Z^{-2} + \ldots\}. \tag{2.5}$$

$$\Psi_E = \Psi_{(n)}{}^{(0)} + Z^{-1}\Psi^{(1)} + \ldots. \tag{2.6}$$

$E^{(0)}$ in (2.5) is given by (2.4), and $\Psi_{(n)}{}^{(0)}$ in (2.6) is a linear combination of antisymmetrized products of hydrogenic wave functions, each product being characterized by the same set of principal quantum numbers (n).

To secure faster convergence, one should in practice replace Z in equation (2.5) by $Z-Z_0$, where Z_0 is the shielding constant given by Slater's rules (**8**).

The expansions (2.5), (2.6) are valid for sufficiently small values of Z^{-1}. We shall assume that they hold for all $Z^{-1} \leqslant N^{-1}$.

We shall call a group of terms belonging to a particular set (n) and a particular parity p a *complex*. According to (2.4) and (2.5) the terms of a given complex are "intertwined": the interval between terms of the same complex is asymptotically proportional to Z, while the interval between terms that belong to complexes characterized by different sets (n) is asymptotically proportional to Z^2.

We may conveniently designate a complex by the symbol $(1^p 2^q 3^r \ldots)$, adding the superscript o if the parity is odd.

A complex contains one or more entire configurations. For example, the complex $(1^2 2\,3)^0$ contains the configurations $(1s^2)\,(2s3p)$, $(1s^2)\,(2p3d)$, and $(1s^2)\,(2p3s)$.

2.2. *Configuration mixing in isoelectronic sequences.*—For the matrix representation of $H(N, Z)$ we adopt, as is usually done, an LS-coupling scheme. But in addition we shall assume that the radial wave functions contain Z explicitly, and are so constructed that the diagonal matrix elements have the proper quadratic dependence on Z, as given by (2.4) and (2.5).*

$H(N, Z)$ is diagonal in L, S, and p. Off-diagonal elements connect terms belonging to different configurations, as well as terms of different seniority within the same configuration. All the off-diagonal terms are asymptotically proportional to Z. Using this fact (which follows from the form of (2.3) and the requirement that the diagonal matrix elements have the proper quadratic dependence on Z),

* A method for constructing such radial wave functions has been developed by the writer and applied to the complex $(1^2)\,(2^2)$. Only an abstract has been published (**10**).

and the usual formulae of perturbation theory, one can easily demonstrate the following theorem. The coefficient $E^{(1)}$ in the expansion (2.5) of a given term energy is completely determined by the submatrix whose elements connect terms belonging to the same complex. Moreover, in the expansion

$$\Psi_{(n)^p\beta LS}=\sum_{(n'l')\alpha'} a_{(n)^p\beta LS;\,(n'l')\alpha' LS}\Psi_{(n'l')\alpha' LS} \tag{2.7}$$

of an eigenfunction in terms of the basic functions, the coefficients have the following asymptotic dependence on Z:

$$a_{(n)^p\beta LS;\,(n'l')\alpha' LS}\simeq\begin{cases}\text{const. } Z^{-1} & \text{if } (n')\neq(n)\\ \text{const.} & \text{if } (n')\equiv(n).\end{cases} \tag{2.8}$$

Thus, the coupling between terms of the same kind that belong to the same complex approaches constancy with increasing Z, while the coupling between the terms of the same kind that belong to different complexes tends to zero with increasing Z.

Since a complex contains more than one configuration in general, the relations between term intervals predicted by the standard theory will not ordinarily hold true even in the limit $Z\rightarrow\infty$.

2.3. *Extrapolation along isoelectronic sequences.*—Let $E_{(n)^p\Gamma}$ denote the energy of the term Γ of the complex $(n)^p$. We define the difference operator Δ_z in the usual way:

$$\Delta_z f(Z)=f(Z+1)-f(Z).$$

From equation (2.5) we obtain the equations

$$\Delta_z(E_{(n)^p\Gamma}-E_{(n)^{p'}\Gamma'})=E^{(1)}_{(n)^p\Gamma}-E^{(1)}_{(n)^{p'}\Gamma'}+O(Z^{-2}), \tag{2.9}$$

and

$$\Delta_z^2(E_{(n)^p\Gamma}-E_{(n')^{p'}\Gamma'})=2(E^{(0)}_{(n)^p\Gamma}-E^{(0)}_{(n')^{p'}\Gamma'})+O(Z^{-3}). \tag{2.10}$$

Because of the rapidity with which the differences (2.9) and (2.10) approach constancy, these rules enable one to extrapolate term spectra with high accuracy along isoelectronic sequences. The constant term on the right-hand side of (2.10) is given explicitly by (2.4).

3. *Application to Ca* XV

The theoretical energy levels of an atom (N, Z) are the eigenvalues of the Hamiltonian $H(N, Z)+V(N, Z)$, where $H(N, Z)$ is given by (2.1) and $V(N, Z)$ represents the spin-dependent interactions, which cause the splitting of terms into levels.

In view of the preceding discussion we may reasonably assume that in Ca XV the configuration $(1s^2)$ $(2s^2)$ $(2p^2)$ is coupled much more strongly with the configuration $(1s^2)$ $(2p^4)$, which belongs to the same complex, than with any other configuration. On the simplifying assumption of zero coupling between the complex $(1^2 2^4)$ and other complexes, the energy levels of $(1^2 2^4)$ are the eigenvalues of the matrices (3·1 abc).

The notation is standard* except for the symbol Φ, which represents a numerical multiple of the Slater integral $G_1(2s, 2p)$, the symbol L, which represents a linear combination of Slater integrals F_0, and the asterisks, which serve to distinguish corresponding parameters in the two configurations.

* The coefficients a and b have not yet been calculated. Their values are unimportant in the present calculation, where, for the sake of simplicity, they have been set equal to 2.8 and 1 respectively.

	$2p^2\ {}^3\mathrm{P}_2$	$2p^2\ {}^1\mathrm{D}_2$	$2p^4\ {}^3\mathrm{P}_2$	$2p^4\ {}^1\mathrm{D}_2$
$2p^2\ {}^3\mathrm{P}_2$	$\cdot 5\zeta-6\cdot 4\eta$	$2^{-1/2}(\zeta+2\cdot 8\eta)$	Φ	0
$2p^2\ {}^1\mathrm{D}_2$	$2^{-1/2}(\zeta+2\cdot 8\eta)$	$6F_2$	0	Φ
$2p^4\ {}^3\mathrm{P}_2$	Φ	0	$L-\cdot 5\zeta^*-3\cdot 4\eta^*$	$-2^{-1/2}(\zeta^*+a\eta^*)$
$2p^4\ {}^1\mathrm{D}_2$	0	Φ	$-2^{-1/2}(\zeta^*+a\eta^*)$	$L+6F_2$

(3.1 a)

	$2p^2\ {}^3\mathrm{P}_1$	$2p^4\ {}^3\mathrm{P}_1$
$2p^2\ {}^3\mathrm{P}_1$	$-\cdot 5\zeta+8\eta$	Φ
$2p^4\ {}^3\mathrm{P}_1$	Φ	$L+\cdot 5\zeta^*+5\eta^*$

(3.1 b)

	$2p^2\ {}^3\mathrm{P}_0$	$2p^2\ {}^1\mathrm{S}_0$	$2p^4\ {}^3\mathrm{P}_0$	$2p^4\ {}^1\mathrm{S}_0$
$2p^2\ {}^3\mathrm{P}_0$	$-\zeta+8\eta$	$-2^{1/2}(\zeta+\eta)$	Φ	0
$2p^2\ {}^1\mathrm{S}_0$	$-2^{1/2}(\zeta+\eta)$	$15F_2$	0	2Φ
$2p^4\ {}^3\mathrm{P}_0$	Φ	0	$L+\zeta^*+2\eta^*$	$2^{1/2}(\zeta^*+b\eta^*)$
$2p^4\ {}^1\mathrm{S}_0$	0	2Φ	$2^{1/2}(\zeta^*+b\eta^*)$	$L+15F_2^*$

(3.1 c)

The nine independent intervals between the eigenvalues of (3.1) involve only eight undetermined parameters. Unfortunately, the experimental data* for the configuration $(1s^2)\ (2p^4)$ are so scanty that one cannot determine the values of all eight parameters in Ca XV by extrapolation along the isoelectronic sequence. However, by a simple theoretical argument we can reduce the number of independent parameters from eight to five.

According to Slater (**8**), the shielding constant of a $2s$ electron for a $2p$ electron is the same as that of a $2p$ electron. A $2p$ electron in the configuration $(1s^2)$ $(2s^2)\ (2p^2)$ should therefore "see" virtually the same electrostatic field as a $2p$ electron in the configuration $(1s^2)\ (2p^4)$. Hence to a good approximation we may set

$$F_2^*=F_2,\quad \zeta^*=\zeta,\quad \eta^*=\eta. \tag{3.2}$$

This approximation should be particularly good in a highly ionized atom like Ca XV, since small changes in the shielding will not alter the total electrostatic field appreciably.

We shall use Feenberg's (**9**) fifth-order perturbation theory to calculate the three smallest eigenvalues of the matrices (3.1). In Ca XV the results are accurate to about one part in a thousand. Since the calculation as a whole is accurate only to about one part in a hundred, this method of solving the secular equations is precise enough for our purpose.

* All the experimental data used in this paper are taken from Charlotte Moore's compilation (**11**).

We obtain:

$$E(^3P_2)=0{\cdot}5\zeta-6{\cdot}4\eta$$
$$-\frac{(\zeta+2{\cdot}8\eta)^2/2}{\left(6F_2-\dfrac{\Phi^2}{L+6F_2-0{\cdot}5\zeta+6{\cdot}4\eta}\right)-\left(0{\cdot}5\zeta-6{\cdot}4\eta-\dfrac{(\zeta+2{\cdot}8\eta)^2/2}{6F_2-0{\cdot}5\zeta+6{\cdot}4\eta}-\dfrac{\Phi^2}{L-\zeta+3\eta}\right)}$$
$$-\frac{\Phi^2}{\left(L-0{\cdot}5\zeta-3{\cdot}4\eta-\dfrac{(\zeta+2{\cdot}8\eta)^2/2}{L+6F_2-0{\cdot}5\zeta+6{\cdot}4\eta}\right)-\left(0{\cdot}5\zeta-6{\cdot}4\eta-\dfrac{(\zeta+2{\cdot}8\eta)^2/2}{6F_2-0{\cdot}5\zeta+6{\cdot}4\eta}-\dfrac{\Phi^2}{L-\zeta+3\eta}\right)}$$
$$+\frac{2\Phi^2(\zeta+2{\cdot}8\eta)^2/2}{(6F_2-0{\cdot}5\zeta+6{\cdot}4\eta)(L-\zeta+3\eta)(L+6F_2-0{\cdot}5\zeta+6{\cdot}4\eta)}. \tag{3.3 a}$$

$$E(^3P_1)=-0{\cdot}5\zeta+8\eta-\frac{\Phi^2}{L+0{\cdot}5\zeta+5\eta-\left(-0{\cdot}5\zeta+8\eta-\dfrac{\Phi^2}{L+\zeta-3\eta}\right)}. \tag{3.3 b}$$

$$E(^3P_0)=-\zeta+8\eta$$
$$-\frac{2(\zeta+\eta)^2}{\left(15F_2-\dfrac{4\Phi^2}{L+15F_2+\zeta-8\eta}\right)-\left(-\zeta+8\eta-\dfrac{2(\zeta+\eta)^2}{15F_2+\zeta-8\eta}-\dfrac{\Phi^2}{L+2\zeta-6\eta}\right)}$$
$$-\frac{\Phi^2}{\left(L+\zeta+2\eta-\dfrac{2(\zeta+\eta)^2}{L+15F_2+\zeta-8\eta}\right)-\left(-\zeta+8\eta-\dfrac{2(\zeta+\eta)^2}{15F_2+\zeta-8\eta}-\dfrac{\Phi^2}{L+2\zeta-6\eta}\right)}$$
$$+\frac{2\times 2\Phi^2\times 2(\zeta+\eta)^2}{(15F_2+\zeta-8\eta)(L+2\zeta-6\eta)(L+15F_2+\zeta-8\eta)}. \tag{3.3 c}$$

We shall also need the formulae

$$E(2p^{4}\,^3P_1)=L+0{\cdot}5\zeta+5\eta+\frac{\Phi^2}{L+0{\cdot}5\zeta+5\eta-\left(-0{\cdot}5\zeta+8\eta-\dfrac{\Phi^2}{L+\zeta-3\eta}\right)}, \tag{3.4}$$

$$E(^1S)=15F_2-\frac{4\Phi^2}{L+4\Phi^2/L}, \tag{3.5 a}$$

$$E(^3P)=-\frac{\Phi^2}{L+\Phi^2/L}, \tag{3.5 b}$$

$$E(^1D)=6F_2-\frac{\Phi^2}{L+\Phi^2/L}. \tag{3.5 c}$$

From (3.5) we obtain

$$\mathrm{DP}\equiv E(^1D)-E(^3P)=6F_2, \tag{3.6}$$

$$\mathrm{SD}\equiv E(^1S)-E(^1D)=9F_2-\frac{\Phi^2}{L}\left(\frac{4}{1+4\Phi^2/L^2}-\frac{1}{1+\Phi^2/L^2}\right). \tag{3.7}$$

By (3.4) and (3.3 a)

$$E(2p^{4}\,^3P_1)-E(2p^{2}\,^3P_1)=L+\zeta-3\eta+\frac{2\Phi^2}{L+\zeta-3\eta+\dfrac{\Phi^2}{L+\zeta-3\eta}}. \tag{3.8}$$

Garstang has derived values of SD, PD, ζ and η for the first ten members of the isoelectronic sequence, and, by extrapolation, for Ca XV as well. The extrapolation is probably quite accurate, since the approximations underlying the calculation are valid for the early members of the sequence. One could probably derive improved values of ζ and η for Si IX and P X by using the more accurate formulae given above; but Garstang seems to have given little weight to these ions in extrapolating the values of ζ and η. We shall therefore use his extrapolated parameters in the present calculation. This step not only saves labour, but also puts the essential differences between Garstang's calculation and the present one in the sharpest possible focus.

Garstang's values of SD and PD are well represented beyond Ne V by the formulae

$$\left.\begin{aligned} \mathrm{SD} &= 5250\,(Z-3.25)-1785\ \mathrm{cm}^{-1},\\ \mathrm{DP} &= 4660\,(Z-3.25)-1930\ \mathrm{cm}^{-1}. \end{aligned}\right\} \tag{3.9}$$

The shielding constant, 3.25, is that given by Slater (**8**). The smallness of the constant terms in these expressions justifies our assumption of zero coupling between the complex $(1^2 2^4)$ and other complexes.

Experimental values for the interval $E(2p^4\,{}^3\mathrm{P}_1)-E(2p^2\,{}^3\mathrm{P}_1)$ are available for O III, F IV, Ne V and Na VI. Garstang's calculations give SD, DP, ζ and η for these ions. We can therefore solve equations (3.7) and (3.8) for Φ and L. The derived values of L are well represented by the formula

$$L = 63\,175\,(Z-3.25)-21\,380\ \mathrm{cm}^{-1}. \tag{3.10}$$

Hence

$$L = 1\,036\,800\ \mathrm{cm}^{-1}\ \text{in Ca XV}. \tag{3.11 a}$$

Garstang's extrapolated parameters are

$$\left.\begin{aligned} 6F_2 = \mathrm{DP} &= 76\,400\ \mathrm{cm}^{-1},\\ \mathrm{SD} &= 86\,300\ \mathrm{cm}^{-1},\\ \zeta &= 24\,210\ \mathrm{cm}^{-1},\\ \eta &= 91\ \mathrm{cm}^{-1}, \end{aligned}\right\}\ \text{in Ca XV}. \tag{3.11 b}$$

From (3.11 a, b) and (3.7) we obtain

$$\Phi = 101\,310\ \mathrm{cm}^{-1}\quad \text{in Ca XV}. \tag{3.11 c}$$

Finally, we insert the values (3.11) in the equations (3.3) and obtain

$$\left.\begin{aligned} E({}^3\mathrm{P}_2) &= -\ \ 2\,639\ \mathrm{cm}^{-1},\\ E({}^3\mathrm{P}_1) &= -20\,966\ \mathrm{cm}^{-1},\\ E({}^3\mathrm{P}_0) &= -38\,667\ \mathrm{cm}^{-1}. \end{aligned}\right\} \tag{3.12}$$

The intervals are

$$\left.\begin{aligned} E(10) &= 17\,701\ \mathrm{cm}^{-1} = 5650\,\mathrm{A}\quad (\text{observed: } 5694\,\mathrm{A}),\\ E(21) &= 18\,327\ \mathrm{cm}^{-1} = 5456\,\mathrm{A}\quad (\text{observed: } 5445\,\mathrm{A}). \end{aligned}\right\} \tag{3.13}$$

In view of the approximations we have made, the agreement is satisfactory; the results tend to confirm the identifications of Edlén and Waldmeier.

The research reported in this paper has been supported by the Geophysics Research Directorate, Air Force Cambridge Research Center, under Contract AF19(604)-146 with Harvard University.

Harvard College Observatory,
Cambridge, Massachusetts :
1954 *November* 11.

References

(1) B. Edlén, *Zs. f. Astrophys.*, **22,** 30, 1942.
(2) M. Waldmeier, *Astr. Mitt. Zürich*, Nr. **151,** 1947.
(3) M. Waldmeier, *Zs. f. Astrophys.*, **29,** 29, 1951.
(4) I. Shklovsky, *Annals of the Crimean Astrophys. Obs.*, **5,** 86, 1950.
(5) Charlotte Pecker, D. Billings and W. Roberts, *C.R.*, **238,** 1101, 1954.
(6) R. H. Garstang, *M.N.*, **111,** 115, 1951.
(7) R. H. Garstang, *Ap. J.*, **115,** 569, 1952.
(8) J. C. Slater, *Phys. Rev.*, **36,** 57, 1930.
(9) E. Feenberg, *Phys. Rev.*, **74,** 206, 1948.
(10) D. Layzer, *A.J.*, **56,** 43, 1951.
(11) Charlotte E. Moore, " Atomic Energy Levels ", *Circ. Nat. Bur. Standards*, No. 467, 1949.

ON THE IDENTIFICATION OF Ca XV AND A XIV IN THE SOLAR CORONA

Bengt Edlén

(Communicated by F. J. M. Stratton)

(Received 1955 February 9)

Summary

The interpretation of the coronal wave-lengths λ 5694 and λ 5446 as transitions in Ca XV is shown to be compatible with known isoelectronic data on level intervals. The original suggestion concerning A XIV is revised and the identification transferred from λ 4359 to the new coronal line λ 4412.

The interpretation (**1, 2**) of the coronal lines λ 5694 and λ 5446 as transitions within the ground term $2s^2 2p^2\,{}^3\mathrm{P}$ of Ca XV has been subject to much discussion with arguments for and against the identifications (e.g. **3, 4**). The present note is intended to show in a simple and direct way what evidence the known data in the isoelectronic sequence actually provide as far as the size of the intervals is concerned.

The data are collected in Table I, where columns 2, 3 and 4 give all usable observed values of the relevant intervals. In some cases the values differ slightly from those in the literature (**5**), which is due to re-examination of existing or, in the case of Al VIII, utilization of unpublished measurements. The values given in brackets for Si IX and P X have been extrapolated in the present investigation*, and the values given for Ca XV are the wave-numbers of the coronal lines.

TABLE I

Isoelectronic data for the configuration $2s^2 2p^2$

Ion	${}^3\mathrm{P}_2$–${}^3\mathrm{P}_1$	${}^3\mathrm{P}_1$–${}^3\mathrm{P}_0$	${}^1\mathrm{D}_2$–${}^3\mathrm{P}_2$	χ	α_{2-1}	α_{1-0}	ζ_{2-1}	ζ_{1-0}
	cm^{-1}	cm^{-1}	cm^{-1}					
C I	27·03	16·36	10149	0·0034	0·9986	0·5023	27·07	32·57
N II	82·2	49·1	15184	0·0069	0·9971	0·5046	82·4	97·3
O III	193·0	113·6	19967	0·0122	0·9949	0·5081	194·0	223·6
F IV	388·2	225·2	24628	0·0198	0·9917	0·5131	391·4	438·9
Ne V	698	414	29182	0·0300	0·9874	0·5198	707	797
Na VI	1161	696	33620	0·0432	0·9817	0·5284	1183	1317
Mg VII	1812	1127	37982	0·0600	0·9744	0·5392	1860	2090
Al VIII	2704	1716	...	0·0806	0·9654	0·5522	2801	3107
Si IX	3864	(2563)	...	0·1054	0·9542	0·5677	4049	(4515)
P X	(5345)	(3705)	...	0·1350	0·9408	0·5858	(5681)	(6325)
– – – –								
Ca XV	18355	17556	...	$0{\cdot}3673_7$	$0{\cdot}8297_4$	$0{\cdot}7132_3$	22121	24615

* This extrapolation confirms the suggestion by Garstang (**6**) and Naqvi (**7**) that the published values for P X need revision.

The following treatment is, in principle, identical with that used in my original paper (1). It is based on the intermediate-coupling formulae which express the level intervals as functions of the parameters ζ and F_2 (see **8** and **9**). Introducing the coupling parameter $\chi=\zeta/5F_2$ and the following abbreviations

$$\left.\begin{aligned}\alpha_{i-k}&=({}^3\mathrm{P}_i-{}^3\mathrm{P}_k)/\zeta,\\ \beta&=({}^1\mathrm{D}_2-{}^3\mathrm{P}_2)/5F_2,\end{aligned}\right\} \tag{1}$$

we obtain from the intermediate-coupling formulae the relations

$$\left.\begin{aligned}\chi\alpha_{2-1}&=\frac{3}{5}+\frac{3}{4}\chi-\left(\frac{9}{25}-\frac{3}{10}\chi+\frac{9}{16}\chi^2\right)^{1/2},\\ \chi\alpha_{1-0}&=-\frac{3}{2}+\frac{3}{2}\left(1+\frac{2}{3}\chi+\chi^2\right)^{1/2},\\ \beta&=\left(\frac{36}{25}-\frac{6}{5}\chi+\frac{9}{4}\chi^2\right)^{1/2}.\end{aligned}\right\} \tag{2}$$

The parameter χ has been defined in the present case by identifying the observed ratio $R_\mathrm{C}=({}^3\mathrm{P}_2-{}^3\mathrm{P}_0)/({}^1\mathrm{D}_2-{}^3\mathrm{P}_2)$ with its theoretical expression ($R_\mathrm{C}=\chi\alpha_{2-0}/\beta$) as a function of χ according to formulae (1) and (2).* The χ-values obtained in this way for the 7 ions from C I through Mg VII are represented within their error limits by the empirical formula

$$\sqrt[3]{\chi}=0{\cdot}04080Z-0{\cdot}1022+0{\cdot}048/Z, \tag{3}$$

which yields the χ-values in col. 5 of Table I and, by way of formulae (2), the α's in cols. 6 and 7. Finally, the ζ-values in the last two columns of the table are obtained by dividing the observed intervals by the corresponding α:

$$\left.\begin{aligned}\zeta_{2-1}&=({}^3\mathrm{P}_2-{}^3\mathrm{P}_1)/\alpha_{2-1},\\ \zeta_{1-0}&=({}^3\mathrm{P}_1-{}^3\mathrm{P}_0)/\alpha_{1-0}.\end{aligned}\right\} \tag{4}$$

The difference between ζ_{2-1} and ζ_{1-0} is a measure of the inaccuracy of the intermediate-coupling formulae, and is due to their neglecting spin-spin interaction and the perturbing influence of other configurations.† This deficiency, however, is of no consequence for the present purpose, as long as the parameters obtained are suitable for isoelectronic comparison and extrapolation.

The results are best demonstrated by a graph (Fig. 1) showing the variation of $\sqrt[4]{\zeta}$ with atomic number. A suitable linear function of Z is subtracted to get an adequate scale. As the figure shows, the curve for ζ_{2-1} is definitely pointing towards the value which corresponds to λ 5446 in Ca XV, providing a clear evidence in favour of the identification. For ζ_{1-0} the evidence is less definite because the points are considerably more affected by observational errors, this being due both to larger errors in the intervals themselves and to the smaller value of α. The graph shows in any case that an interval in Ca XV corresponding to λ 5694 is in no conflict with the isoelectronic data as far as they are known.

The curves in Fig. 1 can be represented by simple interpolation formulae which for some purposes may be more useful than a graph. For ζ_{2-1} the values

* For convenience the α's, β and $\chi\alpha_{2-0}/\beta$ were calculated to 5 decimals for $\chi=0{\cdot}00$ (0·01) 0·80 and tabulated. The tables could be duplicated if they should turn out to be of interest to others.

† I am grateful to Dr Garstang for a discussion on this point,

through the whole sequence, including Ca XV, are represented within the limits of observational errors by the formula

$$\sqrt[4]{\zeta_{2-1}} = 0{\cdot}70124Z - 1{\cdot}8118 - 0{\cdot}2889/(Z - 3{\cdot}48). \quad (5)$$

Expressions of the same form, $AZ - B - C/(Z-a)$, were tested in the course of a comprehensive investigation (unpublished) and found well adapted to represent $\sqrt[4]{\zeta}$, F_2 and $\sqrt[3]{\chi}$ for all configurations $2s^n2p^m$ and $3s^n3p^m$. A theoretical justification for this form is implicit in a paper by Layzer (**10**).*

The conclusion of this discussion is, then, that the identifications of λ 5694 and λ 5446 with $^3P_{1-0}$ and $^3P_{2-1}$ of Ca XV are perfectly compatible with observed isoelectronic data. Taken together with other evidence (**4**) this would seem to remove further doubts regarding the interpretation of these lines.

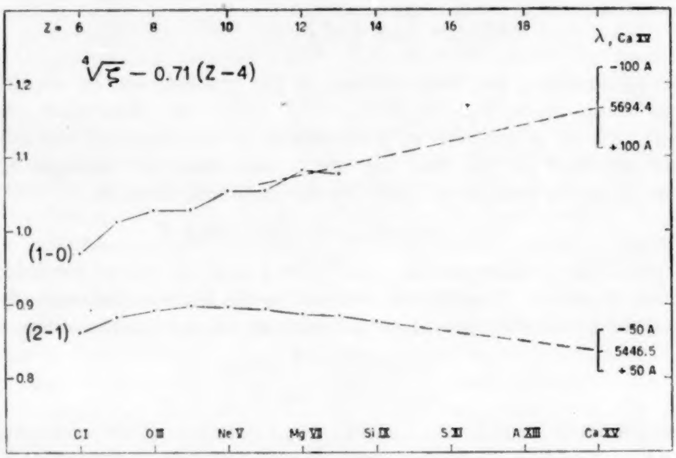

FIG. 1.—*Graph of* $\sqrt[4]{\zeta} - 0{\cdot}71(Z-4)$ *referring to the intervals* $^3P_{2-1}$ *and* $^3P_{1-0}$ *of the configuration* $2s^22p^2$.

It is of interest to mention also the following point which, in a way, provides further evidence for the same interpretation and, at the same time, removes the last question-mark from the list of coronal identifications. After the recent discovery by Lyot and Dollfus (**11**) of the coronal line λ 4412·4 it appears that the original, tentative identification of λ 4359 with A XIV $2s^22p\ ^2P_{3/2} - {}^2P_{1/2}$ should be revised and the assignment transferred to the new line. This fits the isoelectronic data definitely better. Moreover, the characteristic appearance of λ 4412 is similar to that of λ 5694 and λ 5446, the three lines forming a group of their own, precisely as one should expect from the fact that both A XIV and Ca XV are exceptional with regard to ionization potentials.

* I am much obliged to Dr Layzer for his kindness in sending me a manuscript copy of his paper. It incited me to publish the present note.

Department of Physics,
University of Lund,
Lund (Sweden) :
1955 *February* 5.

References

(1) B. Edlén, *Zs. f. Astroph.*, **22,** 30, 1942.
(2) M. Waldmeier, *Zs. f. Astroph.*, **29,** 29, 1951.
(3) R. H. Garstang, *Ap. J.*, **115,** 569, 1952.
(4) Ch. Pecker, D. E. Billings and W. O. Roberts, *Ap. J.*, **120,** 509, 1954.
(5) *Atomic Energy Levels*, NBS Circular 467, Vol. I, 1949.
(6) R. H. Garstang, *M.N.*, **111,** 115, 1951.
(7) Ali M. Naqvi, *Proc. Nat. Inst. Sc., India*, **19,** 461, 1953.
(8) E. U. Condon and G. H. Shortley, *The Theory of Atomic Spectra*, Cambridge Univ. Press, 1935.
(9) H. A. Robinson and G. H. Shortley, *Phys. Rev.*, **52,** 713, 1937.
(10) D. Layzer, *M.N.*, **114,** 692, 1954.
(11) B. Lyot and A. Dollfus, *C.R.*, **237,** 855, 1953.

CONTENTS

Printed in London by Taylor & Francis, Ltd., 1955 July